International Conference on Recent Trends in Geoscience Research and Applications 2025

15–19 September 2025, Belgrade, Serbia & virtual

BOOK OF ABSTRACTS AND CONTRIBUTED PAPERS

Edited by Aleksandra Nina, Snežana Dragović, Maja Kuzmanoski, Milan Đorđević, and Mrđan Đokić

Belgrade, 2025

International Conference on Recent Trends in Geoscience Research and Applications 2025

Venue: Institute of Physics Belgrade, National Institute of the Republic of Serbia, University of Belgrade, Serbia & virtual

Date: 15–19 September 2025

Conference type: International scientific conference

Organizers:

Faculty of Civil Engineering, University of Belgrade, Belgrade, Serbia

Institute of Physics Belgrade, National Institute of the Republic of Serbia, University of Belgrade, Belgrade, Serbia

Technical organizer: PanaComp Wonderland Travel, Novi Sad, Serbia

Scientific Rationale

Geoscience research and applications are of crucial interest in science and many areas of modern life. For this reason, exchanging knowledge in various relevant areas is essential for development in scientific, engineering and programming activities. The conference aims to highlight the importance of joint research of experts in these fields and provide a platform for knowledge exchange.

Scientific Organizing Committee

Aleksandra Nina, Institute of Physics Belgrade, National Institute of the Republic of Serbia, University of Belgrade, Belgrade, Serbia, chair

Snežana Dragović, "VINČA" Institute of Nuclear Sciences - National Institute of the Republic of Serbia, University of Belgrade, Belgrade, Serbia, co-chair

Mirela Voiculescu, Faculty of Sciences and Environment, University Dunărea de Jos of Galați, Galați, Romania, co-chair

Oleg Odalović, University of Belgrade, Faculty of Civil Engineering, Department of Geodesy and Geoinformatics, Belgrade, Serbia, co-chair

Pier Francesco Biagi, Department of Physics, University of Bari, Bari, Italy

Peter Butka, Department of Cybernetics and Artificial Intelligence, Faculty of Electrical Engineering and Informatics, Technical University of Kosice, Kosice, Slovakia

Vladica Cvetković, University of Belgrade, Faculty of Mining and Geology, Belgrade, Serbia

Ranko Dragović, University of Niš, Faculty of Sciences and Mathematics, Niš, Serbia

Hans U. Eichelberger, Space Research Institute, Austrian Academy of Sciences, Graz, Austria

Maria Gritsevich, Finnish Geospatial Research Institute Department of Physics, University of Helsinki, Helsinki, Finland

Ljubica Ivanović Bibić, University of Novi Sad, Faculty of Sciences, Department of Geography, Tourism and Hotel Management, Novi Sad, Serbia

Anđelija Ivkov-Džigurski, University of Novi Sad, Faculty of Sciences, Department of Geography, Tourism and Hotel Management, Novi Sad, Serbia

Konstantinos Kourtidis, Physics Department, Aristotle University of Thessaloniki

Ivan Lizaga, Instituto Pirenaico de Ecología (IPE-CSIC), Spanish National Research Council, Zaragoza, Spain

Slavica Malinović-Milićević, Geographical Institute „Jovan Cvijić“, Serbian Academy of Sciences and Arts, Belgrade, Serbia

Ana Milanović Pešić, Geographical Institute „Jovan Cvijić“, Serbian Academy of Sciences and Arts, Belgrade, Serbia

Irina Mironova, St. Petersburg State University, St. Petersburg, Russia

Giovanni Nico, Institute for Applied Mathematics, National Research Council, Bari, Italy

Luka Č. Popović, Astronomical Observatory, Belgrade, Serbia

Sergey Pulinets, Space Research Institute, Russian Academy of Sciences (IKI), Moscow, Russia

Eugene Rozanov,
Physikalisch-Meteorologisches Observatorium Davos/World Radiation Center, Davos, Switzerland

Xuhui Shen, National Space Science Center of CAS, Beijing, China

Elizabeth A. Silber, Department of Earth Sciences, Western University, London, ON, Canada

Ivana Smičiklas, "VINČA" Institute of Nuclear Sciences - National Institute of the Republic of Serbia, University of Belgrade, Belgrade, Serbia

Vladimir Srećković, Institute of Physics Belgrade, National Institute of the Republic of Serbia, University of Belgrade, Belgrade, Serbia

Earle R. Williams, Parsons Laboratory, Massachusetts Institute of Technology, Cambridge, MA, USA

Local Organizing Committee

Aleksandra Nina, Institute of Physics Belgrade, National Institute of the Republic of Serbia, University of Belgrade, Belgrade, Serbia, chair

Snežana Dragović, "VINČA" Institute of Nuclear Sciences - National Institute of the Republic of Serbia, University of Belgrade, Belgrade, Serbia, co-chair

Đorđe Trajković, Institute of Physics Belgrade, National Institute of the Republic of Serbia, University of Belgrade, Belgrade, Serbia, co-chair

Aleksandar Čupić, "VINČA" Institute of Nuclear Sciences - National Institute of the Republic of Serbia, University of Belgrade, Belgrade, Serbia

Mrđan Đokić, University of Niš, Faculty of Sciences and Mathematics, Niš, Serbia

Milan Đorđević, University of Niš, Faculty of Sciences and Mathematics, Niš, Serbia

Sanja Grekulović, University of Belgrade, Faculty of Civil Engineering, Department of Geodesy and Geoinformatics, Belgrade, Serbia

Aleksandra Kolarski, Institute of Physics Belgrade, National Institute of the Republic of Serbia, University of Belgrade, Belgrade, Serbia

Maja Kuzmanoski, Institute of Physics Belgrade, National Institute of the Republic of Serbia, University of Belgrade, Belgrade, Serbia

Milica Langović, Institute of Physics Belgrade, National Institute of the Republic of Serbia, University of Belgrade, Belgrade, Serbia

Ana Milanović Pešić, Geographical Institute „Jovan Cvijić“, Serbian Academy of Sciences and Arts, Belgrade, Serbia

Dušan Petković, University of Belgrade, Faculty of Civil Engineering, Department of Geodesy and Geoinformatics, Belgrade, Serbia

Miljana Todorović Drakul, University of Belgrade, Faculty of Civil Engineering, Department of Geodesy and Geoinformatics, Belgrade, Serbia

Published by:
Faculty of Civil Engineering, University of Belgrade, Belgrade, Serbia

Institute of Physics Belgrade, National Institute of the Republic of Serbia, University of Belgrade, Belgrade, Serbia

Picture on the first cover: Dejan Doljak
ISBN 978-86-7518-253-5

List of reviewers:

Filip Arnaut, Institute of Physics Belgrade, National Institute of the Republic of Serbia, University of Belgrade, Belgrade, Serbia

Vladica Cvetković, University of Belgrade, Faculty of Mining and Geology, Belgrade, Serbia

Ranko Dragović, University of Niš, Faculty of Sciences and Mathematics, Niš, Serbia

Snežana Dragović, "VINČA" Institute of Nuclear Sciences - National Institute of the Republic of Serbia, University of Belgrade, Belgrade, Serbia

Luka Ilić, Department of Earth Sciences, Barcelona Supercomputing Center, Barcelona, Spain

Aleksandra Kolarski, Institute of Physics Belgrade, National Institute of the Republic of Serbia, University of Belgrade, Belgrade, Serbia

Anđelka Kovačević, University of Belgrade, Faculty of Mathematics, Department of Astronomy, Belgrade, Serbia

Zoran Mijić, Institute of Physics Belgrade, National Institute of the Republic of Serbia, University of Belgrade, Belgrade, Serbia

Ana Milanović Pešić, Geographical Institute „Jovan Cvijić“, Serbian Academy of Sciences and Arts, Belgrade, Serbia

Aleksandra Nina, Institute of Physics Belgrade, National Institute of the Republic of Serbia, University of Belgrade, Belgrade, Serbia

Oleg Odalović, University of Belgrade, Faculty of Civil Engineering, Department of Geodesy and Geoinformatics, Belgrade, Serbia

Dušan Petković, University of Belgrade, Faculty of Civil Engineering, Department of Geodesy and Geoinformatics, Belgrade, Serbia

Zorica Podraščanin, Faculty of Sciences, Department of Physics, University of Novi Sad, Novi Sad, Serbia

Nikola Veselinović, Institute of Physics Belgrade, National Institute of the Republic of Serbia, University of Belgrade, Belgrade, Serbia

CONTENTS

Invited Lectures

Invited Progress Reports

Progress Reports

Posters

INVITED LECTURES

GeosciRA25

Book of Abstracts and Contributed Papers
International Conference on Recent Trends in Geoscience Research and Applications 2025 Belgrade, Serbia and Virtual, 15–19 September 2025
Editors: Aleksandra Nina, Snežana Dragović, Maja Kuzmanoski, Milan Đorđević, and Mrđan Đokić

Original scientific paper
Abstract

THE COUPLING PHENOMENA AND MECHANISMS BETWEEN EARTH INTERIOR EVENTS AND SPACE ENVIRONMENT

Xuhui SHEN[1,2,3*], Xuemin ZHANG[1,4], Shufan ZHAO[1], Qinqin LIU[1], Wenxiu LIU[1], Yatong CUI[1]

[1]National Space Science Center of CAS, Beijing, China;
e-mails: shenxuhui@nssc.ac.cn, zxm@ief.ac.cn, zsf2008bj@126.com, liuqinqin@nssc.ac.cn, liuwenxiu@nssc.ac.cn, cuiyatong@nssc.ac.cn
[2]College of Advanced Interdisciplinary Studies, National University of Defence Technology, Changsha, China; e-mail: shenxuhui@nssc.ac.cn
[3]College of Science and Technology of Emergency Management, University of CAS, Beijing, China; e-mail: shenxuhui@nssc.ac.cn
[4]Institute of Earthquake Forecasting of CEA, Beijing, China; e-mail: zxm@ief.ac.cn

In the last 20 years, China launched the CSES (China Seismo-Electromagnetic Satellit) mission, High resolution RS Observation and CMP (Chinese Meridian Program) and acquired a significant amount of data related to natural hazards, space weather, as well as their coupling processes. By checking all these data using both event analysis and statistical research, we reach the understanding that most of the large natural hazard activities may cause significant disturbance in the atmosphere and ionosphere. The statistical results show that the temporal-spatial distribution features of ionospheric disturbance before earthquake occurrence are as follows: 1) main disturbance parameters are geomagnetic field, ULF/ELF/VLF electromagnetic waves, ionospheric plasma and charged particles; 2) the related precursors usually occur a few hundred kilometers away from the epicenter; 3) the related precursors usually occur a few days before the event's occurrence; and 4) the probability of these kinds of precursors may be more than 60% before an earthquake with M$\geqslant$6. Based on the preliminary understanding above, we try to develop the mechanisms to understand how these signals below ground propagate up into the ionosphere. In general, strong underground activities, such as earthquakes and volcanic eruptions, may release large amounts of matter and energy to the surface. These emissions of matter and energy could spread into the atmosphere and some may penetrate into the ionosphere by the following three main mechanisms: electromagnetic waves propagation and electrodynamics, acoustic gravity waves propagation and fluid dynamics, as well as geochemistry spreading and thermodynamics. We are currently developing a new project of ground-based IMCP (International Meridian Circle Program), to promote the integrated observation and research of the lithosphere-atmosphere-ionosphere coupling mechanisms as well as their impacts on natural hazard mitigation and global change tendency.

**Corresponding author*

Acknowledgements

This work was supported by the China National Space Administration (CNSA), the Ministry of Sciences and Technologies of China (MOST), Chinese Academy of Sciences (CAS), China Earthquake Administration (CEA) as well as the cooperation with Italian Space Agency (ASI) and European Space Agency (ESA).

References

Shen, X. H., Zhang, X. M., Yuan, S. G. et al. (2018). *Sci. China. Tech. Sci.*, 61, 634.
Shen, X., Zeren, Z., Yuan, S. et al. (2020). *Aerosp. China*, 21(1), 5.
Qinqin, L., Lu, G., Jianqiang, L. et al. (2023). *Remote Sens.,* 15, 2661.
Shufan, Z., Xuhui, S., Chen, Z. et al. (2023). *Front. Astron. Space Sci.* 10, 1335615.
Shufan, Z., Xuhui, S., Chen, Z. et al. (2020). *Results Phys.,* 18, A08310.
Shen, X., Huang, J., Lin, J. et al. (2022). *Prog. Earthq. Sci.* 52(1), 1.
Shen, X. H., Zhang, X. M., Hong, S. Y. et al. (2013). *Earthq. Sci.,* 26(6), 427.
Shen, X., Yuan, S., and Zeren, Z. (2023). *Space Int.*, 2023(3), 31.
Zhang, X., Frolov, V., Shen, X. et al. (2020). *Radio Sci.*, 55(8), e2019RS007040.
Li, M., Shen, X., Parrot, M. et al. (2020). *J. Geophys. Res. - Space*, 125(12), e2020JA028116.
Shen, X., Zhang, X., Cui, J. et al. (2018). *J. Remote Sens.*, 22, 1.

GeosciRA25

Book of Abstracts and Contributed Papers
International Conference on Recent Trends in Geoscience Research and Applications 2025 Belgrade, Serbia and Virtual, 15–19 September 2025
Editors: Aleksandra Nina, Snežana Dragović, Maja Kuzmanoski, Milan Đorđević, and Mrđan Đokić

Original scientific paper
Abstract

MITIGATION OF TORRENTIAL HAZARDS IN A TYPICAL ALPINE CATCHMENT IN SLOVENIA

Nejc BEZAK[1*], Maximilian KRAMER[2], Sascha SCHULTES[2], Jošt SODNIK[1,3], Klemen KOZMUS TRAJKOVSKI[1], Matjaž MIKOŠ[1]

[1]University of Ljubljana, Faculty of Civil and Geodetic Engineering, Ljubljana, Slovenia; e-mails: nejc.bezak@fgg.uni-lj.si, jost.sodnik@tempos.si, klemen.kozmus-trajkovski@fgg.uni-lj.si, matjaz.mikos@fgg.uni-lj.si
[2]Geobrugg AG, Romanshorn, Switzerland; e-mails: maximilian.kramer@geobrugg.com, sascha.schultes@geobrugg.com
[3]Tempos, Environmental Engineering, Ljubljana, Slovenia; e-mail: jost.sodnik@tempos.si

Various sediment-related disasters such as flash floods, debris flows and landslides can occur in Alpine areas. To protect built infrastructure and human lives, various structural and non-structural (grey, green and hybrid infrastructure) protection measures can be used. Within this presentation, an overview is provided about the mitigation measures implemented near the Krvavec ski resort in north-western Slovenia. In May 2018, an extreme debris flood occurred in this area, causing considerable economic damage and leading to intense erosion and sediment transport processes. After the May 2018 event, various field investigations (e.g., geological and topographical surveys) and modeling applications (e.g., hydrological modeling, debris flow) were carried out to obtain the required input data for the design of mitigation measures. Mitigation measures include the river engineering works at local streams, the construction of a large silt check dam for sediment retention, the construction of several smaller retention dams and the construction of 16 flexible net barriers with an estimated retention volume of around 8000 m^3. A comprehensive monitoring system was also set up in the study area to observe and monitor potential future extreme events. The August 2023 extreme flood event also caused damage in this part of Slovenia. The results of this abstract show that the flexible net barriers were able to retain large amounts of sediments and protect downstream infrastructure despite the extreme rainfall with a return period of over 250 years. High impacts were detected by monitoring devices installed on flexible net barriers. Due to the installation of flexible net barriers,he erosion and sediment transport dynamics in the investigated area decreased. The presence of flexible net barriers also altered the natural deposition process by trapping material and slowing the flow and leading to sediment deposition.

Acknowledgements

This work was partly supported by the Interreg TORRENT project, the UNESCO Chair on Water-related Disaster Risk Reduction and research projects P2-0180, J6-4628, N2-0313 (Slovenian Research and Innovation Agency).

**Corresponding author*

Book of Abstracts and Contributed Papers
International Conference on Recent Trends in Geoscience Research and Applications 2025 Belgrade, Serbia and Virtual, 15–19 September 2025
Editors: Aleksandra Nina, Snežana Dragović, Maja Kuzmanoski, Milan Đorđević, and Mrđan Đokić

Original scientific paper
Abstract

THE ANNOUNCEMENT OF THE LONG-TERM PROBABILITY OF A "MAJOR EARTHQUAKE" OCCURRING IN JAPAN AND THE SOCIAL IMPACT OF "AMBIGUOUS" INFORMATION ANNOUNCED WHEN THE PROBABILITY OF OCCURRENCE BECOMES RELATIVELY HIGH

Toshiyasu NAGAO[1*]

[1]*Institute of Oceanic Research and Development, Tokai University, Shizuoka, Japan; e-mail: toshi.nagao@gmail.com*

In Japan, the government publishes the long-term probability of earthquakes (30-year probability) based on the geological active fault investigation. This reflects the consensus among seismologists that “earthquakes can only be predicted in the long term,” therefore, the government does not issue any short-term earthquake prediction information. In the past, the Seismological Society of Japan (SSJ) had a committee named "earthquake prediction", but in 2014, the committee was abolished because the name “prediction” could lead to misunderstandings that prediction was possible. Considering this situation, the Earthquake Prediction Society of Japan was established in 2014, and the current presenter serves as its representative. At present, instead of prediction information, a system has been established to issue “Special Information on the Nankai Trough Mega-Earthquake,” which is expected to affect more than half of Japan. This system was launched in 2019 and was first announced in August 2024, causing significant confusion throughout Japan. In the presentation, I will explain the impact of this “Special Information” and the basis on which it is issued. Internationally, however, short-term earthquake prediction research has made significant progress. In 2001, EMSEV (Electromagnetic Studies of Earthquakes and Volcanoes) was established within the IUGG, based on the IAGA/IASPEI/IAVCEI. EMSEV focuses particularly on electromagnetic precursor phenomena research, and statistically significant phenomena have been discovered even through satellite-based observations of precursory phenomena. In this presentation, I will also introduce the activities of EMSEV.

*Corresponding author

GeosciRA25

Book of Abstracts and Contributed Papers
International Conference on Recent Trends in Geoscience Research and Applications 2025 Belgrade, Serbia and Virtual, 15–19 September 2025
Editors: Aleksandra Nina, Snežana Dragović, Maja Kuzmanoski, Milan Đorđević, and Mrđan Đokić

Original scientific paper
Abstract

DELTASENSE: AFRICA'S REMOTE SENSING GUARDIAN OF LANDSCAPE DEGRADATION

Ivan LIZAGA[1,2*], Borja LATORRE[3], Montfort BAGALWA[4], Landry CIZUNGU[5], Joseph OKELLO[6], Muhumuza MOSES[6], Linus MUNISHI[7], Kristof VAN OOST[8], William BLAKE[9], Ana NAVAS[3], Pascal BOECKX[2]

[1]Instituto Pirenaico de Ecología (IPE-CSIC), Spanish National Research Council, Zaragoza, Spain; e-mail: ivan.lizaga@ugent.be
[2]Isotope Bioscience Laboratory - ISOFYS, Department of Green Chemistry and Technology, Ghent University, Gent, Belgium; e-mails: ivan.lizaga@ugent.be, pascal.boeckx@ugent.be
[3]Estación Experimental de Aula-Dei (EEAD-CSIC), Spanish National Research Council, Zaragoza, Spain; e-mails: borja.latorre@csic.es, anavas@eead.csic.es
[4]Service Environnement, Observatoire Volcanologique de Goma (OVG), Goma, Democratic Republic of Congo; e-mail: montfortbagalwa2021@gmail.com
[5]Université catholique de Bukavu (UCB), Bukavu, Democratic Republic of the Congo; e-mail: landrycizunngu@gmail.com
[6]Mountains of The Moon University (MMU), Fort Portal, Uganda; e-mails: joseph.okello@mmu.ac.ug, mmuhumuza@mmu.ac.ug
[7]School of Life Sciences and Bio-Engineering, The Nelson Mandela-African Institute of Science and Technology (NM-AIST), Arusha, Tanzania; e-mail: linus.munishi@nm-aist.ac.tz
[8]Earth and Life Institute, UCLouvain, Louvain-la-Neuve, Belgium; e-mail: kristof.vanoost@uclouvain.be
[9]School of Geography, Earth and Environmental Sciences, University of Plymouth, Plymouth, UK; e-mail: william.blake@plymouth.ac.uk

Land degradation across East Africa continues to threaten ecological stability and livelihoods. While traditional monitoring approaches often focus on direct land-use changes, they tend to overlook subtle yet critical indicators of environmental disruption. Our newly developed tool, DeltaSense, introduces a novel strategy by leveraging inland lake deltas as natural integrators of landscape processes, providing an early warning system for regional degradation dynamics. Building upon a successful pilot in the Lake Kivu region, this newly funded initiative now scales up across the Democratic Republic of the Congo, Uganda, Burundi, Tanzania, and Mozambique. The system integrates multi-decadal satellite time series with in-situ observations, ranging from UAV imagery to bathymetric surveys, allowing degradation to be assessed across temporal and spatial gradients. Key partnerships with regional institutions such as OVG, UCB, RWB, MMU, and NM-AIST enable local co-development of the tool and enhanced data interpretation, fostering both technical capacity and long-term sustainability. By analysing over 40

*Corresponding author

years of delta dynamics alongside present-day satellite imagery, DeltaSense captures the impacts of land-use change, conflict, and resource extraction. Recent analyses in Uganda revealed sedimentation anomalies downstream of a newly established gold mine, which were later confirmed through field campaigns and water sampling in a contaminated lake. These results highlight the platform's utility for rapid identification and on-the-ground verification of degradation events. In addition to its scientific and diagnostic value, DeltaSense offers an open-access web platform that allows users such as researchers, decision-makers, and local communities alike to visualise historical trends, monitor ongoing changes, and receive early alerts on abrupt upstream disturbances. This reinforces its potential as a decision-support tool for sustainable landscape and resource management.

GeosciRA25

Book of Abstracts and Contributed Papers
International Conference on Recent Trends in Geoscience Research and Applications 2025 Belgrade, Serbia and Virtual, 15–19 September 2025
Editors: Aleksandra Nina, Snežana Dragović, Maja Kuzmanoski, Milan Đorđević, and Mrđan Đokić

Original scientific paper
Abstract

THE IONOSPHERE AS A SENSITIVE INDICATOR AND MEDIUM OF GEOSPHERES' INTERACTION

Sergey PULINETS[1*], Konstantin TSYBULYA[2], Nadezhda KOTONAEVA[2]

[1]Space Research Institute, Russian Academy of Sciences (IKI), Moscow, Russia;
e-mail: pulse@cosmos.ru
[2]Fedorov Institute of Applied Geophysics (IPG), Moscow, Russia;
e-mails: kgc@ipg.geospace.ru, kotonaeva@ipg.geospace.ru

The duality of the ionosphere's properties as a medium makes it an important player in the chain of processes of the geospheres' interaction. Being the upper part of atmosphere, it conserves the main features of atmospheric dynamics, but on the other hand, being a conductive medium, it is strongly controlled by magnetospheric processes. It converts the energy of the solar wind and magnetospheric currents into the large-scale movements of matter in the form of travelling ionospheric disturbances (TID) and acoustic gravity waves (AGW), heat release and inducing the currents in the Earth's crust. Simultaneously it "works" as a sensor reacting on the processes in the atmosphere (hurricanes, sand storms, volcano eruptions) and on the underground activity in the form of earthquake preparation processes. Earthquakes and tsunamis induce large-scale wave movements of different nature in the ionosphere. It means that monitoring the ionospheric parameters and their dynamics, we can get information on a variety of processes in the atmosphere and magnetosphere. In this regard the creation of the Ionozond 2025 constellation consisting of four Ionosphere-M satellites with topside sounder onboard will be an important contribution to the geospheres' interaction studies. The results obtained during the first months of Ionozond 2025 constellation activity will be reported.

Acknowledgements

The work was supported by the Ministry of Science and Higher Education of the Russian Federation (theme "Monitoring", state registration No. 122042500031-8).

*Corresponding author

GeosciRA25

Book of Abstracts and Contributed Papers
International Conference on Recent Trends in Geoscience Research and Applications 2025 Belgrade, Serbia and Virtual, 15–19 September 2025
Editors: Aleksandra Nina, Snežana Dragović, Maja Kuzmanoski, Milan Đorđević, and Mrđan Đokić

Original scientific paper
Abstract

MESOSPHERIC OZONE DEPLETION UNDER SOLAR AND GEOMAGNETIC FORCING IN 2024

Irina MIRONOVA[1*]

[1]*St. Petersburg State University, St. Petersburg, Russia; e-mail: i.a.mironova@spbu.ru*

In 2024, a series of solar eruptive events occurred that resulted in powerful geomagnetic disturbances. An extreme geomagnetic storm was recorded on May 10–11, 2024 and became the most powerful geomagnetic event according to the Dst index over the last two solar activity cycles since the geomagnetic storms in 2003. Several more powerful geoeffective solar events resulted in geomagnetic storms in March, June, and October. All events were accompanied by precipitation of high-energy electrons and protons, which in turn affected variations in the winter composition of the upper and middle atmosphere/ionosphere. The paper presents the latitude-longitude distribution of precipitation of energetic particles, electrons, and protons with energies greater than 40 keV, the estimates of which are important for studying the reaction of the inner ionosphere, upper and middle atmosphere during geomagnetic disturbances. The paper presents analyzed fluxes of protons and energetic electrons obtained from the POES satellites (METOP01, METOP03, NOAA15, NOAA18 and NOAA19) during events associated with solar eruptive and geomagnetic events in 2024. Here, we also evaluate the vulnerability of the ozone layer to space weather processes. Seasonal and latitudinal effects of ozone depletion linked to strong geomagnetic storms and geoeffective solar events are considered separately.

Acknowledgements

The authors acknowledge Saint-Petersburg State University for a research project 124032000025-1.

*Corresponding author

INVITED PROGRESS REPORTS

GeosciRA25

Book of Abstracts and Contributed Papers
International Conference on Recent Trends in Geoscience Research and Applications 2025 Belgrade, Serbia and Virtual, 15–19 September 2025
Editors: Aleksandra Nina, Snežana Dragović, Maja Kuzmanoski, Milan Đorđević, and Mrđan Đokić

Original scientific paper
Abstract

PERTURBATIONS OF VLF RADIO SIGNALS DUE TO LEP EFFECT MONITORED IN BELGRADE - A CASE STUDY

Aleksandra KOLARSKI[1*]

[1]*Institute of Physics Belgrade, National Institute of the Republic of Serbia, University of Belgrade, Belgrade, Serbia; e-mail: aleksandra.kolarski@ipb.ac.rs*

A typical amplitude (A) and phase (P) perturbations of Very Low Frequency (3-30 kHz) radio signals related to Lightning induced Electron Precipitation (LEP) process is analyzed and presented here as a case study event. LEP event-induced variations in A & P, characteristic in their amount, duration and pattern, were recorded by the Absolute Phase and Amplitude Logger narrowband receiving system located in Belgrade (Serbia). The LEP effect simultaneously occurred on five VLF signals in total, emitted from four European and one American transmitter. The related perturbation was modeled through numerical simulations to assess related electron density changes within the altitude range corresponding to the nocturnal mid-latitude lower ionospheric D region over the central European sector. These changes affected propagation of monitored VLF signals transmitted subionospherically within the Earth-ionosphere waveguide. Through the application of the LWPCv21 numerical routine, by adjusting the parametrization of perturbed ionospheric profiles in iterative approximations, regions of enhanced ionization along the Great Circle Paths of monitored VLF signals were identified and located. This enabled positioning of the causative Localized Ionospheric Enhancement and the determination of its spatial and structural features.

Acknowledgements

The author acknowledges funding provided by the Institute of Physics Belgrade through the grant by the Ministry of Science, Technological Development and Innovation of the Republic of Serbia. Author thanks Prof. D. Šulić for instrumental set-up.

*Corresponding author

PROGRESS REPORTS

GeosciRA25

Book of Abstracts and Contributed Papers
International Conference on Recent Trends in Geoscience Research and Applications 2025 Belgrade, Serbia and Virtual, 15–19 September 2025
Editors: Aleksandra Nina, Snežana Dragović, Maja Kuzmanoski, Milan Đorđević, and Mrđan Đokić

Original scientific paper
Abstract

CLIMATOLOGY OF CLOUDS AT AN ACTRIS STATION IN THE SE EUROPE

Mirela VOICULESCU[1*], Adrian ROȘU[1], Daniel CONSTANTIN[1], Cătălin NEGOIȚĂ[1]

[1]Faculty of Sciences and Environment, REXDAN RI, University Dunărea de Jos of Galați, Galați, Romania; e-mails: mirela.voiculescu@ugal.ro, adrian.rosu@ugal.ro, daniel.constantin@ugal.ro, c.negoita@ugal.ro

The Aerosol, Clouds and Trace Gases Research Infrastructure (ACTRIS) is a European distributed research infrastructure which got an ERIC (European Research Infrastructure Consortium) status in April 2023. The Cloud Remote Sensing Station (CCRES) in Galati (RADO-Galati) is part of the REXDAN Research Infrastructure at the University Dunarea de Jos of Galati, Romania (e.g. www.rexdan.ugal.ro). The station is equipped with five equipment that started to work synergistically as a cloud observation platform at the beginning of February 2022: cloud radar (RPG, dual polarization, FMCW, operating at 94 GHz), multichannel microwave radiometer (RPG HAPTRO), ceilometer (LUFFT backscatter lidar), disdrometer (Parsivel) and a built in meteorological station that includes a rain gauge (Thies Clima). All equipment is set on an open terrace at about 10 m height (40 m ASL). All instruments work on a continuous basis and feed the Cloudnet site with live data. Based on three years of data (2022-2024), a climatology of the clouds is presented, along with other characteristics.

Acknowledgements

Support from the project “Operational support for Romanian research national facilities of ACTRIS ERIC", PCIDIF/144/PCIDIF_P1/OP1/RSO1.1/PCIDIF_A3, Smis 309113, is acknowledged. Ewan O'Connor, Simo Tukiainen are acknowledged for the Cloudnet processing suite. ECMWF is acknowledged for providing IFS model data. ACTRIS (RADO – Galati, part of REXDAN RI) and Finnish Meteorological Institute are acknowledged for providing data sets, available for download from https://cloudnet.fmi.fi.

*Corresponding author

GeosciRA25

Book of Abstracts and Contributed Papers
International Conference on Recent Trends in Geoscience Research and Applications 2025 Belgrade, Serbia and Virtual, 15–19 September 2025
Editors: Aleksandra Nina, Snežana Dragović, Maja Kuzmanoski, Milan Đorđević, and Mrđan Đokić

Original scientific paper
Abstract

LOCAL MAGNETIC FIELD CHANGES ON THE ADRIATIC TECTONIC MICROPLATE

Rudi ČOP[1*]

[1]*Institute Terra Viva, Sečovlje, Slovenia; e-mail: rudi@artal.si*

The Adriatic tectonic microplate is an ideal natural geophysical laboratory due to its location and exploration (Kiraly et al, 2018; Kissling, 2024). The magnetic field measured on it contains a very high level of noise compared to measurements on the neighboring Eurasian tectonic plate (Čop et al, 2011; Čop, 2025). The sources of this noise discovered so far are the passage of weather fronts MCS *(mesoscale convective system) (*Čop et al, 2014; Čop, 2015) and the change in the position of the Moon in relation to the Earth (Kuhar et al, 2020). The sources of the noise are also the tensions of Adriatic tectonic microplate. This noise increases significantly in the period before earthquakes or volcanic eruptions occurring on or within its immediate vicinity (Čop et al, 2021). The change in the tension of the Adriatic tectonic microplate is predominantly in the direction of the vertical component of the geomagnetic field. Influences from space are detected mainly in the horizontal plane. A strong geomagnetic storm of category G5, the initial phase of which was registered on May 11, 2024, is among the twenty strongest magnetic storms in the last 500 years. From the magnetograms measured at the PIA geomagnetic observatory (Piran, Slovenia), we calculated the standard geomagnetic indices K and A. The indices do not fully describe the effects of the geomagnetic storm. Therefore, we calculated the change in the energy density of the geomagnetic field for each day and checked its usefulness. The obtained results served us well as a reference for all previous and also for future exceptional events in the local magnetic field measured on the Adriatic tectonic microplate. In addition, the influence of the Solar Weather on the lithosphere as well as on the biosphere (Čop and Jere Jakulin, 2022) is better defined with the help of the change in energy density.

References

Čop, R. (2015). *Geosci. Instrum. Method. Data Syst.*, 4, 155.

Čop, R. (2025). Zemljino magnetno polje in njegovo opazovanje v Sloveniji. The Earth's magnetic field and its observation in Slovenia (in Slovenian). *Alternator. Misli znanosti.* https://doi.org/10.3986/alternator.2025.08

Čop, R., Deželjin, D., Mihajlović, J. S. et al. (2011). *Elektroteh. Vestn. (English Edition)*, 78(3), 96.

Čop, R., Milev, G., Deželjin, D. et al. (2014). *Geosci. Instrum. Methods Data Syst.*, 3, 135.

Čop, R., Rasson, L. J., and Bilc, A. (2021). *Open J. Earthq. Res.*, 10, 95.

Čop, R., and Jere Jakulin, T. (2022). *Int. J. Qual. Res.*, 16(3), 703.

Kiraly, A., Faccenna, C., and Funiciello, F. (2018). *Tectonics*, 37, 3941.

Kissling, E. (2024). *Ann. Geophys.*, 67(4), S431.

Kuhar, M., Čop, R., and Pavlovčič Prešeren, P. (2020). *Geod. Vestn.*, 64(2), 30.

*Corresponding author

GeosciRA25

Book of Abstracts and Contributed Papers
International Conference on Recent Trends in Geoscience Research and Applications 2025 Belgrade, Serbia and Virtual, 15–19 September 2025
Editors: Aleksandra Nina, Snežana Dragović, Maja Kuzmanoski, Milan Đorđević, and Mrđan Đokić

Original scientific paper
Abstract

IONOSPHERIC VARIATIONS IN THE SOLAR CYCLE 25 INFERRED FROM VLF/LF ELECTRIC FIELD MEASUREMENTS

Hans U. EICHELBERGER[1*], Aleksandra NINA[2], Mohammed Y. BOUDJADA[1], Pier Francesco BIAGI[3], Maria SOLOVIEVA[4], Patrick H. M. GALOPEAU[5], Iren-Adelina MOLDOVAN[6], Giovanni NICO[7], Aleksandra KOLARSKI[2], Nikola VESELINOVIĆ[2], Vladimir SREĆKOVIĆ[2], Manfred STACHEL[1], Bruno P. BESSER[1]

[1]Space Research Institute, Austrian Academy of Sciences, Graz, Austria;
e-mails: hue@oeaw.ac.at, mohammed.boudjada@oeaw.ac.at,
manfred.stachel@oeaw.ac.at, bruno.besser@oeaw.ac.at
[2]Institute of Physics Belgrade, National Institute of the Republic of Serbia, University of Belgrade, Belgrade, Serbia; e-mails: sandrast@ipb.ac.rs,
aleksandra.kolarski@ipb.ac.rs, veselinovic@ipb.ac.rs, vlada@ipb.ac.rs
[3]Department of Physics, University of Bari, Bari, Italy; e-mail: pf.biagi@gmail.com
[4]Schmidt Institute of Physics of the Earth, RAS, Moscow, Russia;
e-mail: mcsolovieva@gmail.com
[5]LATMOS-CNRS, UVSQ Université Paris-Saclay, Guyancourt, France;
e-mail: patrick.galopeau@latmos.ipsl.fr
[6]National Institute for Earth Physics, Magurele, Romania;
e-mail: irenutza_67@yahoo.com
[7]Institute of Applied Mathematics, National Research Council, Bari, Italy;
e-mail: giovanni.nico@cnr.it

In this study we investigate electric field amplitude variations between narrowband very low- and low-frequency (VLF/LF) transmitters and receivers related to X-class solar flares since the beginning of the solar cycle 25. These VLF/LF (3 kHz – 300 kHz) radio signals which propagate in the Earth's waveguide, defined by the lithosphere and lower ionosphere (D/E-layer during day/night), are sampled with ground-based receivers from the International Network for Frontier Research on Earthquake Precursors (INFREP) network (Biagi et al., 2019; Moldovan et al., 2015; Galopeau et al., 2023). The remote sensing of processes within the VLF/LF cavity (Nina, 2022; Kolarski and Grubor, 2014) allows us to investigate the consequence of solar x-ray outbursts on the ionospheric D- and E-layers. The considered x-ray fluxes data are from NOAA GOES satellites. We compare amplitude and phase measurements from VLF/LF transmitter-receiver ray paths, in time- and frequency-domain, with 86 X-class solar flares related excitations from 71 days in the time span July 2021 to June 2025. The scientific objective is to enhance our understanding of VLF/LF waveguide dynamics and establish

*Corresponding author

benchmarks for the comprehension of physical excitation processes at the origin of electric field amplitude disturbances generated by solar x-rays. We emphasize and underscore in this analysis the importance related changes in the lower ionosphere. This leads us to open up prospects for an automated real-time monitoring and characterization of the connection between solar activity and the Earth's ionosphere plasma environment.

Acknowledgements

The authors acknowledge the support provided by the Ministry of Science, Technological Development and Innovation of the Republic of Serbia (projects 337-00-216/2023-05/188) and the Austrian Federal Ministry of Women, Science and Research (BMFWF) (project no. RS 22/2024). This work was carried out in the frame of the Serbian Austrian bilateral project. The authors acknowledge funding provided by the Institute of Physics Belgrade through the grant by the Ministry of Science, Technological Development and Innovation of the Republic of Serbia.

References

Biagi, P. F., Colella R., Schiavulli L. et al. (2019). *Open J. Earthq. Res.*, 8, 101.

Galopeau, P. H. M., Maxworth, A.S. Boudjada, M.Y. et al. (2023). *Geosci. Instrum. Methods Data Syst.*, 12, 231.

Moldovan, I. A., Constantin A.P., Biagi P. F. et al. (2015). *Rom. J. Phys.*, 60(7-8), 1203.

Nina, A. (2022). *Remote Sens.,* 14, 54.

Kolarski, A., Grubor, D. (2014). *Adv. Space Res.*, 53(11), 1595.

Book of Abstracts and Contributed Papers
International Conference on Recent Trends in Geoscience Research and Applications 2025 Belgrade, Serbia and Virtual, 15–19 September 2025
Editors: Aleksandra Nina, Snežana Dragović, Maja Kuzmanoski, Milan Đorđević, and Mrđan Đokić

Original scientific paper
Abstract

MAGNETIC MOMENT OF THE HELIOSPHERIC CURRENT SHEET

Roman KISLOV[1*]

[1]*Pushkov institute of terrestrial magnetism, ionosphere and radio wave propagation of the Russian academy of sciences (IZMIRAN), Moscow, Russia; e-mail: kr-rk@bk.ru*

The heliospheric current sheet (HCS) is a separator between regions with opposite polarities of the interplanetary magnetic field in the solar wind. HCS can be approximately regarded as a giant disk with a current and corresponding magnetic moment. The magnitude of the current depends on interplanetary magnetic field components and their spatial distribution. We estimate magnetic moment of the HCS using two methods. In the first method we calculate the total current of HCS using spatial distribution of the interplanetary magnetic field from multi-spacecraft observations (Khabarova and Obridko, 2012; Khabarova, 2013) performed during solar activity minima. In the second method the total current can be calculated within framework of different models of the interplanetary magnetic field (Parker, 1958; Kislov et al., 2015; Kislov et al., 2019). It was found that regardless of the method used for the interplanetary magnetic field calculation, the total magnetic moment of the heliospheric current sheet exceeds the solar dipole magnetic moment by several orders of magnitude during solar activity minimum. This result leads to hypothesis that the Sun and the HCS should be considered as couple interacting object. We illustrate this idea by estimations of possible effect of the interaction in the global heliospheric current circuit proposed by Alfvén (Alfvén, 1977).

References

Alfvén, H. (1977). *Rev. Geophys. Space Phys.*, 15(3), 271.
Khabarova, O., and Obridko, V. (2012). *Astrophys. J.*, 761(2), 82.
Khabarova, O. (2013). *Astron. Rep.*, 57(11), 844.
Kislov, R. A., Khabarova, O. V., and Malova, H. V. (2015). *J. Geophys. Res. - Space,* 120(10), 8210.
Kislov, R. A., Khabarova, O. V., and Malova, H. V. (2019). *Astrophys. J.*, 875(1), 28.
Parker, E. N. (1958). *Astrophys. J.*, 128, 664.

*Corresponding author

Book of Abstracts and Contributed Papers
International Conference on Recent Trends in Geoscience Research and Applications 2025 Belgrade, Serbia and Virtual, 15–19 September 2025
Editors: Aleksandra Nina, Snežana Dragović, Maja Kuzmanoski, Milan Đorđević, and Mrđan Đokić

Original scientific paper
Abstract

CHARACTERIZATION OF DIURNAL AND SEASONAL VARIABILITY OF IONOSPHERIC TEC OVER THE INDIAN EQUATORIAL REGION USING GPS OBSERVATIONS

Lekshmi O NAIR[1*], Lijo JOSE[2]

[1]Mahatma Gandhi University Kottayam, Kerala, India;
e-mail: lekshmikochuchira@gmail.com
[2]St. Berchmans College, Changanassery, India; e-mail: lijojosek@gmail.com

The Indian low-latitude ionospheric region, particularly over Bangalore (13.0°N, 77.6°E), exhibits strong temporal variability driven by complex electrodynamic processes such as the Equatorial Ionization Anomaly (EIA), Equatorial Electrojet (EEJ), and Equatorial Plasma Bubbles (EPBs) (Kelley, 2009). These phenomena significantly affect trans-ionospheric radio signal propagation, impacting satellite-based navigation and communication systems. This study investigates the diurnal and seasonal behaviour of Vertical Total Electron Content (VTEC) over Bangalore using dual-frequency GPS data extracted from RINEX observation files processed via the Gopi TEC toolbox. The analysis covers key seasonal months March, June, September, and December during the solar maximum period of 2013 to 2014, when ionospheric activity is enhanced (Arons, 1993). Slant TEC data are mapped to vertical TEC using appropriate mapping functions, and elevation filtering is applied to minimize multipath errors. The results show a clear diurnal pattern, with a post-sunrise increase, a noon-time maximum, and a post-sunset decline in VTEC. Seasonal differences are evident, with equinoctial months showing stronger TEC enhancements due to favourable solar and electrodynamic conditions. Signatures of EPBs are identified as post-sunset VTEC depletions on several equinoctial days, consistent with equatorial irregularity behaviour (Rama Rao, 2006). These observations demonstrate the highly dynamic nature of the equatorial ionosphere and emphasize the need for continuous TEC monitoring in this region. This study contributes valuable insights into ionospheric dynamics over the Indian sector and supports improved GNSS-based positioning, ionospheric modelling, and space weather forecasting.

Acknowledgements

The authors gratefully acknowledge the International GNSS Service for providing access to RINEX GPS data and GPS-TEC software by Gopi k Seemala.

*Corresponding author

References

Arons, J. (1993). *Space Sci. Rev.*, 63, 209.

Kelley, M. C. (2009). *The Earth's Ionosphere: Plasma Physics and Electrodynamics,* Academic Press., San Diego, CA, USA.

Rama Rao, P. V. S., Gopi, D., and Niranjan, K. (2006). *Ann. Geophys.*, 24, 3279.

GeosciRA25

Book of Abstracts and Contributed Papers
International Conference on Recent Trends in Geoscience Research and Applications 2025 Belgrade, Serbia and Virtual, 15–19 September 2025
Editors: Aleksandra Nina, Snežana Dragović, Maja Kuzmanoski, Milan Đorđević, and Mrđan Đokić

Original scientific paper
Abstract

PRELIMINARY ANALYSIS OF FORBUSH DECREASES IN OCTOBER 2024 USING OBSERVATIONS FROM BELGRADE MUON STATION

Nikola VESELINOVIĆ[1*], Mihailo SAVIĆ[1], Aleksandar DRAGIĆ[1], Dimitrije MALETIĆ[1], Dejan JOKOVIĆ[1], Radomir BANJANAC[1], Vladimir UDOVIČIĆ[1]

[1]Institute of Physics Belgrade, National Institute of the Republic of Serbia, University of Belgrade, Belgrade, Serbia; e-mails: veselinovic@ipb.ac.rs, msavic@ipb.ac.rs, dragic@ipb.ac.rs, maletic@ipb.ac.rs, yokovic@ipb.ac.rs, banjanac@ipb.ac.rs, udovicic@ipb.ac.rs

In this work, a pronounced Forbush decrease observed in October 2024, near the peak of Solar Cycle 25, is investigated. Forbush decreases are transient depressions in cosmic ray flux, typically triggered by interplanetary disturbances such as coronal mass ejections (Belov et al., 2022). During the observed period, these Forbush decreases were recorded using scintillating muon detectors at the Belgrade Muon Station, Serbia. The detectors were recently incorporated into the global gLOWCOST network of portable muon detectors (Mubashir et al, 2025), enabling the results presented here to be correlated with and compared to global muon monitoring efforts. Two sets of detector arrays, one at ground level (+75 m a.s.l.) and another at a shallow underground depth (25 m w.e.), operate continuously, measuring secondary cosmic ray muon fluxes with distinct median rigidities (Veselinović et al., 2023). This configuration permits energy-dependent analysis of cosmic ray modulation during solar transients. We performed a comparative study of muon flux variations from both detector systems, alongside in-situ interplanetary measurements, including solar wind proton flux at Lagrange Point 1 and in near-Earth space. The characteristics of the Forbush decreases were evaluated to quantify their relationship with solar wind structures and geomagnetic conditions. This integrated approach provides a more comprehensive assessment of how large-scale solar eruptions influence the modulation of galactic cosmic rays, with broader implications for understanding solar-terrestrial coupling processes and space weather forecasting.

Acknowledgements

The authors acknowledge funding provided by the Institute of Physics Belgrade through the grants by the Ministry of Science, Technological Development and Innovation of the Republic of Serbia

**Corresponding author*

References

Belov, A., Shlyk, N., Abunina, M. et al. (2022). *Universe*, 8, 403.

Veselinović, N. B., Savić, M. B., Maletić, D. M. et al. (2023). *Contrib. Astron. Obs. Skaln.*, 53(3), 148.

Mubashir A., Ashok A., Connors M. et al. (2025). *Adv. Space Res*., Available online

GeosciRA25

Book of Abstracts and Contributed Papers
International Conference on Recent Trends in Geoscience Research and Applications 2025 Belgrade, Serbia and Virtual, 15–19 September 2025
Editors: Aleksandra Nina, Snežana Dragović, Maja Kuzmanoski, Milan Đorđević, and Mrđan Đokić

Original scientific paper
Abstract

OPTIMIZATION OF OBSERVATION TIME IN PRECISE POINT POSITIONING BY COMBINING ERROR MODELS

Miloš MARKOVIĆ[1*], Dušan PETKOVIĆ[2], Miljana TODOROVIĆ DRAKUL[2], Stefan KRSTIĆ[2]

[1]Academy of Technical and Artistic Vocational Studies, Department for Civil Engineering and Geodesy, Belgrade, Serbia; e-mail: milmarkovic85@gmail.com
[2]Faculty of Civil Engineering, Department of Geodesy and Geoinformatics, University of Belgrade, Belgrade, Serbia; e-mails: dpetkovic@grf.bg.ac.rs, mtodorovic@grf.bg.ac.rs, skrstic@grf.bg.ac.rs

This study addresses the optimization of observation duration within the Precise Point Positioning (PPP) technique, focusing on determining the minimal observation time required to achieve stable and accurate coordinate solutions while accounting for various error sources, such as precise ephemerides and satellite clock files. The numerical analysis was conducted using the Bernese GNSS Software, applying different processing scenarios that included four types of ephemerides (CODE, IGS, IGR, and IGU) and clock files with sampling intervals of 5 and 30 seconds. Observations were collected from three permanent GNSS stations over a multi-year period (2017–2019) and all results were expressed within the IGS14 reference frame. The processed data were organized into three datasets, enabling a comprehensive evaluation of the influence of ephemeris quality, seasonal stability and temporal dynamics of coordinate convergence. The results demonstrate a clear convergence trend dependent on both the quality of ephemerides and the length of the observation session, while the inclusion of high-rate clock products (5-second intervals) should further improve positioning precision under certain conditions. These findings provide valuable insights into the optimization of observation strategies in scientific and technical GNSS applications, allowing for more efficient planning of observation durations without compromising the accuracy of positioning results. The study thus contributes to the rationalization of data acquisition processes in geodetic and geophysical surveys, where efficient resource utilization is often critical.

*Corresponding author

GeosciRA25

Book of Abstracts and Contributed Papers
International Conference on Recent Trends in Geoscience Research and Applications 2025 Belgrade, Serbia and Virtual, 15–19 September 2025
Editors: Aleksandra Nina, Snežana Dragović, Maja Kuzmanoski, Milan Đorđević, and Mrđan Đokić

Original scientific paper
Abstract

GEOID MODELING BASED ON GLOBAL GEOPOTENTIAL MODELS AND DIGITAL TERRAIN MODELS

Marko STANKOVIĆ[1*], Sanja GREKULOVIĆ[2], Danilo JOKSIMOVIĆ[3], Sofija NAOD[4]

[1]Geodetic Technical Secondary School, Belgrade, Serbia; e-mail: stankovic.d.marko@gmail.com
[2]Department of Geodesy and Geoinformatics, Faculty of Civil Engineering, University of Belgrade, Belgrade, Serbia; e-mail: sanjag@grf.bg.ac.rs
[3]D.O.O. Geodeting, Bijelo Polje, Montenegro; e-mail: danilo.s.joksimovic@gmail.com
[4]Department for Civil Engineering and Geodesy, Academy of Technical and Art Applied Studies Belgrade, Belgrade, Serbia; e-mail: naodsofija@vggs.rs

This paper presents a methodology for high-resolution, centimeter-accuracy geoid modeling in local areas using only publicly available data, eliminating the need for terrestrial gravity measurements. The approach synthesizes long- and short-wavelength components of the height anomaly, along with ellipsoidal correction, to efficiently determine geoid surfaces, following the remove-restore method (Barzaghi, 2016). Three test areas with varying terrain characteristics and spatial distributions of high-precision geodetic network points were selected: the Republic of Serbia, the Auvergne region in France, and the state of Colorado, USA. At each geodetic point (latitude, longitude, ellipsoidal height), three key parameters were modeled: the long-wavelength component of the height anomaly, $\zeta^{EGM2008}$, computed using the Earth Gravitational Model 2008 (EGM2008) (Pavlis et al., 2012); the short-wavelength component, ζ^{RTM}, derived from a Residual Terrain Model (RTM) (Forsberg, 1985), based on Digital Terrain Models (DTM) obtained from the Shuttle Radar Topography Mission (SRTM) (Farr and Kobrick, 2000); and the ellipsoidal correction, EC, defined with respect to the Geodetic Reference System 1980 (GRS80) (Odalović, 2010; Hofmann-Wellenhof and Moritz, 2006). The sum of these three components yielded the total modeled height anomaly, ζ^{LMQG}, representing the Local Model of the Quasi-Geoid (LMQG). A 5′×5′ regular grid, matching the EGM2008 resolution, was generated for each area, and height anomalies were computed at each grid node to derive the local geoid surface. Model validation was conducted using existing high-accuracy GPS/levelling data (Kenyeres, 2016). Three distinct external validation procedures were applied, tailored to the spatial distribution and availability of control points in each region. Validation involved four-parameter transformations and least squares estimation to assess the agreement between modeled and reference values. The results confirm that the proposed method yields accurate and reproducible geoid surfaces, achieving centimeter-level precision suitable for engineering, surveying, and mapping applications. Its particular strength lies in regions lacking terrestrial gravity data, where it provides a practical and cost-effective solution for geoid determination, relying solely on globally available geopotential models and

*Corresponding author

terrain data. Keywords: geoid modeling, global geopotential model, digital terrain model, undulation, height anomaly, residual terrain model, ellipsoidal correction.

References

Barzaghi, R. (2016). *The Remove-Restore Method*. In M. G. Sideris (Ed.), Encyclopedia of Geodesy (57). Springer International Publishing, Cham, Switzerland.

Farr, T. G., and Kobrick, M. (2000). *Eos Trans. AGU,* 81(48), 583.

Forsberg, R. (1985). *Bull. Geodesique*, 59(4), 342.

Hofmann-Wellenhof, B., and Moritz, H. (2006). *Physical Geodesy.* Springer-Verlag, Vienna, Austria.

Kenyeres, A. (2016). *GPS/Leveling*. In M. G. Sideris (Ed.), Encyclopedia of Geodesy (129). Springer International Publishing, Cham, Switzerland.

Odalović, O. (2010). *Physical Geodesy* (in Serbian). University of Belgrade, Belgrade, Serbia.

Pavlis, N. K., Holmes, S.A., Kenyon, S.C. et al. (2012). *J. Geophys. Res. Solid Earth*, 117(B4), B04406.

GeosciRA25

Book of Abstracts and Contributed Papers
International Conference on Recent Trends in Geoscience Research and Applications 2025 Belgrade, Serbia and Virtual, 15–19 September 2025
Editors: Aleksandra Nina, Snežana Dragović, Maja Kuzmanoski, Milan Đorđević, and Mrđan Đokić

Original scientific paper
Abstract

MINING, ECOSYSTEMS, AND COMMUNITY HEALTH: A ONE HEALTH APPROACH TO THE HOLISTIC IMPACTS OF ACID MINE DRAINAGE IN THE WITWATERSRAND BASIN, SOUTH AFRICA

Zeynep Ceylin ECER[1*], Vasile GRAMA[2]

[1]Firat Unıversity Faculty of Human and Social Sciences, Geography Department, Elaziğ, Turkey; e-mail: ecerzeynepceylin@gmail.com
[2]Oradea University Faculty of Geography, Tourism and Sports, Department of Geography, Tourism and Regional Planning, Oradea, Romania; e-mail: vgrama@uoradea.ro

Gold mining, while economically significant globally, is an industrial activity often associated with severe environmental challenges. The Witwatersrand Basin in South Africa, a historical epicenter of world gold production for over a century, starkly exemplifies the extensive environmental degradation resulting from such activities. Since its discovery in 1886, the basin has yielded approximately 43,500 tons of gold (around 30% of all gold mined in history) and 73,000 tons of uranium, leading to widespread and long-term impacts on the region's water resources, soil quality, air, and local ecosystems. One of the most prominent environmental consequences of mining in the Witwatersrand Basin is Acid Mine Drainage (AMD). Originating from approximately 270 tailings dams, which cover an area of 400 km² and contain an estimated 6 billion tons of pyrite waste with around 600,000 tons of residual uranium, AMD has caused severe pollution in watercourses such as the Wonderfonteinspruit. The acidic conditions and high metal concentrations created by AMD not only disrupt aquatic ecosystems but also threaten the water sources supplying drinking water to local communities. This paper employs the One Health/EcoHealth Approach to investigate the impacts of AMD from gold mining in the Witwatersrand Basin on ecosystems, human health, and societal well-being. The One Health/EcoHealth Approach considers environmental health, human health, and societal well-being as interconnected systems, evaluating their complex interactions within a holistic framework. The study undertakes an integrated examination of the impact pathways extending from ecosystem degradation to human communities, including food chain contamination, adverse health effects, and socio-economic consequences. By adopting this comprehensive perspective, the research aims to provide a deeper understanding of the multifaceted legacy of gold mining and inform strategies for mitigation and sustainable development in historically impacted regions. Keywords: Acid Mine Drainage (AMD), Gold Mining, Witwatersrand Basin, One Health, EcoHealth, Environmental Impact, South Africa, Water Pollution.

*Corresponding author

GeosciRA25

Book of Abstracts and Contributed Papers
International Conference on Recent Trends in Geoscience Research and Applications 2025 Belgrade, Serbia and Virtual, 15–19 September 2025
Editors: Aleksandra Nina, Snežana Dragović, Maja Kuzmanoski, Milan Đorđević, and Mrđan Đokić

Original scientific paper
Abstract

EXTRACTION OF GULLY BOUNDARIES IN FORESTED TERRAIN USING HIGH-RESOLUTION UAV LiDAR DATA

Milan ĐORĐEVIĆ[1*], Miloš MANIĆ[2], Mrđan ĐOKIĆ[1], Ranko DRAGOVIĆ[1], Ivana SMIČIKLAS[3], Snežana DRAGOVIĆ[3]

[1]University of Niš, Faculty of Sciences and Mathematics, Niš, Serbia;
e-mails: milan.djordjevic@pmf.edu.rs, mrdjan.djokic@pmf.edu.rs, dragovicr@pmf.ni.ac.rs
[2]University of Belgrade, Faculty of Geography, Belgrade, Serbia;
e-mail: dd18011@studenti.gef.bg.ac
[3]"VINČA" Institute of Nuclear Sciences - National Institute of the Republic of Serbia, University of Belgrade, Belgrade, Serbia; e-mails: ivanat@vin.bg.ac.rs, sdragovic@vin.bg.ac.rs

Accurate delineation of gully shoulder lines as vector boundaries in forested environments presents a considerable challenge due to canopy cover and the limitations of traditional remote sensing approaches, including satellite imagery, aerial photogrammetry, and orthophotos. In contrast, data acquired by unmanned aerial vehicle light detection and ranging (UAV LiDAR) can enable reliable detection of gully and small channel networks beneath dense vegetation with high planimetric accuracy. Conventional approaches based on digital elevation models (DEMs) primarily rely on flow accumulation to extract linear drainage networks, often resulting in pseudo-channels, parallel artifacts, and subjectivity in threshold definition. Other approaches, based on slope, curvature, or bidirectional and multidirectional hillshades, and machine learning, have also been employed for the identification and extraction of gully boundaries. Topographic openness has proven to be a handy morphometric index for highlighting convex and concave microrelief, making it suitable for distinguishing gully zones in high-resolution elevation models. This study investigates the applicability of topographic openness-based techniques for gully boundary extraction in forested terrain using high-resolution UAV-based LiDAR data collected in the northern part of the Crveni Potok catchment in eastern Serbia. The workflow included point cloud processing steps, such as trajectory splitting, pass matching, overlap trimming, noise removal, and smoothing, followed by classification into ground, low, and high vegetation. A high-resolution DEM was generated and used to compute positive topographic openness. The resulting raster was analyzed to evaluate the variation in topographic openness index values between gullies and surrounding terrain. Based on this analysis, the raster was reclassified into classes, converted to vector format, and further processed through generalization and smoothing, including the removal of polygons smaller than a specified minimum size. Field validation is performed using Global Navigation Satellite System (GNSS) measurements of characteristic shoulder points and representative cross-sections. Accuracy is quantified by using spatial metrics

*Corresponding author

between semi-automatically measured and field-measured gully boundaries. Automated gully mapping significantly enhances erosion monitoring in challenging forest environments, contributing to more effective conservation efforts.

Acknowledgements

This research was supported by the Science Fund of the Republic of Serbia, Grant No. 7047, Development of erosion prediction tool for sustainable soil management - Predict-Er. This paper was also supported by the Ministry of Science, Technological Development and Innovation of the Republic of Serbia (contracts 451-03-137/2025-03/200124 and 451-03-136/2025-03/200017).

Book of Abstracts and Contributed Papers
International Conference on Recent Trends in Geoscience Research and Applications 2025 Belgrade, Serbia and Virtual, 15–19 September 2025
Editors: Aleksandra Nina, Snežana Dragović, Maja Kuzmanoski, Milan Đorđević, and Mrđan Đokić

Original scientific paper
Abstract

THE WAITING TIME PARADOX AND GLOBAL RISK ANALYSIS: LESSONS FROM GEOPHYSICAL HAZARDS

Milan M. ĆIRKOVIĆ[1*]

[1]*Astronomical Observatory of Belgrade, Belgrade, Serbia; e-mail: mcirkovic@aob.rs*

Study of global catastrophic and existential risks is an emerging area of risk analysis. There are multiple selection effects plaguing the analysis of these risks, like the well-known survivorship or the "anthropic shadow" bias. Here, I would like to add possible role for another selection effect, based on the waiting time paradox known for quite some time, but elaborated upon by Didier Sornette and Leon Knopoff in 1997. The conventional resolution of the paradox is based upon limitation of our historical database on the referent class events (say earthquakes or volcano eruptions). As I shall show, the difficulties are only exacerbated in the global case not only by practical issues, but also by the strongly non-ergodic nature of the underlying geophysical process. I also briefly discuss how studies of extrasolar planets can help us to obtain less biased picture of the underlying risk landscape.

References

Sornette, D., and Knopoff, L. (1997). *Bull. Seismol. Soc. Am.* 87, 789.

*Corresponding author

GeosciRA25

Book of Abstracts and Contributed Papers
International Conference on Recent Trends in Geoscience Research and Applications 2025 Belgrade, Serbia and Virtual, 15–19 September 2025
Editors: Aleksandra Nina, Snežana Dragović, Maja Kuzmanoski, Milan Đorđević, and Mrđan Đokić

Original scientific paper
Abstract

A COMPARATIVE DROUGHT ANALYSIS FOR AUSTRIA, SLOVAKIA, AND BULGARIA USING DROUGHT INDICES

Nina NIKOLOVA[1], Simeon MATEV[1*], Petko BOZHKOV[1], Martin GERA[2], Sabina THALER[3], Josef EITZINGER[3], Marian MELO[2], Jaroslava SLAVKOVA[2]

[1]Faculty of Geology and Geography, Sofia University "St. Kliment Ohridski", Sofia, Bulgaria; e-mails: nina@gea.uni-sofia.bg, matev@gea.uni-sofia.bg, pbozhkov@gea.uni-sofia.bg
[2]Faculty of Mathematics, Physics, and Informatics, Comenius University, Bratislava, Slovakia; e-mails: martin.gera@fmph.uniba.sk, marian.melo@fmph.uniba.sk, jaroslava.slavkova@fmph.uniba.sk
[3]Institute of Meteorology and Climatology, BOKU University, Vienna, Austria; e-mails: sabina.thaler@boku.ac.at, josef.eitzinger@boku.ac.at

Understanding and assessing drought is increasingly important due to its growing impact on agriculture, water resources, and ecosystems, particularly in the context of climate change. This study presents a comparative drought assessment for Austria, Slovakia, and Bulgaria using the Pálfai Drought Index (PaDI), a modified aridity index derived from key meteorological parameters such as temperature and precipitation. The PaDI, calculated using data from selected meteorological stations, provides insights into the severity and frequency of drought events across different regions (Pálfai & Herceg, 2011; Mezősi et al., 2016). The results from the present study indicate that mild and moderate droughts are common in all three countries, while serious droughts have been recorded primarily in Bulgaria and Slovakia (only in Bratislava and Hurbanovo). Bulgaria appears to be the most vulnerable to drought conditions, though none of the countries experienced extreme drought events during the study period. The findings reinforce the need to complement PaDI with other indices such as the Standardized Precipitation Evapotranspiration Index (SPEI) for a more comprehensive understanding of drought dynamics. Using the SPEI (Vicente-Serrano et al., 2010), the occurrence and frequency of drought events in selected areas of the three countries were studied. The relative share of dry months out of all months during the 25-year period (2000–2024) ranges from 18 to 21. Austria shows lower total dry month frequencies (18–19%), whereas Slovakia and Bulgaria show slightly higher and more variable values (up to 21%). Most locations show that extremely dry months are rare across the region. Slovakia has the lowest extreme drought frequency but the highest overall dry month percentage. The research emphasizes the importance of multi-indicator approaches for accurate drought monitoring.

*Corresponding author

Acknowledgements

The study was conducted under the project Extreme Droughts and their Impact on Agriculture in Selected Continental Climates of Europe, funded by the Programme for Multilateral Scientific and Technological Cooperation in the Danube Region (Agreement № KP-06-DANUBE/1, 18.07.2023, Ministry of Education and Science of Bulgaria; OeAD-GmbH - Austria's Agency for Education and Internationalization, Project № MULT 10/23), and grant DSFR-22-0017 - Slovak Research and Development Agency).

References

Mezősi, G., Blanka, V., Ladányi, Z. et al. (2016). *Carpathian J. Earth Environ. Sci.*, 11(2), 355.

Pálfai, I., and Herceg Á. (2011). *Riscuri catastrofe,* 9(2), 145.

Vicente-Serrano, S. M., Beguería, S., and López-Moreno, J. I. (2010). *J. Clim.*, 23(7), 1696.

GeosciRA25

Book of Abstracts and Contributed Papers
International Conference on Recent Trends in Geoscience Research and Applications 2025 Belgrade, Serbia and Virtual, 15–19 September 2025
Editors: Aleksandra Nina, Snežana Dragović, Maja Kuzmanoski, Milan Đorđević, and Mrđan Đokić

Original scientific paper
Abstract

STUDY OF THE SEISMIC ACTIVITY AT THE DODECANESE ISLANDS (JANUARY AND FEBRUARY 2025) BASED ON THE ANALYSIS OF THE SWARM MISSION DATA

Giovanni NICO[1*], Hans U. EICHELBERGER[2], Mohammed Y. BOUDJADA[2], Aleksandra NINA[3], Pier Francesco BIAGI[4], Iren-Adelina MOLDOVAN[5], Luka Č. POPOVIĆ[6]

[1]Institute for Applied Mathematics, National Research Council, Bari, Italy; e-mail: giovanni.nico@cnr.it
[2] Space Research Institute, Austrian Academy of Sciences, Graz, Austria; e-mails: hue@oeaw.ac.at, mohammed.boudjada@oeaw.ac.at
[3]Institute of Physics Belgrade, National Institute of the Republic of Serbia, University of Belgrade, Belgrade, Serbia; e-mail: sandrast@ipb.ac.rs
[4]Department of Physics, University of Bari, Bari, Italy; e-mail: pf.biagi@gmail.com
[5]National Institute for Earth Physics, Magurele-Bucharest, Romania; e-mail: iren@infp.ro
[6]Astronomical Observatory, Belgrade, Serbia; e-mail: lpopovic@aob.rs

Satellite missions in the low Earth orbit (LEO), such as CSES and ESA's Swarm, can provide data at altitudes of about 500 km useful for the detection of seismic precursors (e.g., De Santis et al., 2016 and Akhoondzadeh et al., 2018). In this work we present the first result of the analysis of magnetic field data acquired by the Swarm satellites to identify earthquake precursors related to the seismic sequence which occurred at the beginning of the year 2025 in the Dodecanese islands (Greece). The magnetic field and electron density data recorded by the Swarm satellites have been studied and correlated to the strong earthquakes with magnitude greater than M6.1 (e.g., see De Santis et al., 2016). In particular, it has been found that the time derivative of the magnetic field components can provide useful information about seismic precursors. In this analysis, we apply the same methodology to the Dodecanese earthquake which occurred in January and February 2025. We compute the time derivatives of the three components of the magnetic field measured by the Swarm A satellite on 22nd January 2025 and the Swarm B satellite on 24th January 2025, along the closest orbits to the Dodecanese islands. In both cases, the IGRF modelled field has been removed from the Swarm magnetic measurements, before computing the time derivatives. Anomalies have been identified in the time derivative of the east component of the magnetic field, in a latitude range between 33°N and 38°N. The discovered seismic precursors are compared to those identified in VLF/LF sub-ionospheric radio signals recorded by the European INFREP (Biagi et al., 2019) ground-based network.

*Corresponding author

Acknowledgements

The authors acknowledge funding provided by the Institute of Physics Belgrade and the Astronomical Observatory (the contract 451-03-136/2025-03/200002) through the grants by the Ministry of Science, Technological Development and Innovation of the Republic of Serbia.

References

De Santis, A., Balasis, G., Pavón-Carrasco, F. J. et al. (2017). *Earth Planet. Sci. Lett.*, 461, 119.

Akhoondzadeh, M., De Santis, A., Marchetti et al. (2018). *Adv. Space Res.*, 61(1), 248.

Biagi, P. F., Colella, R., Schiavulli, L. et al. (2019). *Open J. Earthq. Res.*, 8, 101.

GeosciRA25

Book of Abstracts and Contributed Papers
International Conference on Recent Trends in Geoscience Research and Applications 2025 Belgrade, Serbia and Virtual, 15–19 September 2025
Editors: Aleksandra Nina, Snežana Dragović, Maja Kuzmanoski, Milan Đorđević, and Mrđan Đokić

Review paper
Abstract

VLF/LF EARTHQUAKE PRECURSORS: REVIEW AND COMPARISONS

Aleksandra NINA[1*], Pier Francesco BIAGI[2], Giovanni NICO[3], Hans U. EICHELBERGER[4], Mohammed Y. BOUDJADA[4], Jovan BAJČETIĆ[5,6], Danilo LAZOVIĆ[5], Peter BUTKA[7], Peter BEDNÁR[7], Martin SARNOVSKÝ[7], Martin HUMENÍK[7], Luka Č. POPOVIĆ[8]

[1]*Institute of Physics Belgrade, National Institute of the Republic of Serbia, University of Belgrade, Belgrade, Serbia; e-mail: sandrast@ipb.ac.rs*
[2]*Department of Physics, University of Bari, Bari, Italy; e-mail: pf.biagi@gmail.com*
[3]*Institute of Applied Mathematics, National Research Council, Bari, Italy; e-mail: giovanni.nico@cnr.it*
[4]*Space Research Institute, Austrian Academy of Sciences, Graz, Austria; e-mails: hue@oeaw.ac.at, mohammed.boudjada@oeaw.ac.at*
[5]*Khaoticen doo, Belgrade, Serbia; e-mails: bajce05@gmail.com, danilo.lazovic136@gmail.com*
[6]*Professional Science and Technology, Zrenjanin, Serbia; e-mail: jbajcetic@pro-sci-tech.com*
[7]*Department of Cybernetics and Artificial Intelligence, Faculty of Electrical Engineering and Informatics, Technical University of Kosice, Kosice, Slovakia; e-mails: peter.butka@tuke.sk, peter.bednar@tuke.sk, martin.sarnovsky@tuke.sk, martin.humenik@student.tuke.sk*
[8]*Astronomical Observatory, Belgrade, Serbia; e-mail: lpopovic@aob.rs*

One of the scientific areas which use data obtained by monitoring the lower ionosphere by very low/low frequency (VLF/LF, 3 kHz – 300 kHz) radio signals is the research of earthquake precursors. Previous studies have indicated at least four types of variations in the time evolution of amplitude and phase that are recorded before the earthquake and are considered as their possible precursors: 1. reduction of amplitude during the night, 2. shift of solar terminator time (STT) defined as the time of the minimum amplitude during sunrise and sunset, 3. reduction of the amplitude and phase noise, 4. excitation and attenuation of waves at different wave periods. In this study, we analyze the characteristics of the mentioned changes related to the time of their occurrence before the earthquake, the area around the epicenter of the earthquake where they were observed, and the magnitudes that can be expected after their detections. We point out the advantages and disadvantages of individual types of variations, their compatibility and the importance of their simultaneous analysis. Additionally, we show the necessity of a multidisciplinary approach in the development of spatially distributed receiver networks and combined data processing in research aimed at examining the feasibility of finding sufficiently reliable methods that could include ionospheric

*Corresponding author

VLF/LF signal observations in near future multi-instrument earthquake warning systems.

Acknowledgements

The authors acknowledge the support provided by the Ministry of Science, Technological Development and Innovation of the Republic of Serbia (projects 337-00-216/2023-05/188 and 337-00-3/2024-05/11), the Austrian Federal Ministry of Women, Science and Research (BMFWF) (project no. RS 22/2024), and the Slovak APVV agency (project SK-SRB-23-0029). The authors acknowledge funding provided by the Institute of Physics Belgrade and the Astronomical Observatory (the contract 451-03-136/2025-03/200002) through the grants by the Ministry of Science, Technological Development and Innovation of the Republic of Serbia.

GeosciRA25

Book of Abstracts and Contributed Papers
International Conference on Recent Trends in Geoscience Research and Applications 2025 Belgrade, Serbia and Virtual, 15–19 September 2025
Editors: Aleksandra Nina, Snežana Dragović, Maja Kuzmanoski, Milan Đorđević, and Mrđan Đokić

Original scientific paper
Abstract

MULTISPECTRAL IMAGE ANALYSIS FOR MAPPING EROSION AND DEBRIS FLOW-PRONE AREAS IN THE BUYUKDERE RIVER CATCHMENT (EASTERN RHODOPES, BULGARIA)

Miloslava STEFANOVA[1*]

[1]*University of Mining and Geology "St. Ivan Rilski", Sofia, Bulgaria;*
e-mail: m.sstefanova@mgu.bg

Erosion and debris flows are among the most significant geomorphological hazards in mountainous terrains. This study aims to identify vulnerable areas within the Buyukdere River catchment (Eastern Rhodopes, Bulgaria) using a remote sensing and GIS-based approach. The catchment covers approximately 27 km² and, despite its low-mountainous relief, is prone to erosion and debris flows due to steep slopes, sparsely vegetated terrain, and intense rainfall. To assess the role of vegetation in controlling these processes, Sentinel-2 multispectral images from spring and autumn of 2020 and 2023 were analyzed. The Normalized Difference Vegetation Index (NDVI), a widely used indicator of vegetation cover, was calculated to evaluate land cover state. NDVI results were compared with slope data derived from a 12.5 m ALOS PALSAR (2009) digital elevation model in a GIS environment. NDVI values from November 2023 indicate a notable increase in bare or sparsely vegetated areas compared to November 2020, while spring imagery from both years shows similar vegetation conditions. Areas with NDVI below 0.2 and slopes greater than 15° were identified as highly susceptible to erosion and debris flows. Based on land cover and slope gradient analysis, the areas most susceptible to erosion and debris flows are concentrated in the northern and eastern parts of the catchment, particularly within the 1st and 2nd order sub-catchments as defined by Strahler's method (Strahler, 1957). Steep slopes in the lower catchment, combined with bare or sparsely vegetated terrain, increase erosion susceptibility. Integrating NDVI-based vegetation dynamics with topographic factors provides a spatially explicit framework that supports preliminary hazard assessment within broader erosion and debris flow evaluations.

Acknowledgements

Contract № ГПФ-255 – 01.04.2025, University of Mining and Geology, Sofia

References

ALOS PALSAR (2009). *ALPSRP158530820-RTC_HI_RES.* JAXA/METI Accessed through ASF DAAC

Strahler, A. N. (1957). *Trans. Am. Geophys. Union,* 38, 913.

*Corresponding author

GeosciRA25

Book of Abstracts and Contributed Papers
International Conference on Recent Trends in Geoscience Research and Applications 2025 Belgrade, Serbia and Virtual, 15–19 September 2025
Editors: Aleksandra Nina, Snežana Dragović, Maja Kuzmanoski, Milan Đorđević, and Mrđan Đokić

Original scientific paper
Abstract

TESTING FUNDAMENTAL PHYSICS WITH SEISMOLOGY

Aneta WOJNAR[1,2*]

[1]*Complutense University of Madrid, Madrid, Spain; e-mail: awojnar@ucm.es*
[2]*University of Wroclaw, Wroclaw, Poland; e-mail: aneta.wojnar2@uwr.edu.pl*

I will briefly demonstrate the application of Earth seismic data to constrain quantum and modified gravity proposals. Further, I will discuss essential enhancements needed for this method. Since the idea evolved into a more serious project, I would like to present a new COST Action CA24101 FuSe. At the heart of FuSe is the belief that seismic phenomena could reveal new aspects of fundamental interactions and lead to the discovery of new physics. By analysing seismic data and studying the underlying physical principles, FuSe aims to explore imprints of unknown physics that may be embedded in these natural processes. On the other hand, the study of fundamental physics can also improve our knowledge of the Earth. This effort draws on interdisciplinary expertise, with a focus on how seismic events could deepen our understanding of the fundamental forces that govern the universe. FuSe's innovative approach combines diverse scientific fields to pursue both theoretical and practical advancements. This synergy has the potential to transform our knowledge of both fundamental physics and seismic activity, contributing to a broader understanding of Earth's interior and the cosmos.

*Corresponding author

GeosciRA25

Book of Abstracts and Contributed Papers
International Conference on Recent Trends in Geoscience Research and Applications 2025 Belgrade, Serbia and Virtual, 15–19 September 2025
Editors: Aleksandra Nina, Snežana Dragović, Maja Kuzmanoski, Milan Đorđević, and Mrđan Đokić

Original scientific paper
Abstract

CHARACTERIZATION OF RIVERBED SEDIMENT THROUGH 3D POINT CLOUD PROCESSING AND ANALYSIS

Valentina NIKOLOVA[1*], Laure GUERIT[2], Asparuh KAMBUROV[3], Dobromir FILIPOV[4], Ana M. PETROVIĆ[5], Jan BABEJ[6], Jiří JAKUBÍNSKÝ[6]

[1]University of Mining and Geology, Sofia, Bulgaria; e-mail: v.nikolova@mgu.bg
[2]Géosciences Rennes, University of Rennes, Rennes, France; e-mail: laure.guerit@univ-rennes.fr
[3]University of Mining and Geology, Sofia, Bulgaria; e-mail: asparuh.kamburov@mgu.bg
[4]University of Architecture, Civil Engineering and Geodesy, Sofia, Bulgaria; e-mail: filipov_fgs@uacg.bg
[5]Geographical Institute „Jovan Cvijić", Serbian Academy of Sciences and Arts, Belgrade, Serbia; e-mail: a.petrovic@gi.sanu.ac.rs
[6]The Czech Academy of Sciences, Global Change Research Institute, Brno, Czech Republic; e-mails: babej.j@czechglobe.cz, jakubinsky.j@czechglobe.cz

Characterization of riverbed sediments is essential for understanding sediment dynamics and their hydrogeomorphological aspects in river systems. In particular, riverbed morphology significantly influences sediment transport processes, especially in torrential watersheds. This study aims to quantify riverbed sediment patterns in contrasting fluvial environments — temporary torrential streams and a permanently flowing river — using 3D point cloud technology. High-resolution point clouds were generated through terrestrial photogrammetry and laser scanning of low mountainous study areas in Bulgaria, Serbia and Czechia. The clouds were processed using the G3Point Cloud Compare plugin (Leroy et al., 2025). This method allows a detailed analysis of sediment size, shape, and distribution (Steer et al., 2022), which are important for understanding the conditions of sediment transport and deposition, and thus plays a crucial role in developing measures for decreasing the erosion and debris flow susceptibility. The results of the 3D point clouds analysis of the riverbed sediments show uneven roughness distribution suggesting sediment transport driven by intermittent or torrential flow. In most of the studied cases dip patterns of the grains (ellipsoids segmented from the point cloud) are consistent and steep while the azimuth distributions vary. This aligns with expected complexity in fluvial systems, where bar dynamics, and episodic flow events contribute to variable sedimentary patterns. Overall, the study demonstrates the effectiveness of 3D point cloud analysis for capturing fine-scale sediment processes and understanding the sediment patterns across diverse riverine settings.

*Corresponding author

Acknowledgements

Project Geomorphological interpretation of photogrammetry and laser scanning data in the study of torrential watersheds, Contract № КП-06-Дунав/5, 14.08.2023 (National Science Fund, Bulgaria), PHC Danube n 49921ZG (France); 337-00-140/2023-05/10 (Serbia) and MSMT 8X23015 (Czechia).

References

Leroy, P., Guérit, L., Steer, P. et al. (2025). *G3Point plugin for CloudCompare* [software]. University Rennes, CNRS, Lidar Platform, Rennes, France.

Steer, P., Guérit, L., Lague, D. et al. (2022). *Earth Surf. Dyn.*, 10(6), 1211.

Book of Abstracts and Contributed Papers
International Conference on Recent Trends in Geoscience Research and Applications 2025 Belgrade, Serbia and Virtual, 15–19 September 2025
Editors: Aleksandra Nina, Snežana Dragović, Maja Kuzmanoski, Milan Đorđević, and Mrđan Đokić

https://doi.org/10.46793/Geoscira25.050L

Original scientific paper
Contributed paper

HOT SPRINGS AND THE ORIGIN OF LIFE: SIMULATING ANCIENT ATMOSPHERES IN MODERN GEOTHERMAL ENVIRONMENTS

Dragan LUKIĆ[1*]

[1] *Institute of Physics Belgrade, National Institute of the Republic of Serbia, University of Belgrade, Belgrade, Serbia; e-mail: lukic@ipb.ac.rs*

Abstract: Understanding the origin of life requires investigating the environmental conditions and biochemical processes that shaped the transition from prebiotic chemistry to early cellular life. This study focuses on terrestrial hot springs as analog environments for early Earth, proposing that life may have originated in these geochemically rich, thermally dynamic systems. Geological and molecular evidence suggests early life forms were thermophilic, adapted to high temperatures similar to those in modern hot springs. These environments—characterized by minerals like iron and sulfur, thermal gradients, and wet-dry cycles—facilitate key reactions such as carbon fixation and the formation of protocell structures. Using thermophilic organisms as modern analogs, we propose experiments that simulate early atmospheric compositions within enclosed hot spring systems to study microbial responses and chemical evolution. This approach not only enhances our understanding of early Earth biochemistry but also informs the search for life in analogous extraterrestrial environments, such as Mars and Europa. Our findings aim to shed light on how life may have emerged and evolved under varying atmospheric and geochemical conditions.

Keywords: Hot springs; Origin of Life; Thermophiles; Hydrothermal Vents; Early Earth Atmosphere

1. Introduction

Understanding the origin of life is a central question in science, yet much remains speculative due to the complexity and inaccessibility of the early Earth environment. Rather than focusing solely on how life began, this paper investigates the earliest stages of biological development—particularly how early life adapted to extreme environmental conditions. By examining modern analogs such as hot springs and thermophilic organisms, we can better understand the geochemical and atmospheric interactions that may have fostered the transition from prebiotic chemistry to cellular life.

*Corresponding author

2. Hot springs and Early Life

2.1. Thermal Adaptation and the Evolution of Early Life

Studies of ancient proteins suggest that early life forms were thermophilic, adapted to high-temperature environments comparable to those found in contemporary terrestrial hot springs (Gaucher et al., 2010). Geological data also support this view: Earth's primordial oceans may have approached temperatures similar to modern hot springs (Hoyle, 1972). As Earth's surface cooled over geological time, organisms likely evolved to adapt to increasingly temperate environments. This evolutionary trajectory supports the hypothesis that life may have originated in hot spring ecosystems rather than in the chemically distinct, high-pressure environments of deep-sea hydrothermal vents (Maruyama et al., 2019).

One major argument against deep-sea hydrothermal vents as the origin point of life is the extreme temperature of their central zones—often exceeding 350°C—far beyond the stability limits of proteins and nucleic acids (Kelley et al., 2005; Amend & Shock, 2001; Bada, 2004). Although cooler peripheral regions exist, they are chemically dynamic and biologically populated by thermophiles that likely migrated from more stable environments. These ecosystems may reflect adaptation rather than origin. In contrast, terrestrial hot springs offer a chemically rich, more variable thermal environment that allows for wet-dry cycles, UV exposure, and mineral interactions—conditions potentially conducive to prebiotic chemistry and early evolution.

2.2. Hot Springs as Natural Laboratories for Prebiotic Chemistry

Terrestrial hot springs, enriched with minerals like iron and sulfur, offer unique geochemical environments ideal for exploring the origins of life. Iron sulfides in these systems can catalyze the reduction of carbon dioxide into simple organic molecules such as methanol—key precursors to more complex biomolecules (Nan et al., 2024). This reaction, similar to the reverse water-gas shift process, supports the idea that hot springs may have been important sites for early carbon fixation (Martin et al., 2008).

In addition to their rich chemistry, hot springs exhibit thermal gradients and natural wet-dry cycling. These dynamic conditions promote the polymerization and encapsulation of organic compounds into protocell-like structures, processes that may have played a crucial role in the development of cellular life (Leman et al., 2004). As such, hot spring pools function as natural reactors that simulate the fluctuating conditions of early Earth.

Thermophilic organisms living in modern hot springs provide further clues. Their enzymes and metabolic systems, adapted to high temperatures, serve as living models for understanding how life could have operated under primordial conditions. Laboratory experiments mimicking hot spring chemistry—by mixing hydrogen-rich fluids with CO_2-rich water and iron minerals—have already shown the potential for forming primitive membranes and organic structures (Brocks et al., 1999).

Building on this, we aim to study present-day thermophilic life in actual hot spring environments enclosed under atmospheric chambers that simulate early Earth's gaseous composition. This approach allows us to observe how different atmospheric conditions might have influenced the chemical and biological evolution of early life, offering a window into the interaction between ancient atmospheres and emerging biosystems.

2.3. Research Methodology: Simulating Ancient Atmospheres in Modern Hot Springs

We propose an experimental framework to investigate how early atmospheric compositions could have shaped the metabolism and chemical evolution of primitive life. This involves deploying a transparent dome-like chamber canopy over portions of a modern terrestrial hot spring. The chamber allows precise control over gas concentrations, replicating early Earth atmospheres with mixtures of CO_2, N_2, H_2, CH_4, and H_2S. Internal temperature sensors, gas input regulators, and spectrophotometric sampling ports will allow us to monitor microbial behavior and chemical changes in real time.

Initial pilot studies would have involved enclosing Cyanidiales (a thermophilic algal lineage) within a chamber filled with a CO_2-dominant atmosphere and tracking changes in gene expression, pH, redox potential, and organic compound formation.

Future experiments will include tracking the synthesis of fatty acids, nucleotide-like precursors, and membrane structures. We will also test whether mineral substrates, such as iron sulfide and clays placed within the chamber, enhance catalysis and polymer formation. These data will provide empirical evidence to support or refute proposed pathways for prebiotic chemistry and early metabolism under simulated early Earth conditions.

2.4. Astrobiological Implications

The implications of hot spring research extend beyond Earth. The geochemical environments of hot springs are analogous to potential habitats on Mars and icy moons such as Europa and Enceladus, which may host geothermal activity. By understanding how life might emerge under hot spring-like conditions on Earth, we can refine our models for detecting biosignatures and assessing habitability elsewhere in the solar system. By examining extremophiles in these environments, scientists can develop models to predict where and how life might arise elsewhere in the universe.

3. Conclusion

Terrestrial hot springs serve as accessible and informative analogs for the environments that may have fostered the origin of life. Their mineral-rich waters, variable thermal regimes, and capacity for wet-dry cycling make them ideal settings for exploring how prebiotic molecules could have assembled into increasingly complex systems.

While our current research focuses on chamber-based simulations of early atmospheres, several limitations remain. Replicating long-term evolutionary processes within short experimental timescales is inherently challenging, and modern thermophiles, though informative, are not perfect stand-ins for primordial organisms. Additionally, the variability in hot spring geochemistry makes standardization difficult.

Future studies will involve more comprehensive chemical analyses, the use of synthetic protocells, and comparative experiments across different geothermal systems. These efforts aim to bridge the gap between geochemical potential and biological emergence, advancing our understanding of how life might originate on Earth—and possibly elsewhere in the universe.

Acknowledgements

"This research was supported by the Science Fund of the Republic of Serbia, grant no. 6775, Urban Observatory of Belgrade – UrbObsBel, and Ministry of Science, Technological Development and Innovation". The authors acknowledge funding provided by the Institute of Physics Belgrade through the grants by the Ministry of Science, Technological Development and Innovation of the Republic of Serbia.

References

Amend, J. P., and Shock, E. L. (2001). Energetics of overall metabolic reactions of thermophilic and hyperthermophilic Archaea and Bacteria. *FEMS Microbiol. Rev.*, 25(2), 175.

Bada, J. L. (2004). How life began on Earth: A status report. *Earth Planet. Sci. Lett*., 226(1–2), 1.

Brocks, J. J., Logan, G. A., Buick, R. et al. (1999). Archean molecular fossils and the early rise of eukaryotes. *Science*, 285(5430), 1033.

Gaucher, E. A., Kratzer, J. T., and Randall, R. N. (2010). Deep phylogeny—how a tree can help characterize early life on Earth. *Cold Spring Harb. Perspect. Biol.*, 2(1), a002238.

Hoyle, F. (1972). The History of the Earth. *Quart. J. Roy. Astron. Soc*., 13, 328.

Kelley, D.S., Karson, J. A., Früh-Green, G.L. et al. (2005). A serpentinite-hosted ecosystem: The Lost City hydrothermal field. *Science*, 307(5714), 1428.

Leman, L., Orgel, L., and Ghadiri, M.R. (2004). Carbonyl sulfide–mediated prebiotic formation of peptides. *Science*, 306(5694), 283.

Maruyama, S., Kurokawa, K., Ebisuzaki, T. et al. (2019). Nine requirements for the origin of Earth's life: Not at the hydrothermal vent, but in a nuclear geyser system. *Geosci. Front.*, 10(4), 1337.

Martin, W., Baross, J., Kelley, D. et al. (2008). Hydrothermal vents and the origin of life. *Nat. Rev. Microbiol.*, 6(11), 805.

Nan, J., Luo, S., Tran, Q.P. et al. (2024). Iron sulfide-catalyzed gaseous CO_2 reduction and prebiotic carbon fixation in terrestrial hot springs. *Nat. Commun.*, 15, 10280.

Book of Abstracts and Contributed Papers
International Conference on Recent Trends in Geoscience Research and Applications 2025 Belgrade, Serbia and Virtual, 15–19 September 2025
Editors: Aleksandra Nina, Snežana Dragović, Maja Kuzmanoski, Milan Đorđević, and Mrđan Đokić

https://doi.org/10.46793/Geoscira25.054V

Original scientific paper
Contributed paper

COMPARISON OF TWO-DIMENSIONAL AND THREE-DIMENSIONAL DYNAMIC RESPONSE OF AN EARTH AND ROCKFILL DAM

Sebastian Palacios VIDAL[1*], Denys Parra MURRUGARRA[2]

[1]University of Belgrade, Faculty of Civil Engineering, Department of Geodesy and Geoinformatics, Belgrade, Serbia; e-mail: 704_24@student.grf.bg.ac.rs
[2]National University of Engineering, Lima, Peru; e-mail: dparra@uni.edu.pe

Abstract: This study compares the 2D and 3D dynamic response of a rockfill dam for water storage, which will be located in southern Peru, in a zone of high seismicity. The geotechnical characterization of the materials that compose the dam and the foundation was estimated based on field and laboratory geotechnical investigations. The synthetic seismic records used in the dynamic analyses were obtained from the spectral matching of representative earthquake records, which were previously corrected for baseline and filtered. A numerical modeling strategy is presented, employing the finite element methodology by using constitutive models such as Hardening Soil (HS) and Hardening Soil Small Strains (HS-Small). As part of the results, higher displacement and deformation values were obtained from the 2D dynamic analysis, unlike the acceleration, where higher values were obtained from the 3D dynamic analysis. The 2D structural period of the dam is greater than the 3D period, which demonstrates a strict dependence of this parameter on the geometry of the dam and its topography. Finally, the results obtained in this study show us a notable difference between the 2D and 3D dynamic response of the dam, so it is important to consider 3D dynamic behavior in the design of this type of geotechnical structure.

Keywords: Dynamic response, constitutive models, finite element, dynamic analysis, structural period.

1. Introduction

The construction of earth and rockfill dams for water storage has increased globally due to the growing demand for human and industrial consumption, irrigation, electricity generation, etc. Since many of these structures are located in seismic zones, it is crucial to understand their seismic behavior through dynamic analyses, which are performed based on criteria recommended by international standards.

In dams located in canyon valleys, dynamic behavior is largely influenced by their 3D geometry. Mejia and Seed, 1983 indicate that the natural frequency of vibration of an earth dam depends strictly on the type of canyon (topography) where it is located, and its geometry, specifically the ratio between the length of the crest (L) and the height of the

*Corresponding author

dam (H). Likewise, Gazetas and Dakoulas, 1992 presented a comprehensive compilation of information on the state of the art in seismic design and analysis of rockfill dams. They indicated that the relationship between the 3D (T_D) and 2D ($T_{D\infty}$) fundamental periods depends on the L/H ratio and the type of canyon in the valley in which they are located (see Figure 1).

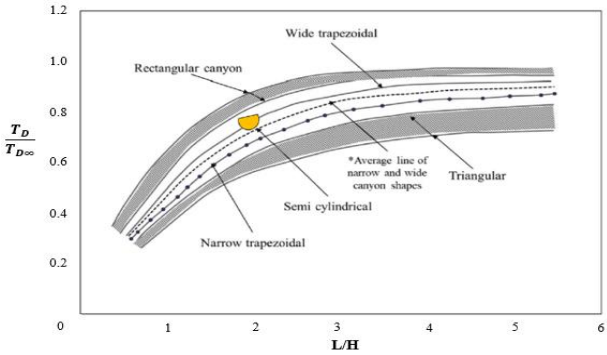

Figure 1. Effect of canyon geometry on the natural fundamental period (Gazetas and Dakoulas, 1992)

The rockfill dam analyzed in this study was designed using two-dimensional analyses and is currently under construction. This dam will have the following characteristics: (1) it will be located in an area of high seismicity, (2) will have a maximum height of 58 m and (3) will be built in a relatively narrow valley.

Based on the above mentioned, understanding the 3D dynamic behavior is essential, since 2D analysis does not adequately capture the actual dynamic response of the dam. In addition, this three-dimensional analysis will capture the actual 3D topography of the dam (see Figure 2) rather than an approximation, as is usually done in this type of analysis (Mejia and Seed, 1983; Gazetas and Dakoulas, 1992)

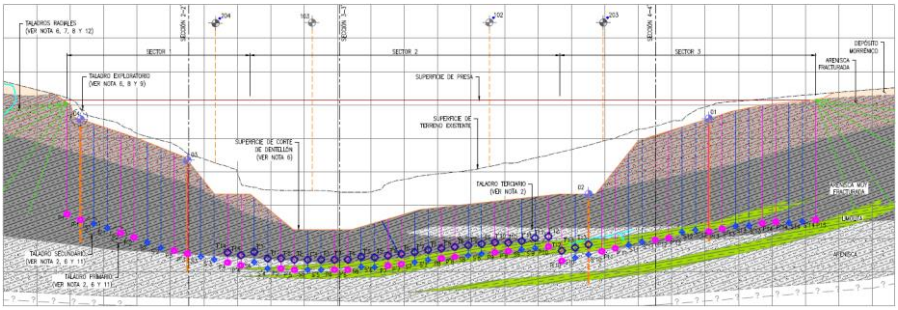

Figure 2. Cross-section of the dam foundation.

The main geometric characteristics of the dam are described in Table 1.

Table 1. Geometric characteristics of the dam

Description	Values
Dam crest elevation (masl)	4512.0
Reservoir level (masl)	4509.5
Free edge (m)	2.5
Crest width / length (m)	10 / 167
Dam height (m)	58
Upstream / Downstream slope	2H:1V / 2.25H:1V

2. Geotechnical characterization

The dam geotechnical model includes the following materials: clay core classified as a sandy clay (CL) and compacted to 95% (Sector 1) and 100% (Sector 2) of its standard Proctor maximum density; upstream and downstream rockfill shoulder obtained by crushing a sandstone rock existing close to the dam area; a moraine deposit classified as a clayey gravel (GC) as foundation soil; and a sandstone bedrock. Also, the model includes filter and drain materials. Figure 3 shows the materials that make up the rockfill dam under analysis.

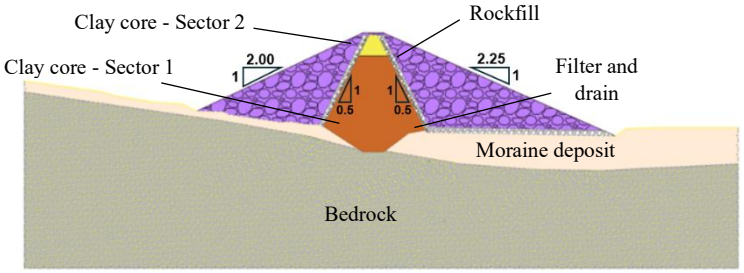

Figure 3. Typical section of rockfill dam for the 2D numerical model

Table 2 shows the shear wave velocities of the foundation soil and rock as determined by MASW (Multichannel Analysis of Surface Waves) and MAM (Microtremor Array Measurements) geophysical tests.

Table 2. Shear wave velocity of the foundation

Description	Vs (m/s)
Medium dense to dense moraine soil	300-600
Bedrock	760-900

2.1. Shear strength properties

Consolidated drained (CD) and consolidated undrained (CU) triaxial tests were carried out on 4-inch specimen of representative samples of the moraine deposit and clay core, respectively.

The nonlinear shear strength envelope of the rockfill was estimated according to the empirical failure criterion proposed by Barton, 2013. However, in order to determine the value of cohesion and angle of friction of the rockfill, the nonlinear shear strength envelope was compared with the Mohr Coulomb envelope. The strength properties of the filter and drain were assumed according to materials with the same characteristics.

2.2. Dynamic properties

Dynamic properties of the moraine deposit and clay core were obtained from resonant column and torsional shear (RCTS) tests performed at different confining pressures. The results obtained were compared with the curves proposed by Darendeli, 2001 in order to know the dynamic behavior of the materials in a wider range of shear strains. For the moraine deposit, the small strain shear modulus determined in the field using geophysics has been compared with the shear modulus predicted by the HS-Small model (Plaxis, 2023). The small strain modulus of the clay core was determined using the correlation proposed by Hardin and Black, 1969 for cohesive materials.

Due to the large particle size of the rockfill, RCTS tests could not be performed. Therefore, the dynamic curves proposed by Rollins et al., 2020, which are applicable for gravelly soils and rockfills, were used. The shear modulus at small strains of the rockfill was determined using the formulation of Kokusho and Esashi, 1981 for granular materials from a rock crushing process.

The dynamic properties of the filter and drain materials were estimated using the curves proposed by Rollins et al., 1998. The shear modulus at small strains of these materials was determined by the correlation proposed by Seed et al., 1986 for granular materials.

3. Numerical modeling

The numerical modeling process adopted for the analysis of the dam's dynamic behavior begins with the development of three important points: geotechnical characterization of the materials (see Chapter 2), creation of the 2D and 3D geometries of the dam, and generation of seismic records for dynamic analysis. After that, the finite element mesh for the 2D and 3D models is generated, and the parameters of the previously calibrated constitutive models are assigned to the materials.

The next step is to define the dam construction process, which is important for performing the static analysis. Prior to the dynamic analyses, the seismic records generated as a time-history of accelerations are entered, and dynamic boundaries are assigned to the model to prevent seismic wave reflection. Results are obtained in terms of displacements, deformations, and accelerations, which will be compared to determine the differences in two-dimensional and three-dimensional dynamic behavior. Finally, from the accelerations induced in the dam body (base and crest), the structural period is determined to evaluate the influence of the canyon topography and the dam geometry.

Each step of this process will be explained in detail in the following sections. Figure

4 presents a schematic diagram summarizing the numerical modeling process used in this study.

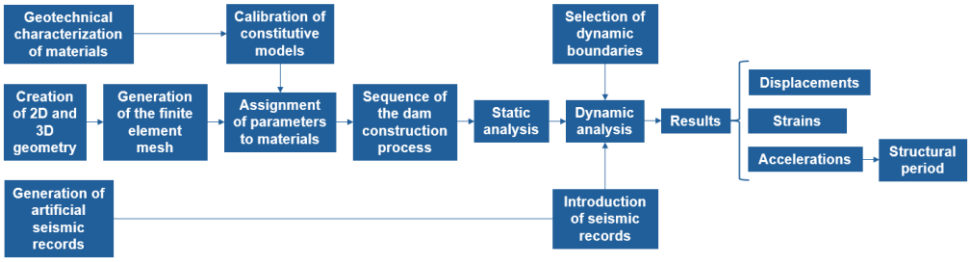

Figure 4. Schematic diagram of the numerical modeling process

It is important to mention that a static analysis was performed to evaluate the stress state prior to the dynamic analysis, as a consequence of the dam construction process. The dynamic analyses were carried out on the final geometry of the dam. The cross section for the 2D numerical analysis is shown in Figure 3 while the 3D geometry of the dam is presented in Figure 5.

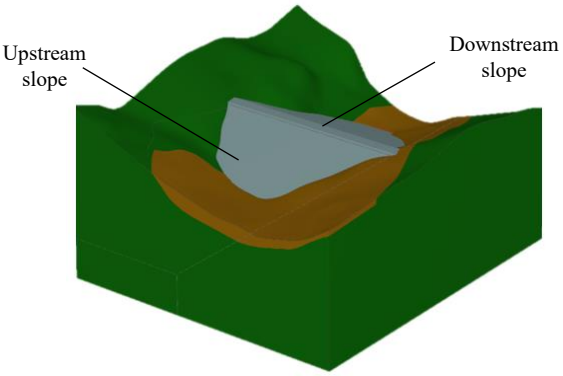

Figure 5. 3D numerical model of the rockfill dam

3.1. Calibration of constitutive models

For the moraine deposit and clay core, Hardening Soil (HS) and Hardening Soil Small Strains (HS-Small) models were selected and calibrated with results of triaxial tests (see Figure 6) and RCTS tests (see Figure 7), respectively.

Regarding the rockfill, filter and drain, the HS-Small model was selected and calibrated with the dynamic curves defined for these materials (see Figure 5); however, the properties of the HS model chosen for these materials were estimated from the dynamic parameters by applying a degradation factor, which allows working with equivalent elastic shear modulus to represent the critical behavior of the materials in the plasticity range (Hammam and Eliwa, 2013).

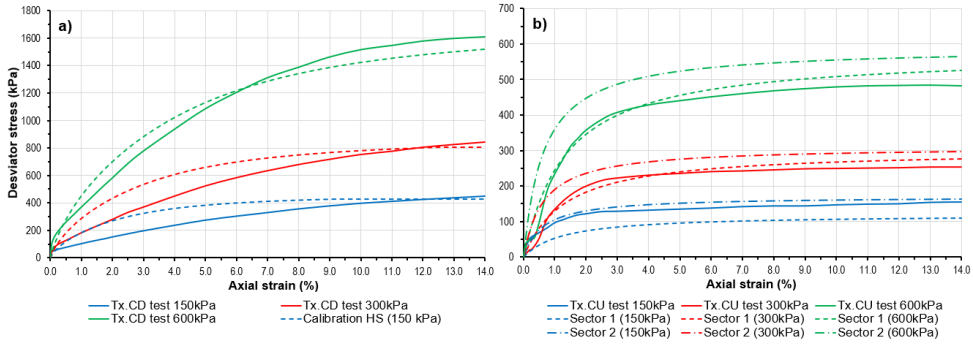

Figure 6. Calibration of static parameters: stress-strain curves from triaxial tests (CD and CU) and the HS model for the moraine deposit (a) and clay core (Sector 1 and 2) (b)

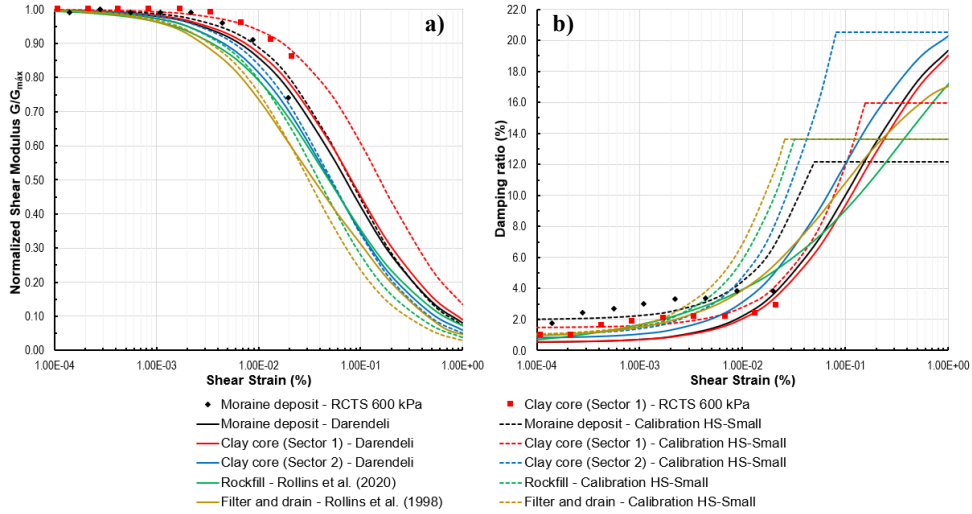

Figure 7. Calibration of dynamic parameters: Normalized shear modulus (a) and Damping ratio (b) curves from RCTS tests and the HS-Small model for the moraine deposit, clay core (Sector 1 and 2), rockfill and filter and drain

For the bedrock, the Linear-Elastic model was selected and calibrated with the shear wave velocities of this material (see Table 1). A reduction factor was also applied to the bedrock to simulate the elastic behavior as mentioned above.

The damping curves predicted by the HS-Small model do not correctly capture the minimum damping values of the materials. This missing hysteretic damping will be compensated by viscous or Rayleigh damping (Brinkgreve et al., 2007), which is frequency-dependent. Regarding the bedrock, Rayleigh damping parameters were defined to facilitate the convergence of the model, so that this material can dissipate a minimum of energy of the seismic loading, for which a damping value equal to 0.5% was adopted (Schnabel, 1973).

Table 3 presents the summary of the calibrated parameters of the materials used in the numerical model.

Table 3. Summary of the calibrated parameters of the materials

Parameter	Moraine deposit		Clay core Sector 1		Clay core Sector 2		Rockfill		Filter and drain		Bedrock
Constitutive model	HS	HS-Small	HS	HS-Small	HS	HS-Small	HS	HS-Small	HS	HS-Small	LE
γ (kN/m^3)	20	20	22	22	22	22	23	23	18	18	22
E_{50}^{ref}(MPa)	33	244	15	45	10	15	22	152	7	47	---
E_{oed}^{ref}(MPa)	20	148	15	45	11	16	13	94	4	30	---
E_{ur}^{ref}(MPa)	120	912	80	245	50	72	65	457	20	142	3520
m	0.5	0.5	1.0	0.45	1.0	0.45	0.5	0.5	0.5	0.5	---
p^{ref}(kPa)	600	600	600	600	150	150	300	300	100	100	---
ν_{ur}	0.2	0.2	0.2	0.2	0.2	0.2	0.2	0.2	0.2	0.2	0.25
c' (kPa)	12	12	23	23	23	23	5	5	5	5	---
φ' (°)	34	34	29	29	29	29	38	38	36	36	---
ψ (°)	0	0	0	0	0	0	0	0	0	0	---
G_0^{ref}(MPa)	---	1000	---	410	---	200	---	635	---	197	---
$\gamma_{0.7}$(E-04)	---	3.1	---	6.0	---	2.0	---	1.5	---	1.2	---
Permeability (m/s)	1.3E-05	1.3E-05	2.0E-08	2.0E-08	2.0E-09	2.0E-09	1.0E-02	1.0E-02	1.0E-01	1.0E-01	5.0E-06
Rayleigh α	---	0.2356	---	0.1767	---	0.1178	---	0.1178	---	0.1178	0.00589
Rayleigh β	---	3.98E-04	---	2.98E-04	---	1.99E-04	---	1.99E-04	---	1.99E-04	9.95E-05

3.2. Details of the numerical model

The free-field and compliant base boundary were selected as the dynamic boundaries for the sides and base of the numerical model, respectively; in addition, interfaces were added at those boundaries and a plate at the base. The lateral dynamic boundaries correspond to free-field boundaries, which reduce the extent of the dynamic model and prevent lateral wave reflections, i.e. these waves are absorbed (Plaxis, 2023). The seismic records were input into the models as a prescribed displacement and a dynamic multiplier of 0.5 was used on each seismic record to account for rock outcrop movement at the base of the model.

The input records have been applied in the upstream-downstream direction of the dam, because it constitutes the most severe condition of an earthquake. Vertical movements were not considered, since they do not induce shear stresses as significant as horizontal movements and, therefore, do not affect the stability of the dam (Mejia and Seed, 1983).

The finite element mesh of the 2D model was generated following the recommendation proposed by Kuhlmeyer and Lysmer, 1973 for element sizing in 2D numerical models, which prevents the wave from moving more than one element per computational step. In the case of the 3D model, a fine mesh was prepared, where the parameter to be controlled was the quality of the generated finite element mesh.

3.3. Seismic scenario

The input seismic motions used for the dynamic analysis were the following: Ancash 1970 and Lima 1974. The first record corresponds to an intraslab earthquake and the second to an interface earthquake (see Table 4), with the former better representing the seismicity of the study area according to the seismic hazard study.

Table 4. Original seismic records

Item	Ancash 1970	Lima 1974
PGA (g)	0.107	0.198
Mw	7.9	7.8
Failure mechanism	Subduction Intraslab	Subduction Interface

The seismic records were previously corrected for baseline and filtered using a bandpass filter. They were then spectrally matched to the uniform hazard spectrum (UHS) corresponding to a return period of 1000 years, which is the design earthquake for the dam, determined by evaluating the consequences of a potential dam break or failure.

Due to the high computational time required for the dynamic analysis of the three-dimensional models, the seismic records that present the highest Arias intensity values (a measure of the energy released by an earthquake) were chosen, which correspond to the Ancash 1970 EW and Lima 1974 NS components shown in Figure 8.

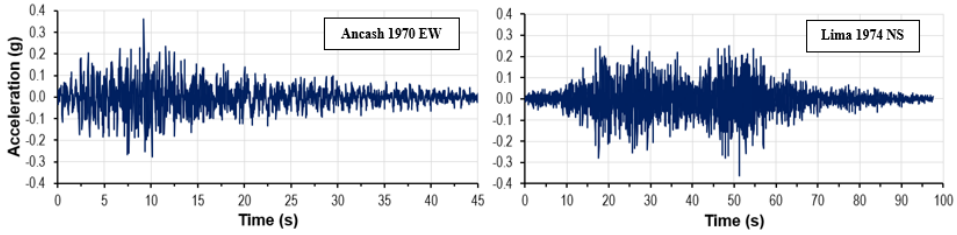

Figure 8. Selected accelerations time-history records of the Ancash 1970 EW and Lima 1974 NS earthquakes

4. Results and discussion

In order to compare the 2D and 3D dynamic behavior of the dam, the results are represented by the displacements, strains and accelerations induced by the seismic records described in chapter 3.1. The calculation of the structural period of the dam is also presented.

4.1. Displacements

The final 2D settlements on the crest results in 0.39 and 1.05 m, and 0.36 and 0.95 m for the 3D dynamic analyses, for the Ancash EW and Lima NS earthquakes, respectively. In general terms, the results obtained from the 2D dynamic analysis are greater than those obtained from the 3D dynamic analysis for both earthquakes used (see Figure 9).

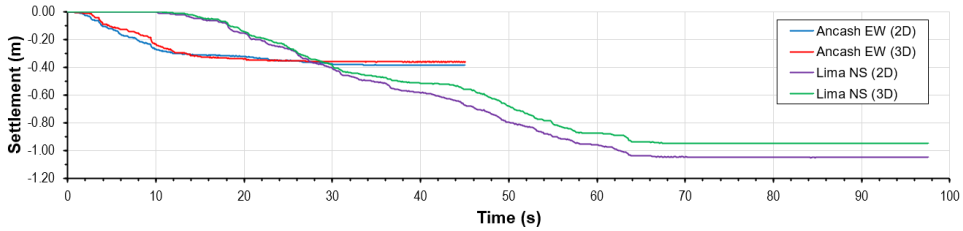

Figure 9. Time-history of settlement on the crest for the Ancash EW and Lima NS earthquakes

As can be seen in the Figure 9, the values obtained from the 2D dynamic analysis are approximately 7 to 9% higher than those obtained from the 3D analysis. Likewise, the settlements induced by the Lima NS earthquake are higher than those induced by the Ancash EW earthquake.

4.2. Strains

Shear strains ranged from 5 to 15% for the 2D dynamic analyses, and from 3.5 to 14% for the 3D analyses, for both earthquakes. Figure 10 shows the maximum shear strains from the 2D and 3D dynamic analyses for the Lima NS earthquake, as these results contain the largest shear strains compared to the Ancash EW earthquake. For both models, the shear strains are mostly concentrated in the clay core and the upper rockfill zone located on the upstream slope of the dam.

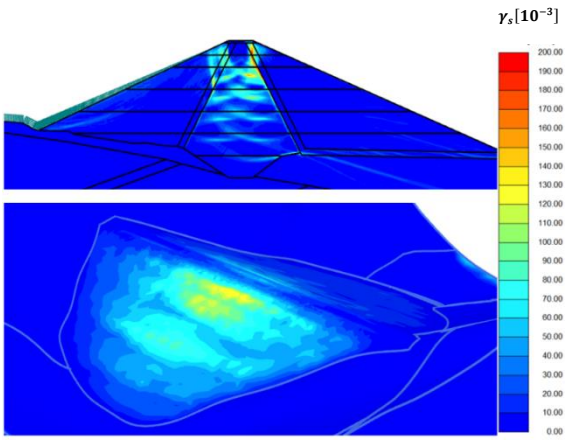

Figure 10. Shear strains obtained from the Lima 1974 NS earthquake for the 2D and 3D models

4.3. Accelerations

The maximum accelerations were obtained at points corresponding to the maximum elevation of each construction stage in the numerical model, from the base to the crest of the dam. The results indicate that the maximum accelerations obtained from the 3D dynamic analysis are greater than those obtained from the 2D analysis for both earthquakes (see Figure 11).

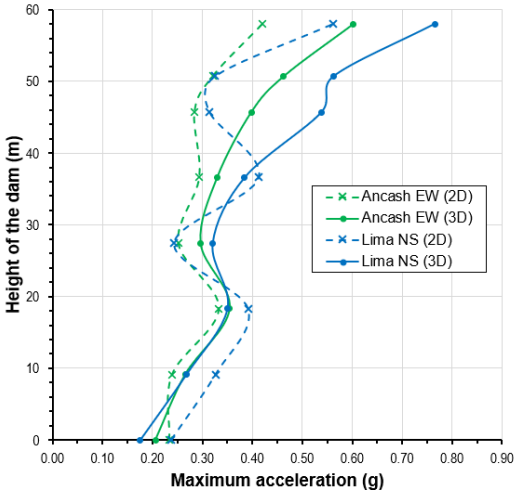

Figure 11. Maximum accelerations at the checkpoints along the clay core

The maximum accelerations along the core of the dam obtained from the 3D dynamic analysis are higher than those from the 2D analysis. It can also be observed that the difference between the 2D and 3D accelerations becomes greater closer to the dam crest.

4.4. Fundamental period

The fundamental period was determined using the method known as Ratio Fourier Amplitude Spectrum (RFAS) (Hwang et al., 2007). In this method, the Fourier Amplitude Spectrum (FAS) was initially calculated by applying the Fourier Transform Function (FTF). Then, the Transfer Function (TF) or spectral ratio was calculated by dividing the FAS on the crest of the dam by that at the base.

The fundamental period was determined as the period corresponding to the highest amplitude of the TF. However, due to unexpected peaks in the TF, it was difficult to determine the fundamental period with high accuracy, due to which in this research the method proposed by Konno and Ohmachi, 1998 was used to smooth the TF, for which a Python routine was developed.

Figure 12 shows the smoothed transfer functions for the 2D and 3D numerical models. The natural frequency of vibration of the 2D model is 2.7 Hz, and that of the 3D model is 4.0 Hz, Since the fundamental period of the dam is the inverse of the frequency, periods of 0.37 s and 0.25 s were obtained for the 2D and 3D models, respectively.

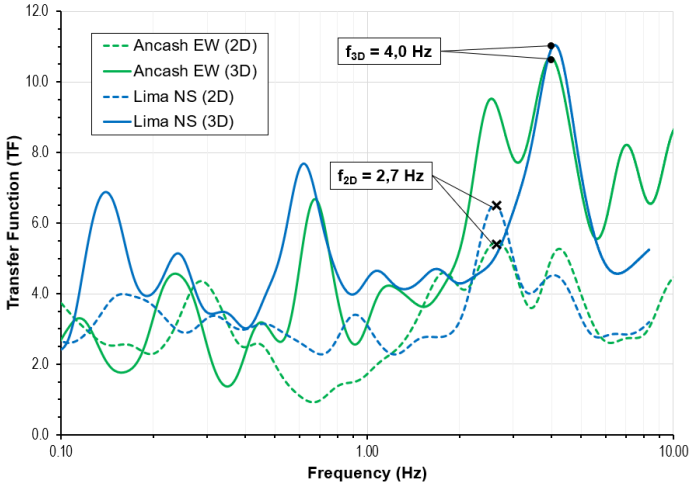

Figure 12. Smoothed crest-to-base transfer functions of the 2D and 3D numerical models

Approximating the geometry of the canyon, where the dam will be located to a triangular or narrow trapezoidal shape, and considering a crest length to dam height ratio of 2.9, a range of values between 0.64 and 0.77 was obtained for the ratio between the 3D and 2D fundamental periods under the criteria defined by Gazetas and Dakoulas, 1992. The ratio T_{3D}/T_{2D} of the dam under analysis is 0.68, which is within the range mentioned above.

5. Conclusions

According to the results of the dynamic analyses, higher values of displacements and deformations were obtained from the 2D dynamic analyses. This is because the dam's rock abutments generate a confinement effect, a behavior that the 2D model does not capture. However, the acceleration values are higher in the 3D dynamic analysis, due to the amplification effect induced by the topography of the canyon.

It can be observed that the structural period obtained for the 2D model is greater than that for the 3D model, which shows a marked dependence of the dynamic period on the geometry of the dam (L/H ratio) as well as on the topography of the canyon. This behavior persists even when considering the actual topography of the site, rather than a simplified approximation.

In terms of functionality and serviceability, the maximum settlement induced at the dam crest (1.05 m) remains below the available freeboard (2.50 m), indicating that overtopping of the reservoir is not expected under the evaluated seismic conditions. Additionally, the deformations recorded within the dam body are of low to moderate magnitude and spatially localized, with no evidence of deformation mechanisms indicative of potential failure surfaces that could compromise the overall structural stability of the dam.

The results obtained in this study show a notable difference between the two-dimensional and three-dimensional dynamic response of the dam, highlighting the importance of incorporating three-dimensional geometric conditions in the evaluation of the dynamic response for a more accurate representation of structural behavior. This observation underscores the need to consider such three-dimensional effects in the design of earth dams, as neglecting them could lead to an underestimation or misrepresentation of key parameters related to seismic performance, potentially compromising the safety and reliability of the structure.

Acknowledgements

The authors would like to express their sincere gratitude to the mining consulting firm Anddes, based in Peru, for the field and laboratory information provided, as well as for funding this research.

References

Barton, N. (2013). Shear strength criteria for rock, joints, rockfill and rock masses: problems and some solutions. *J. Rock Mech. Geotech.,* 5, 249.

Brinkgreve, R. B. J., Kappert, M. H., and Bonnier, P. G. (2007). *Hysteretic damping in a small-strain stiffness model*. Tenth International Symposium on Numerical Models in Geomechanics X, Rhodes, Greece, 737.

Darendeli, M. B. (2001). *Development of a new family of normalized modulus reduction and material damping curves*. University of Texas at Austin, USA.

Gazetas, G., and Dakoulas, P. (1992). Seismic analysis and design of rockfill dams: state-of-the-art. *Soil Dyn. Earthq. Eng.*, 11(1), 27.

Hammam, A. H., and Eliwa, M. (2013). Comparison between results of dynamic & static moduli of soil determined by different methods. *HBRC J.*, 9(2), 144.

Hardin, B. O. and Black, W. L. (1969). Closure to Vibration modulus of normally consolidated clay. *J. Soil Mech. Found. Div.*, 95(6), 1531.

Hwang, J. H., Wu, C. P., Wang, S.C. (2007). Seismic record analysis of the Liyutan earth dam. *Can. Geotech. J*. 44(11), 1351.

Kokusho, T., and Esashi, Y. (1981). *Cyclic triaxial test on sands and coarse materials*. 10th international conference on soil mechanics and foundation engineering, Stockholm, Sweden, 1, 673.

Konno, K., and Ohmachi, T. (1998). Ground-motion characteristics estimated from spectral ratio between horizontal and vertical components of microtremor. *Bull. Seismol. Soc. Am*. 88, 228.

Kuhlemeyer, R. L., and Lysmer, J. (1973). Finite element method accuracy for wave propagation problems, *J. Soil Mech. Found. Div.*, 99, 421.

Mejía, L. H., and Seed, H. B. (1983). Comparison of 2-D and 3-D dynamic analyses of earth dams. *J. Geotech. Eng.*, 109(11), 1383.

Plaxis (2023). *Plaxis 2D reference manual*.

Rollins, K. M., Evans, M. D., Diehl, N. B. et al. (1998). Shear modulus and damping relationships for gravels. *J. Geotech. Geoenviron. Eng.*, 124(5), 396.

Rollins, K. M., Singh, M., and Roy, J. (2020). Simplified equations for shear-modulus degradation and damping of gravels. *J. Geotech. Geoenviron. Eng.*, 146(9), 04020076.

Schnabel, P. B. (1973). Effects of local geology and distance from source on earthquake ground motions. University of California, Berkeley.

Seed, H. B., Wong, R. T., Idriss, I. M. et al. (1986). Moduli and Damping Factors for Dynamic Analyses of Cohesionless Soils. *J. Geotech. Eng.*, 112(11), 1016.

GeosciRA25

Book of Abstracts and Contributed Papers
International Conference on Recent Trends in Geoscience Research and Applications 2025 Belgrade, Serbia and Virtual, 15–19 September 2025
Editors: Aleksandra Nina, Snežana Dragović, Maja Kuzmanoski, Milan Đorđević, and Mrđan Đokić

https://doi.org/10.46793/Geoscira25.067A

Original scientific paper
Contributed paper

COMPARISON OF METHODS FOR MACROSEISMIC MAPPING: A CASE STUDY OF THE 2016 DEBARCA-PLAKENSKA EARTHQUAKE

Monika ANDREESKA[1*], Svemir GORIN[2], Katerina DROGRESHKA[3], Jasmina NAJDOVSKA[3]

[1]Seismological Observatory, Faculty of Natural Sciences and Mathematics, Skopje, North Macedonia; e-mail: mandreeska@pmf.ukim.mk
[2]Institute of Geography, Faculty of Natural Sciences and Mathematics, Skopje, North Macedonia; e-mail:svemir@pmf.ukim.mk
[3]Seismological Observatory, Faculty of Natural Sciences and Mathematics, Skopje, North Macedonia; e-mails: katerinadrogreska@pmf.ukim.mk, najdovskaj@pmf.ukim.mk

Abstract: The isoseismal map can directly reflect the damage degree of an earthquake, and it is an image representation of a seismic influence field or ground motion intensity field. This paper presents a comparative analysis of three methods used for generating macroseismic maps: manual isoseismal drawing, geostatistical interpolation method kriging and deterministic interpolation method natural neighbor. The objective is to test whether more automated methods can support the process of macroseismic mapping and reduce the subjectivity involved in manually drawn isoseismal lines. The analysis is based on data collected from earthquake that occurred on May 21, 2016, in the epicentral area Debarca-Plakenska, in the Republic of North Macedonia. A total of 82 intensity points, based on the European Macroseismic Scale, were supplemented with 17 additional intensity II points to ensure adequate closure of the macroseismic field and enhanced interpolation accuracy. The findings underscore the importance of selecting interpolation methods based on data characteristics. This research highlights the importance of properly collecting complete macroseismic data. Through the calculation examples, the best choice for this case study is the kriging interpolation method, which can be used to directly build a macroseismic field through intensity points.

Keywords: isoseismal map; GIS; interpolation methods; earthquake;

1. Introduction

The Republic of North Macedonia is situated in a seismically active region (Drogreshka et al., 2022), where one of the key approaches to earthquake interpretation involves analyzing its effects on people and material assets. A crucial tool in this process is the use of isoseismal maps, which depict the distribution of seismic intensity using the European Macroseismic Scale (EMS), categorized from level 1 to 12 (Grunthal, 1998,

*Corresponding author

Wald et al., 2024). The impact of an earthquake is influenced by several factors including local geology, topography, attenuation characteristics, earthquake magnitude, and the depth of the hypocentre (Schenková et al., 2007; Sirovich et al., 2002). As part of a broader inquiry into the methodologies for constructing isoseismal maps in Europe, a targeted survey was conducted among seismological institutes. The aim was to identify prevailing practices and to assess whether formalized guidelines exist within institutions. The Czech Republic primarily relies on manual drawing of isoseismal lines, occasionally supplemented with kriging, though the latter reportedly has minimal impact on results. In Greece, systematic macroseismic mapping is no longer practiced, instead, public DYFI (Did You Feel It?) data are utilized. Historical intensity maps and atlases have been published using the manual drawing method. In Hungary, isoseismal maps have traditionally been created manually through expert interpretation of seismic data, however, there is currently a shortage of qualified personnel to perform this work. Slovenia has deliberately discontinued the use of isoseismal lines due to concerns over subjectivity. Instead, only intensity data points are visualized, as studies have shown large discrepancies among experts in drawing isoseismals. Italy employs advanced interpolation methods, particularly kriging, to generate smoothed intensity fields. Their methodology is documented in several scientific publications, and real-time macroseismic impact reports. In the case of North Macedonia, macroseismic maps are produced by the Seismological Observatory at the Faculty of Natural Sciences and Mathematics in Skopje, the country's only official earthquake monitoring institution. While earlier maps were hand-drawn, the observatory has since transitioned to GIS-based workflows (QGIS and ArcMap), enabling faster and more integrated analysis.

This study evaluates three approaches for generating isoseismal maps from: manual drawing, geostatistical interpolation using kriging, and deterministic interpolation using the natural neighbor method in ArcMap 10.8.2. These mapping methods were selected for comparison because, based on the available literature and the conducted survey, they are the most widely recognized and utilized approaches, whereas other existing methods are less documented or less commonly applied. The objective is to determine which of these methods most accurately captures the spatial distribution of macroseismic intensity for the 2016 Debarca-Plakenska earthquake.

2. Data and methods

The analyzed earthquake occurred on May 21, 2016, at 16:41 UTC, in the southwestern region of the Republic of North Macedonia, with an epicenter located near Plakenska Mountain (20.99°E, 41.23°N), approximately 18 km northeast of the city of Ohrid. The earthquake had a local magnitude (ML) of 4.8 and a focal depth of 15 km, with a maximum felt intensity of VI on the European Macroseismic Scale. The area lies within a seismically active zone along the Western-Macedonian fault system, characterized by complex tectonic settings and predominantly Paleozoic and Mesozoic metamorphic and sedimentary rocks (Petrushev, 2021). The local geology includes fractured schists, marbles, and flysch formations, which, combined with topographic effects, may contribute to variations in macroseismic intensity across short distances. Structural damage was limited but included minor cracks in older masonry buildings and instances of fallen plaster or tiles. For this analysis, a dataset of 82 intensity observations was utilized, collected from field questionnaires and citizen reports, and supplemented

by synthetic isoseismals introduced in populated cities where earthquake effects are typically reported. These synthetic points, assigned an intensity of II in areas lacking observed data, were used to support the delineation of the outermost isoseismal, reflecting the practice that seismic effects of low intensity are usually reported in urban centres.

Manual drawing method is the earliest and most traditional approach to isoseismal mapping, with its origins dating back to the early 19th century (Varga, 2008). It involves drawing isoseismal lines by hand, based on expert interpretation of data such as eyewitness reports, building damage and observations of the earthquake's impact. However, it is inherently subjective and can vary between analysts, making it less reproducible and unsuitable for automated or large-scale analyses (Cecic, 1996). Kriging, a geostatistical interpolation method developed in the 1960s offers a more mathematical and data-driven alternative. It estimates unknown values by modeling the spatial correlation among known observations, providing not only predicted values but also estimates of the uncertainty associated with each point (De Rubies et al., 2005, Linkimer, 2007). The natural neighbor method is a deterministic interpolation technique based on Voronoi diagrams, which calculates values at unknown points using weighted contributions from the surrounding observations (Sirovich et al., 2002, Pettenati et al., 1999). Debarca-Plakenska Mountain epicentral area exhibits low to moderate seismic activity over the period from 1900 to 2023. A total of 1250 earthquakes with ML up to 4.8 (case study) have been recorded.

3. Results

By combining observed and synthetic data, a detailed manually drawn isoseismal map was developed for the case study earthquake (Figure 1).

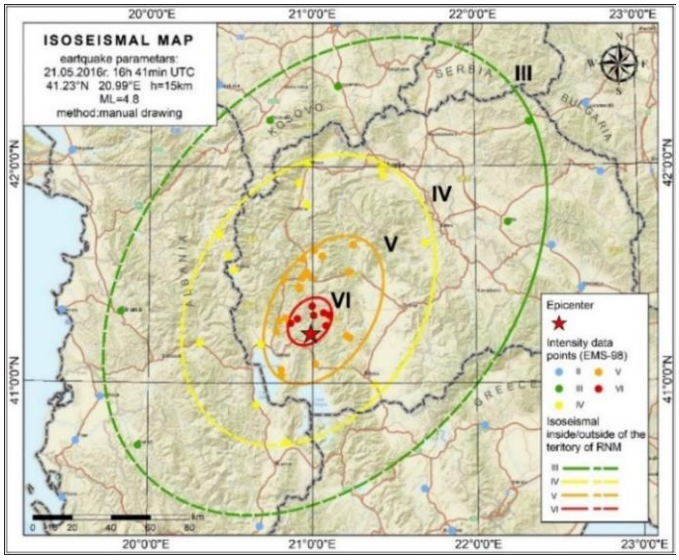

Figure 1. Isoseismal map of the case study earthquake using manual drawing generated in ArcMap 10.8.2

Statistical analysis of the raw intensity data revealed a mean value of 4.48, median of 4.6, and standard deviation of 1.21, with a skewness of -0.27 and kurtosis of 1.78, indicating a near-normal distribution. To enhance the dataset's suitability for geostatistical modeling, a logarithmic transformation was applied, resulting in improved statistical properties: skewness of -0.57, kurtosis of 2.04, and a reduced standard deviation of 0.29. These adjustments help stabilize variance and reduce the impact of outliers, which is essential for producing a reliable and unbiased semivariogram in kriging interpolation. The macroseismic intensity map using kriging interpolation methods (Figure 2) was created based on results from exploratory interpolation analysis (Table 1).

Table 1. Performance metrics of kriging methods using ArcPro's exploratory interpolation tool

Interpolation type	RMSE	ME	MESTD	RMSESTD	ASE	MAX ERROR	PERC ERROR
Empirical Bayesian Kriging - Default	**0.12**	**-0.01**	**-0.08**	**0.81**	**0.21**	**0.40**	**90.26**
Ordinary Kriging – Optimized	**0.12**	**0.00**	**-0.02**	**0.53**	**0.35**	**0.40**	**89.93**
Empirical Bayesian Kriging - Advanced	**0.12**	**-0.01**	**-0.10**	**1.00**	**0.14**	**0.43**	**89.87**

ArcPro's exploratory interpolation tool was utilized to identify the most suitable kriging model among universal, ordinary, and Empirical Bayesian Kriging (EBK). EBK default showed the best performance, with highest prediction accuracy. To further evaluate the reliability of the map, a prediction standard error map was generated. This additional layer visually represents the spatial distribution of uncertainty associated with the intensity predictions, highlighting areas where the model exhibits higher or lower confidence.

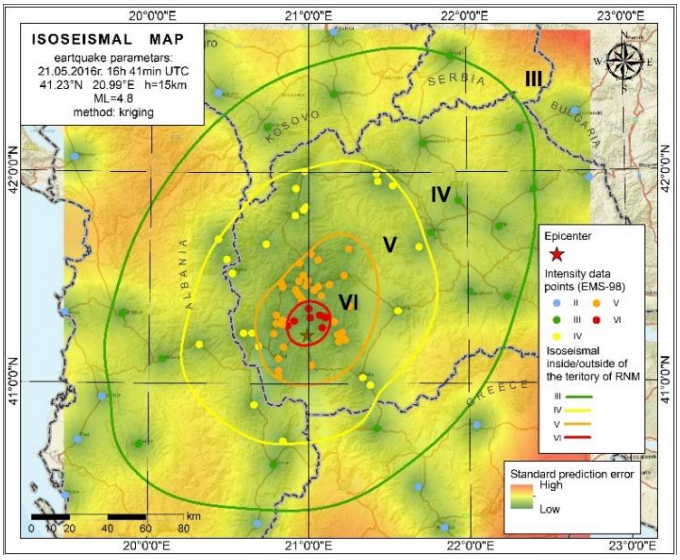

Figure 2. Isoseismal map of the case study earthquake using kriging interpolation generated in ArcMap10.8.2

The isoseismal map (Figure 3) was created using the natural neighbor interpolation method, which accurately represents the distribution of earthquake intensity by estimating values in unsampled areas based on nearby data points. Natural neighbor operates using default parameters in all cases. This approach produces a clear visualization of the spatial seismic intensity distribution.

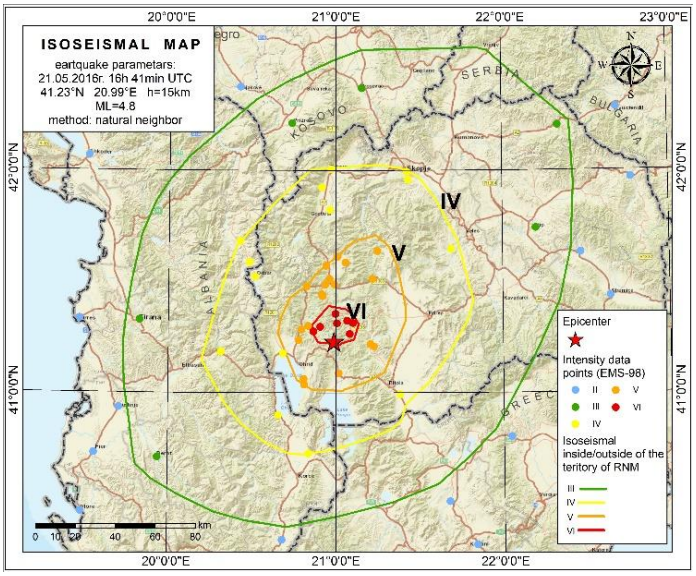

Figure 3. Isoseismal map of the case study earthquake using the natural neighbor interpolation method generated in ArcMap 10.8.2

4. Discussion

Each of the three evaluated methods for macroseismic mapping presents distinct advantages and limitations. The manual drawing method allows expert judgment to account for local geological and contextual knowledge, especially in data-sparse regions. However, it is inherently subjective, lacks reproducibility, and results can vary between analysts. The natural neighbor interpolation method preserves sharp local variations and is simple to implement, making it suitable for preliminary analyses, however, it does not provide uncertainty estimates and may produce fragmented contours not fully aligned with expected seismic attenuation. Kriging, as a geostatistical method, offers the most statistically robust and reproducible results, producing smooth intensity fields and quantifying uncertainty through prediction error maps. It aligns well with expected patterns of intensity decay, making it the most consistent with theoretical and empirical models of ground motion. This method reflects the expected smooth and gradual decrease in seismic intensity with increasing distance from the epicenter, in line with both seismic wave propagation theory, which explains how seismic waves spread and attenuate as they move through the Earth, and patterns observed in real earthquake data.

For seismological services, the practical recommendation is to adopt kriging when sufficient intensity data are available, due to its objectivity and added analytical value. Manual methods may still be useful in cases of low data density or historical events. In general, a combined approach, where automated methods are supplemented with expert review, could offer the best balance.

5. Conclusion

This study compared manual, natural neighbor, and kriging methods for macroseismic mapping of the 2016 Debarca-Plakenska earthquake. Kriging was identified as the most suitable method, offering spatial coherence, reproducibility, and error assessment. It is recommended as the preferred approach for future studies and official macroseismic mapping when data availability allows. In summary, while all methods yielded useful spatial insights, kriging provided an effective balance between detail and generalization, offering a reproducible alternative to subjective manual mapping techniques. Future work should also consider integrating additional parameters such as site effects, soil characteristics, and building vulnerability to further refine intensity modeling and improve the relevance of these maps for civil protection and risk mitigation planning.

References

Cecić, I., Musson, R. M. W., and Stucchi, M. (1996). Do seismologists agree upon epicentre determination from macroseismic data?. *Ann. Geofis.*, 39(5), 1013.

De Rubeis, V., Tosi, P., Gasparini, C., et al. (2005). Application of Kriging Technique to Seismic Intensity Data. *Bull. Seismol. Soc. Am.*, 95(2), 540.

Drogreshka, K., Molerovikj, I., Najdovska, et al. (2022). Series of earthquakes from the border epicentral area Bitola–Florina in January 2022. *Geografski Razgledi*, 55, 75.

Grünthal, G. (1998). European Macroseismic Scale 1998. *Cah. Cent. Eur. Géodyn. Séismol.*, 15, 1.

Linkimer, L. (2008). Application of the Kriging method to draw isoseismal maps of the significant 2002-2003 Costa Rican earthquakes. *Rev. geol. Am. cent.*, 38, 119.

Pettenati, F., Sirovich, L., and Cavallini, F. (1999). Objective treatment and synthesis of macroseismic intensity data sets using tessellation. *Bull. Seismol. Soc. Am.*, 89(5), 1203.

Petrušev, B., and Serafimovski, T. (2021). Geological characteristics of the Republic of North Macedonia. *Geol. Maced.*, 35(1), 13.

Schenková, Z., Schenk, V., Kalogeras, et al. (2007). Isoseismal maps drawing by the kriging method. *J. Seismol.*, 11(3), 345.

Sirovich, L., Cavallini, F., Pettenati, F., et al. (2002). Natural-neighbor isoseismals. *Bull. Seismol. Soc. Am.*, 92(5), 1933.

Varga, P. (2008). History of early isoseismal maps. *Acta Geod. Geophys. Hung.*, 43(2–3), 285.

Wald, D. J., Goded, T., Hortacsu, A., et al. (2024). Developing and implementing an International Macroseismic Scale (IMS) for earthquake engineering, earthquake science, and rapid damage assessment. *U.S. Geological Survey Open-File Report* 2023-1098.

Book of Abstracts and Contributed Papers
International Conference on Recent Trends in Geoscience Research and Applications 2025 Belgrade, Serbia and Virtual, 15–19 September 2025
Editors: Aleksandra Nina, Snežana Dragović, Maja Kuzmanoski, Milan Đorđević, and Mrđan Đokić

https://doi.org/10.46793/Geoscira25.073L

Original scientific paper
Contributed paper

DETECTION OF VLF TRANSMITTERS USING THE ViTRANSFORMER DEEP LEARNING ALGORITHM

Danilo LAZOVIĆ[1*], Olivera PRONIĆ-RANČIĆ[2], Aleksandra NINA[3], Jovan BAJČETIĆ[1,4]

[1]Khaoticen doo, Belgrade, Serbia; e-mails: danilo.lazovic136@gmail.com, bajce05@gmail.com
[2]University of Niš, Faculty of Electronic Engineering, Niš, Serbia; e-mail: olivera.pronic@elfak.ni.ac.rs
[3]Institute of Physics Belgrade, National Institute of the Republic of Serbia, University of Belgrade, Belgrade, Serbia; e-mail: sandrast@ipb.ac.rs
[4]Professional Science and Technology, Zrenjanin, Serbia; e-mail: jbajcetic@pro-sci-tech.com

Abstract: Radio signals of very low frequency (VLF) are used for monitoring the lower ionosphere. Their analysis provides information about ionospheric perturbations in the areas between the transmitter and the receiver of the observed signal, caused by phenomena in space and within Earth's layers. The research presented in this paper demonstrates the capabilities of the ViTransformer neural network for detecting VLF transmitters using images. The images used in this study represent a two-dimensional visualization of the signal emitted by a VLF transmitter and received by a corresponding receiver. For training and testing, the data recorded at the Institute of Physics in Belgrade were used. The database employed contains recorded signals emitted from three different VLF transmitters located in different parts of the world (Germany, the United States, and Australia). The research results show that using the ViTransformer neural network makes it possible to perform classification with high accuracy, reaching nearly 95%.

Keywords: ViTransformer, detection, VLF transmitter.

1. Introduction

The sky component of very low frequency (VLF) electromagnetic waves, which range from 3 to 30 kHz, exhibits low attenuation, making it suitable for long-distance information transmission. This characteristic makes VLF signals particularly suitable for observing the upper atmosphere, specifically the regions below the altitude at which they are reflected. Depending on conditions, these reflections occur at altitudes above 50 km during intense disturbances caused primarily by strong solar radiation during X-ray solar flares, and up to around 85 km during nighttime conditions. (Silber et al., 2017)

The significance of such observations lies not only in the investigation of the characteristics of the lower ionospheric plasma but also in the indirect detection of

*Corresponding author

phenomena that perturb this atmospheric region. These phenomena have sources both in space (e.g., solar radiation, solar energetic particles from our galaxy and others, and the entry of small celestial bodies) and within Earth's layers — primarily the atmosphere and lithosphere. Terrestrial sources cause local perturbations, and the widespread presence of VLF transmitters and receivers allows for their detection (Silber et al., 2017).

This is especially important for investigating potential precursors, characteristics and subsequent processes of natural disasters, as well as for their analysis, and enabling more efficient mitigation and management of their consequences. Such events include earthquakes, tropical cyclones, lightning strikes, volcanic eruptions, and similar phenomena (Silber et al., 2017, Boudjada et al., 2024).

The importance of analyzing these signals has motivated us to classify them based on the shape of their daily amplitude variations, which differ depending on the locations of the transmitter and receiver and the conditions under which the signal propagates through the so-called Earth-ionosphere waveguide. The existence of a global network for their detections has prompted us to apply deep learning algorithms to classify VLF transmitter radio signals (Silber et al., 2017, Nina, 2024).

In this study, we performed classification based on radio signals received by the Absolute Phase and Amplitude Logger (AbsPAL) receiver located at the Institute of Physics Belgrade (Belgrade, Serbia), geographic coordinates 44°51'18"N 20°23'27"E. This technique involves analyzing received signals and processing them using machine learning or deep learning algorithms. Although classical machine learning algorithms continue to yield good results—particularly in certain domains—deep learning algorithms have become dominant in tasks involving large amounts of unstructured data. These algorithms have been widely adopted in the field of RF signal classification because they allow for the processing of large datasets and enable practical use of a model once it has been trained (Nina, 2024).

There are numerous cases where deep learning algorithms outperform traditional machine learning algorithms. (Lai, 2019). The advantage of deep learning lies in its ability to automatically extract relevant features and perform the learning process during neural network training. The downside, however, is the need to provide a database containing labeled samples for each class to ensure proper model training (Lai, 2019).

2. ViT Deep Learning Algorithm

The Transformer neural network architecture was introduced in 2017 and has become highly dominant in recent years. It has largely replaced recurrent neural networks (RNNs) in nearly all-natural language processing (NLP) tasks. All major large language models today are based on the Transformer architecture (Ashish et al., 2017).

Although originally developed for tasks such as translation, Transformers are no longer limited to NLP. Recently, their application has expanded to other domains, including image and video processing, as well as DNA sequence prediction (Ashish et al., 2017).

Since this work uses the ViTransformer algorithm, it is important to note that its architecture is very similar to that of the original Transformer used in NLP. The original Transformer was designed to process sequential data, whereas images are spatial in nature. Assigning a token to each pixel would be computationally expensive. To address this, ViTransformer divides an image into small patches (typically 16×16 pixels), and the

resulting sequence of patches is used as the model's input (Ashish et al., 2017).

Each patch is flattened into a one-dimensional vector and passed through a lower-level linear layer. Positional and class embeddings are added to these vectors, and the sequence is then fed into a standard Transformer encoder. The encoder architecture in ViTransformer is the same as that of the original Transformer (Vakanski, 2023).

According to the literature, there are three main variants of the ViTransformer neural network:

- Base – 12 encoder blocks, 768 hidden dimensions, 86 million parameters
- Large – 24 encoder blocks, 1024 hidden dimensions, 307 million parameters
- Huge – 32 encoder blocks, 1280 hidden dimensions, 632 million parameters

Several variants of the ViTransformer network (such as MaxViT, Swin, DeiT, and T2T-ViT) have outperformed convolutional neural networks (CNNs) such as EffNet, ConvNeXt, and NFNet in terms of classification performance (Vakanski, 2023).

3. Model Description for VLF Signal Detection and Classification

The classification model developed as part of this study was designed to enable straightforward classification of VLF radio signals into three classes: "0", "1", and "2". These correspond to the VLF signals received from different transmitters: DHO (Germany), NAA (United States), and NWC (Australia), respectively. A neural network model was developed (Figure 1) and evaluated based on training accuracy, training loss, validation accuracy, and validation loss, under different complexity settings of the ViTransformer deep learning algorithm.

The ViTransformer neural network, which takes 2D images as input, was used in this study (Figure 2). These images represent 24-hour recordings of signal amplitude from a single VLF transmitter. To expand the image dataset and improve training efficiency, geometric augmentation techniques were applied. Of the total number of images, 60% were used for training, 20% for testing, and 20% for validation.

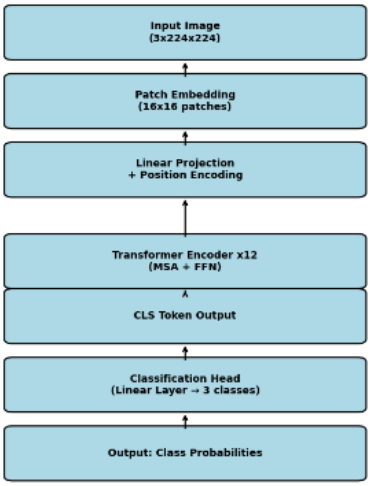

Figure 1. Visual representation of the Neural Network Model

Four different configurations were planned to optimize the network, aiming to balance the number of training epochs, detection accuracy, and training time. In all configurations, the models.vit_l_16 implementation of the ViTransformer algorithm was used.

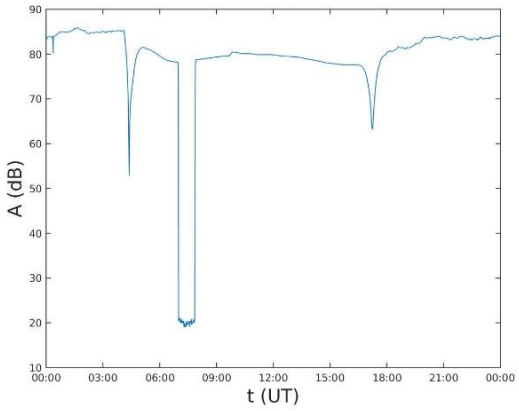

Figure 2. Example of a signal image from one of the VLF transmitters

For all three signal classes used in each configuration, 258 images were used per class, resulting in a total of 774 images.

4. Simulation

The ViTransformer neural network model was trained on the data described above, using four different configurations with varying numbers of epochs for each. Training accuracy is defined as a unitless measure ranging from 0 to 1. Accuracy represents the ratio of correct predictions to the total number of predictions, depending on the number of epochs for all four configurations (Figure 3). Figure 3 shows training and validation loss and accuracy as functions of the number of epochs.

Table 1. Summary of the final training accuracy and training loss values for each configuration.

Configuration	Epochs	Training Accuracy	Training Loss	Validation Accuracy	Validation Loss
First	5	0.87715	0.40681	0.95454	0.23943
Second	10	0.93534	0.19609	0.96103	0.13073
Third	15	0.94827	0.16720	0.96103	0.10466
Fourth	20	0.94827	0.16720	0.96103	0.10466

Based on the results, the following conclusions can be drawn:

- Considering the training accuracy criterion, it can be seen in Table 1 that, except for the first configuration, the accuracy in all other configurations is above 90%.
- The training losses in the second, third, and fourth configurations are also

notably low.

- Regarding validation accuracy and validation loss, all configurations, except the first, show similar or identical results.
- The first configuration performed worse across all four metrics, with final training and validation accuracy values of approximately 0.96103.
- The third configuration represents a compromise between training speed, accuracy, and input data complexity, making it optimal for deployment in an information system intended to operate in real time.

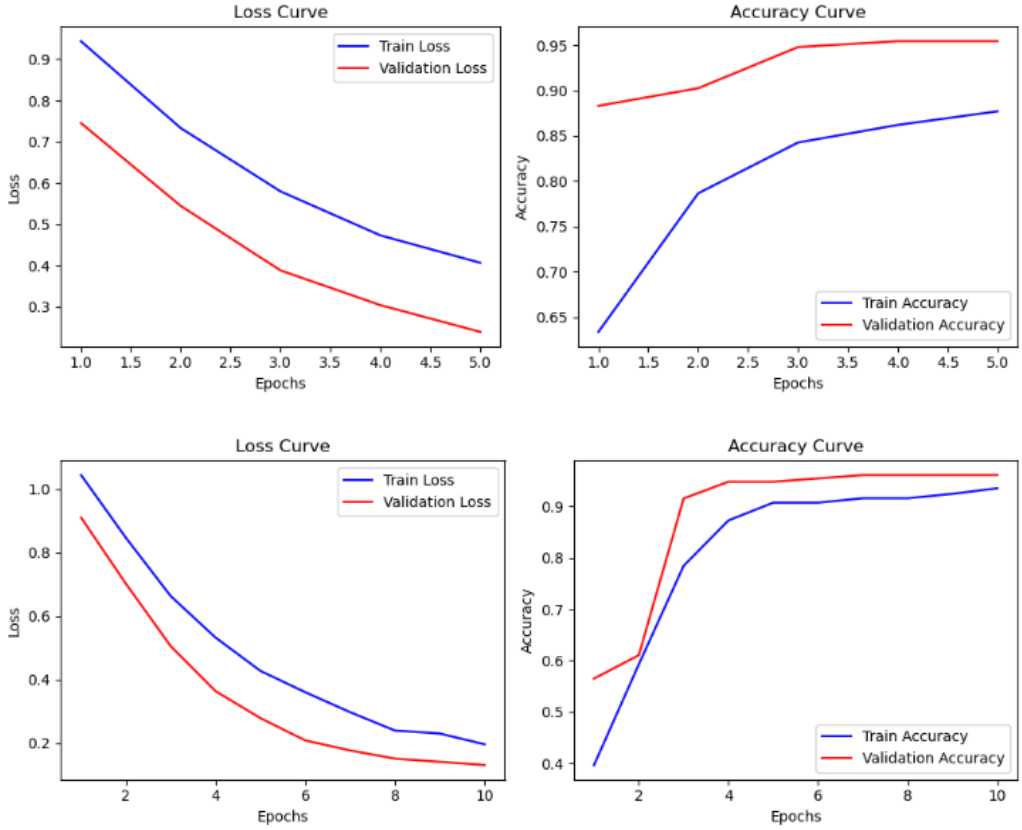

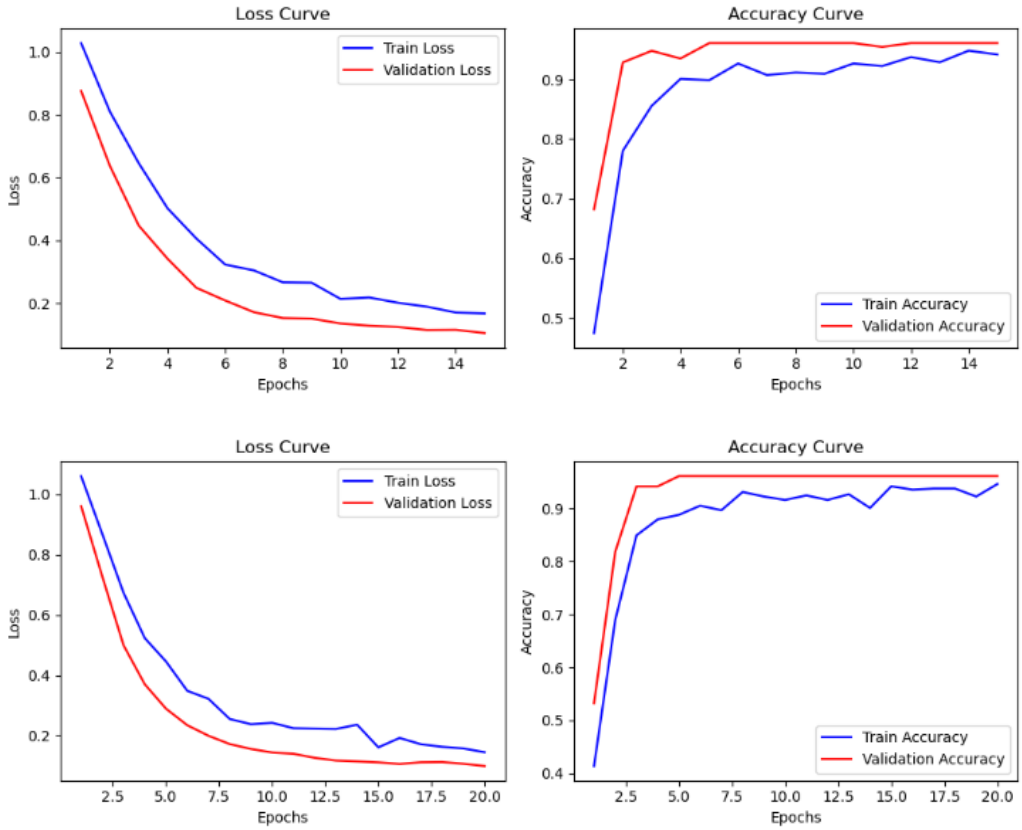

Figure 3: Loss (left panels) and accuracy (right panels) for the first to fourth configurations presented in the first to forth rows, respectively

The full performance of the network is further illustrated by the confusion matrices for all four configurations. Confusion matrices graphically represent classification performance by showing the number of images assigned to each predicted class.

From the confusion matrices, the following observations can be made:

1. The first configuration produced the most errors when classifying signals from transmitter “1”, often misclassifying them as transmitter “2.”
2. It is also evident that the greatest classification challenges involved mixing signals from transmitters “1” and “2”, as well as between “0” and “1”.

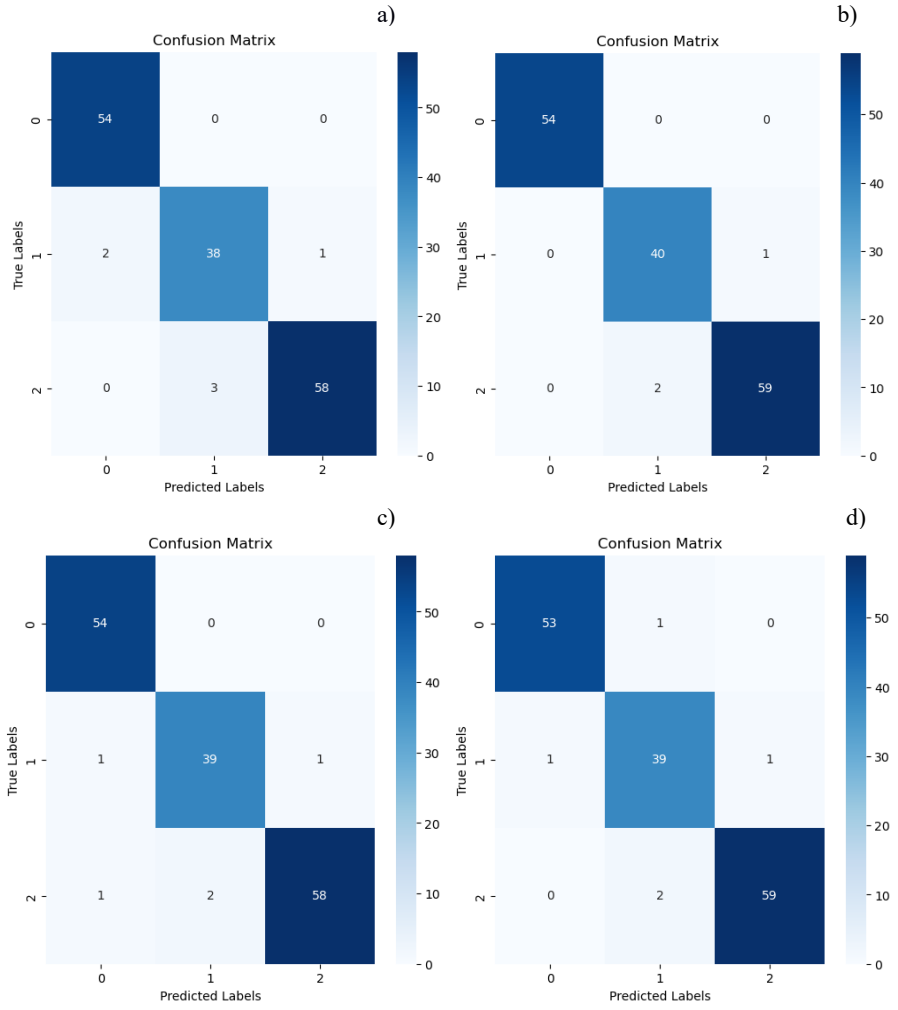

Figure 4: Confusion matrix for the first (a), second (b), third (c) and fourth (d) configuration

5. Conclusion

This paper presents an optimal deep learning model capable of classifying radio emissions from VLF transmitters into three distinct classes with high probability. It has been demonstrated that the use of the ViTransformer model provides strong prediction and classification results with fewer training epochs, achieving higher accuracy and lower training losses.

Additionally, the importance of properly defining and preparing a database containing images of various VLF transmitter radio signals for each configuration is evident.

Future research and improvements to the ViTransformer algorithm will focus on

increasing the number of classes, as well as the detection and classification of a larger variety of states in which radio emissions can occur, along with expanding the total number of radio signals analyzed.

Acknowledgements

The authors acknowledge funding provided by the Institute of Physics Belgrade through the grants by the Ministry of Science, Technological Development and Innovation of the Republic of Serbia.

References

Silber, I., and Price, C. (2017). On the Use of VLF Narrowband Measurements to Study the Lower Ionosphere and the Mesosphere–Lower Thermosphere. *Surv. Geophys.*, 38, 407.

Seybold, J. S. (2005). *Introduction to RF Propagation.* John Wiley and Sons, *New Jersey*, USA.

Lai, Y. (2019). A Comparison of Traditional Machine Learning and Deep Learning in Image. *J. Phys.: Conf. Ser.,* 1314, 012148

Vaswani, A., Shazeer, N., Parmar, N. et al. (2017). Attention Is All You Need. 31st Conference on Neural Information Processing Systems, Long Beach, CA, USA.

Vakanski, A. (2023*).* Lecture 20 - Transformer Networks. https://fall-2023-python-programming-for-data-science.readthedocs.io/en/latest/Lectures/Theme_3-Model_Engineering/Lecture_20-Transformer_Networks/Lecture_20-Transformer_Networks.html#20.9-Vision-Transformers.

Boudjada, M. Y., Biagi, P. F., Eichelberger, H. U. et al. (2024). Analysis of Pre-Seismic Ionospheric Disturbances Prior to 2020 Croatian Earthquakes. *Remote Sens*., 16, 529.

Nina, A. (2024). Analysis of VLF Signal Noise Changes in the Time Domain and Excitations/Attenuations of Short-Period Waves in the Frequency Domain as Potential Earthquake Precursors. *Remote Sens*., 16, 397.

Nina, A., Pulinets, S., Biagi, P. F. et al. (2020). Variation in natural short-period Ionospheric noise, and acoustic and gravity waves revealed by the amplitude analysis of a VLF radio signal on the occasion of the Kraljevo earthquake (Mw = 5.4). *Sci. Total Environ*., 710, 136406.

Nina, A., Radovanović, M., Milovanović, B. et al. (2017). Low ionospheric reactions on tropical depressions prior hurricanes. *Adv. Space Res.* 60, 1866.

Price, C., Asfur, M., Yair, Y. et al. (2009). Maximum hurricane intensity pre-ceded by increase in lightning frequency. *Nat. Geosci*., 2, 329.

POSTERS

GeosciRA25

Book of Abstracts and Contributed Papers
International Conference on Recent Trends in Geoscience Research and Applications 2025 Belgrade, Serbia and Virtual, 15–19 September 2025
Editors: Aleksandra Nina, Snežana Dragović, Maja Kuzmanoski, Milan Đorđević, and Mrđan Đokić

Original scientific paper
Abstract

PRELIMINARY EVALUATION OF CLOUD ENHANCEMENT EVENTS OVER THE SOUTH-WEST OF BUCHAREST, ROMANIA

Emil CARSTEA[1], Konstantinos FRAGKOS[2], Mariana ADAM[1*]

[1]National Institute of Research and Development for Optoelectronics - INOE 2000, Magurele, Romania; e-mails: emil.carstea@inoe.ro, mariana.adam@inoe.ro
[2]Climate and Atmosphere Research Center, the Cyprus Institute, Nicosia, Cyprus; e-mail: k.fragkos@cyi.ac.cy

Global horizontal irradiance (GHI) typically exhibits a well-defined profile under clear sky conditions; however, cloud coverage generally attenuates solar radiation incident on the Earth's surface, reducing overall GHI. Nevertheless, under specific circumstances, particularly involving broken or scattered cloud fields such as cumulus clouds, reflections and refractions of sunlight by cloud edges can increase surface GHI beyond clear sky levels, a phenomenon known as cloud enhancement (Castillejo-Cuberos and Escobar, 2020). These cloud enhancement events significantly influence local and regional irradiance variability, an essential consideration for accurate climate modelling. Climate models thus require region-specific observational data to accurately represent these typically underestimated phenomena. Additionally, short duration cloud enhancements events can lead to transient overproduction in photovoltaic systems, causing operational challenges, including potential energy losses. Therefore, continuous high-resolution observations, ideally at intervals of one minute or less, are crucial for accurately capturing the fine temporal and spatial characteristics of cloud enhancement events. The INO Station, located at Magurele Centre for Atmosphere and Radiation Studies (MARS), aims to deliver long-term, high-quality solar radiation measurements at a temporal resolution of one minute. Established in December 2019, the INO station successfully completed quality assurance and quality control (QA/QC) evaluations and has been an official member of the Baseline Surface Radiation Network (BSRN) since 2021, actively contributing data to the network (Carstea and Fragkos, 2024). This study aims to evaluate the occurrence of cloud enhancement events at the BSRN INO Station (Magurele, Romania), from January 2021 through December 2022, utilizing measured solar irradiance data alongside clear sky irradiance simulations using the McClear model from the Copernicus Atmosphere Monitoring Service (CAMS), which provide accurate estimation of clear-sky irradiance accounting for atmospheric parameters such as aerosol optical depth, total ozone concentration and water vapor.

*Corresponding author

Acknowledgements

The author E.C. acknowledges the support of the Romanian Ministry of Education and Research through the Core Program within the National Research, Development and Innovation Plan 2022-2027, Project PN 23 05 and partly by the European Commission under the Horizon Europe – Research and Innovation Framework Programme, through the PANORAMA project under grant agreement No 101182795.

References

Carstea, E., and Fragkos, K. (2024). *Optoelectron. Adv. Mat.*, 18(11-12), 562.
Castillejo-Cuberos, A., and Escobar, R. (2020). *Sol. Energy*, 209, 547.

GeosciRA25

Book of Abstracts and Contributed Papers
International Conference on Recent Trends in Geoscience Research and Applications 2025 Belgrade, Serbia and Virtual, 15–19 September 2025
Editors: Aleksandra Nina, Snežana Dragović, Maja Kuzmanoski, Milan Đorđević, and Mrđan Đokić

Original scientific paper
Abstract

SEGMENTATION OF SELECTED SOLAR CORONA STRUCTURES USING DEEP LEARNING

Peter BUTKA[1*], Martin SARNOVSKÝ[1], Viera KREŠŇÁKOVÁ[1], Ľubomír LAZOR[1]

[1]Department of Cybernetics and Artificial Intelligence, Faculty of Electrical Engineering and Informatics, Technical University of Kosice, Kosice, Slovakia;
e-mails: peter.butka@tuke.sk, martin.sarnovsky@tuke.sk, viera.kresnakova@tuke.sk, lubomir.lazor@student.tuke.sk

This work addresses the critical need for automated methods to analyze solar imagery, focusing on the segmentation of coronal holes and active regions in solar EUV images. These structures are key indicators of solar activity and are essential for space weather prediction. Traditional manual or heuristic methods are often time-consuming, instrument-sensitive, and struggle with the growing volume of data. The work leverages deep learning, specifically convolutional neural networks, to develop precise and consistent automated segmentation models. Building on the U-Net-based SCSS-Net architecture, the work evaluates its performance and explores modifications and improvements of original SCSS-Net model (Mackovjak et al., 2021). A core contribution is the development of a new data pipeline using images from both SDO/AIA and GOES/SUVI, incorporating detailed preprocessing, automated quality checks, and a chronological data splitting strategy to enhance reliability and prevent data leakage. Combining theoretical background with practical modeling, the work details three experiments: implementing SCSS-Net with the new data, exploring an altered attention U-Net, and applying dynamic data augmentations to SCSS-Net. Augmentations such as flips, rotations, blurring, and distortions were used to improve model generalization, particularly for less obvious features. Evaluation using IoU, Dice, TPR, and FPR on internal and external datasets demonstrates that deep learning provides a reliable and scalable solution for solar structure segmentation, emphasizing the crucial role of thoughtful data handling and model design in achieving robust performance amidst domain-specific challenges like ambiguous boundaries. Our intent for the future is to provide the SCSS-Net as a service which can be used to support the space weather research and applications.

Acknowledgements

This work was supported by the project Development of SCSS-Net: Solar Corona Structures Segmentation algorithm by deep neural networks, within 1st Slovak RPA call under ESA Contract No. 4000143601/24/NL/MH/mp

**Corresponding author*

References

Mackovjak, S., Harman, M., Maslej-Krešňáková, V., and Butka, P. (2021). *Mon. Not. R. Astron. Soc*., 508(3), 3111.

GeosciRA25

Book of Abstracts and Contributed Papers
International Conference on Recent Trends in Geoscience Research and Applications 2025 Belgrade, Serbia and Virtual, 15–19 September 2025
Editors: Aleksandra Nina, Snežana Dragović, Maja Kuzmanoski, Milan Đorđević, and Mrđan Đokić

Original scientific paper
Abstract

TOWARDS UNDERSTANDING ASSOCIATIONS BETWEEN AIR POLLUTION AND MIGRATION: GEOSPATIAL ANALYSIS

Milica LANGOVIĆ[1*], Vladimir SREĆKOVIĆ[1], Marko PETROVIĆ[2]

[1] Institute of Physics Belgrade, National Institute of the Republic of Serbia, University of Belgrade, Belgrade, Serbia;
e-mails: milica.langovic@ipb.ac.rs, vlada@ipb.ac.rs
[2]Faculty of Geography, University of Belgrade, Belgrade, Serbia;
e-mail: marko.petrovic@rect.bg.ac.rs

The environment-migration nexus represents increasingly important research area in the age of intense anthropogenic pressures. Air pollution, as one of the major environmental issues, affects the migration intentions, shapes migration routes and determines the character of the migration cycle. The aim of this paper is to investigate the relationship between air pollution and international migration using the Air Quality Index (AQI) and PM2.5 data, and international migration data by country in 2024. The results of the Kruskal-Wallis test show that there is a statistically significant difference between the groups of countries characterized by different shares of international migrants in the total population, and clearly indicate that the countries in the group with the lowest share of international migrants face the highest level of air pollution. The countries that are characterized by adequate environmental conditions, in this case air quality, are those that attract the most international migrants. However, the question arises as to whether environmental conditions will deteriorate if these trends continue due to possible overpopulation in the countries with the highest proportion of migrants. Accordingly, the research findings may be relevant to the development of environmental strategies at global and regional levels, and thus important in the context of sustainable development.

Acknowledgements

The authors acknowledge funding provided by the Institute of Physics Belgrade through the grant by the Ministry of Science, Technological Development and Innovation of the Republic of Serbia.

*Corresponding author

GeosciRA25

Book of Abstracts and Contributed Papers
International Conference on Recent Trends in Geoscience Research and Applications 2025 Belgrade, Serbia and Virtual, 15–19 September 2025
Editors: Aleksandra Nina, Snežana Dragović, Maja Kuzmanoski, Milan Đorđević, and Mrđan Đokić

Original scientific paper
Abstract

USE OF MACHINE LEARNING FOR ANALYZING IONOSPHERIC SIGNAL PERTURBATIONS PRIOR TO EARTHQUAKES

Peter BEDNÁR[1*], Martin SARNOVSKÝ[1], Peter BUTKA[1], Aleksandra NINA[2], Vladimir SREĆKOVIĆ[2], Luka Č. POPOVIĆ[3], Aleksandra KOLARSKI[2], Filip ARNAUT[2]

[1]Department of Cybernetics and Artificial Intelligence, Faculty of Electrical Engineering and Informatics, Technical University of Kosice, Kosice, Slovakia; e-mails: peter.bednar@tuke.sk, martin.sarnovsky@tuke.sk, peter.butka@tuke.sk
[2] Institute of Physics Belgrade, National Institute of the Republic of Serbia, University of Belgrade, Belgrade, Serbia; e-mails: sandrast@ipb.ac.rs, vlada@ipb.ac.rs, aleksandra.kolarski@ipb.ac.rs, arnaut@ipb.ac.rs
[3]Department of Astronomy, Faculty of Mathematics, University of Belgrade, Belgrade, Serbia; e-mail: lpopovic@aob.rs

This work focuses on analyzing the relationship between changes in the ionosphere and earthquakes using machine learning methods. Recently, changes in the ionosphere have garnered increasing attention as potential indicators of approaching seismic events, with shifts in signal amplitude and frequency potentially offering valuable insights (Nina et al 2024). Data on ionospheric amplitude from several transmitters in Europe and earthquake data (mostly from Italy, Central Europe, and the Balkans) were used, focusing on earthquakes within a 250 km radius of the transmitter-receiver path. Data preprocessing included transforming time domain data into the frequency domain using the Fast Fourier Transform. The primary goal was to confirm the existence of a relationship between changes in the ionosphere and earthquakes through experiments conducted in both time and frequency domains using 6-hour data windows and also attempting a 15-minute earthquake prediction using a 3-hour window. Multiple models were developed, including traditional machine learning and neural networks. The linear SVM achieved the best performance in the time domain with a 74 % accuracy and 0.79 AUC, yielding similar results in the frequency domain (around 72 % for accuracy, precision, and F1-score). Neural networks in the frequency domain obtained metrics around 69-70 % (AUC approximately 0.73-0.75). The achieved results demonstrate that a relationship exists between changes in the ionosphere and earthquakes, as the models could identify earthquake features within the amplitude data. While the current accuracy is not sufficient for reliable prediction of seismic events, the work establishes a valuable foundation for further research.

*Corresponding author

Acknowledgements

This work was supported by the Slovak APVV agency Slovak-Serbian project SK-SRB-23-0029, and the Ministry of Science, Technological Development and Innovation of the Republic of Serbia (Serbian-Slovak project 337-00-3/2024-05/11). The authors acknowledge funding provided by the Institute of Physics Belgrade and the Astronomical Observatory (the contract 451-03-136/2025-03/200002) through the grants by the Ministry of Science, Technological Development and Innovation of the Republic of Serbia.

References

Nina, A. (2024). *Remote Sens.*, 16, 397.

GeosciRA25

Book of Abstracts and Contributed Papers
International Conference on Recent Trends in Geoscience Research and Applications 2025 Belgrade, Serbia and Virtual, 15–19 September 2025
Editors: Aleksandra Nina, Snežana Dragović, Maja Kuzmanoski, Milan Đorđević, and Mrđan Đokić

Original scientific paper
Abstract

A GLOBAL NETWORK OF VLF ANTENNAS FOR STUDYING PRE-SEISMIC IONOSPHERIC DISTURBANCES

Patrick H. M. GALOPEAU[1*], Mohammed Y. BOUDJADA[2], Hans U. EICHELBERGER[2], Ashanthi S. MAXWORTH[3], Pier Francesco BIAGI[4], Giovanni NICO[5]

[1]LATMOS-CNRS, UVSQ Université Paris-Saclay, Guyancourt, France;
e-mail: patrick.galopeau@latmos.ipsl.fr
[2]Space Research Institute, Austrian Academy of Sciences, Graz, Austria;
e-mails: mohammed.boudjada@oeaw.ac.at, hue@oeaw.ac.at
[3]University of Southern Maine, Gorham, ME, USA;
e-mail: ashanthi.maxworth@maine.edu
[4]Department of Physics, University of Bari, Bari, Italy; e-mail: pf.biagi@gmail.com
[5]Institute of Applied Mathematics, National Research Council, Bari, Italy;
e-mail: g.nico@ba.iac.cnr.it

In the framework of studying ionospheric variations, we present a system which records electromagnetic signals, in the Very Low Frequency (VLF: 3 kHz – 30 kHz) and Low Frequency (LF: 30 kHz – 300 kHz) ranges, 24 x 7 x 365. An individual system consists of a monopole antenna, a pre-amplifier, power supply, a central computer, a GPS unit, and a recording device (Galopeau et al., 2023). Several receivers will be implemented around the globe in a network. The first implementation of the system was done in Graz, Austria, the second one will be in Guyancourt (France), a third one in Réunion (France) and a fourth one in Moratuwa (Sri Lanka). Each reception device will allow a continuous daily monitoring of transmitter signals in the VLF and LF frequency bands. This network will be devoted to the study of ionospheric variations, in particular, those linked to the solar activity, but also those associated with seismic activity with the purpose of identifying electromagnetic earthquake precursors.

References

Galopeau, P. H. M., Maxworth, A. S., Boudjada, M. Y. et al. (2023). *Geosci. Instrum. Method. Data Syst.*, 12, 231.

**Corresponding author*

GeosciRA25

Book of Abstracts and Contributed Papers
International Conference on Recent Trends in Geoscience Research and Applications 2025 Belgrade, Serbia and Virtual, 15–19 September 2025
Editors: Aleksandra Nina, Snežana Dragović, Maja Kuzmanoski, Milan Đorđević, and Mrđan Đokić

Original scientific paper
Abstract

BEYOND ENVIRONMENTAL CONTEXT: A FRAMEWORK TO LINK SOLAR ACTIVITY AND FLOOD-INDUCED DISPLACEMENT

Milica LANGOVIĆ[1*], Vladimir SREĆKOVIĆ[1]

[1]Institute of Physics Belgrade, National Institute of the Republic of Serbia, University of Belgrade, Belgrade, Serbia; e-mails: milica.langovic@ipb.ac.rs, vlada@ipb.ac.rs

Considering the established relationship between Solar activity and natural disasters, the aim of this paper is to determine whether the processes resulting from natural disasters, such as population displacement, could also be linked to the dynamics of solar activity. Since flood is one of the most important factors of population mobility in different regions, this paper focuses on characteristics of flood-induced displacement patterns during Solar Cycle 24 in Europe. Using data of both mentioned categories, the research shows a certain connection between flood-induced displacement and the dynamics of Solar Cycle 24. It was found that the intensity of flood-induced displacement was highest during the period of greatest solar activity. Based on the research results, the study opens a discussion on whether solar activity can be considered a valid factor in population displacement. The issue is quite complex and deeper conclusions require that this area be examined from different aspects, with adequate research that will monitor this process during the current Solar Cycle 25. The paper points out that this issue has perspectives to contribute to potential predictions in the field of flood-induced displacement in the future, which would allow the development of preventive measures in the years of solar maximum.

Acknowledgements

The authors acknowledge funding provided by the Institute of Physics Belgrade through the grant by the Ministry of Science, Technological Development and Innovation of the Republic of Serbia.

*Corresponding author

GeosciRA25

Book of Abstracts and Contributed Papers
International Conference on Recent Trends in Geoscience Research and Applications 2025 Belgrade, Serbia and Virtual, 15–19 September 2025
Editors: Aleksandra Nina, Snežana Dragović, Maja Kuzmanoski, Milan Đorđević, and Mrđan Đokić

Original scientific paper
Abstract

TEMPORAL ASPECTS OF NATURAL DISASTER FATALITIES

Milica LANGOVIĆ[1*], Vladimir SREĆKOVIĆ[1], Marko LANGOVIĆ[2]

[1]Institute of Physics Belgrade, National Institute of the Republic of Serbia, University of Belgrade, Belgrade, Serbia;
e-mail: milica.langovic@ipb.ac.rs, vlada@ipb.ac.rs
[2]Faculty of Geography, University of Belgrade, Belgrade, Serbia;
e-mail: marko.langovic@gef.bg.ac.rs

Natural disasters affect population in all parts of the world and frequently have a devastating impact on society. The aim of this paper is to examine global patterns of population affected by natural disasters, focusing on the temporal trends of total deaths by natural disasters in the period 2000-2024. In order to identify the connection between frequency of natural disasters and its impact on total deaths worldwide, the correlation analysis was performed. Results showed that in the observed period natural disasters have influenced death of around 1.5 million people. Temporal analysis revealed that although there are evident variations in the dynamics, a slightly decreasing trend in total deaths by natural disasters in the observed period has been established. Considering the impact of natural disasters on fatalities on a global scale, the paper discusses whether the authorities have done enough to inform about natural disasters, prepare and protect the population, and whether natural disasters are actually perceived as a risk to society equally in all parts of the world. The paper highlights the importance of analyzing the impact of different types of natural disasters on the population in different regions, which will be considered in future research.

Acknowledgements

The authors acknowledge funding provided by the Institute of Physics Belgrade through the grant by the Ministry of Science, Technological Development and Innovation of the Republic of Serbia.

**Corresponding author*

GeosciRA25

Book of Abstracts and Contributed Papers
International Conference on Recent Trends in Geoscience Research and Applications 2025 Belgrade, Serbia and Virtual, 15–19 September 2025
Editors: Aleksandra Nina, Snežana Dragović, Maja Kuzmanoski, Milan Đorđević, and Mrđan Đokić

Original scientific paper
Abstract

SDR-BASED VLF RECEIVER AND SOFTWARE SOLUTION

Jovan BAJČETIĆ[1,2*], Danilo LAZOVIĆ[1], Aleksandra NINA[3]

[1]Khaoticen doo, Belgrade, Serbia; e-mails: jbajcetic@pro-sci-tech.com, dlazovic@khaoticen.com
[2]Professional Science and Technology, Zrenjanin, Serbia; e-mail: jbajcetic@pro-sci-tech.com
[3]Institute of Physics Belgrade, National Institute of the Republic of Serbia, University of Belgrade, Belgrade, Serbia; e-mail: sandrast@ipb.ac.rs

The presented receiving system represents a standalone, remotely operable platform for continuous monitoring of very low (VLF), low (LF), medium (MF) and high (HF) frequency radio waves, with the goal of identifying ionospheric and other natural perturbations related to various natural phenomena. The current implementation comprises the reception module which is utilized as a KiwiSDR software-defined radio optimized for the 16–46 kHz frequency band, interfaced with a BeagleBone Green embedded controller running Linux. Additional hardware components include an active Mini-Whip antenna, precision GNSS timing, SSD storage, and a power supply designed to minimize noise. The Functional Software, executed onboard, enables continuous acquisition of IQ data, locally buffered with GNSS timestamps and transferred securely to a central processing console. The implemented software suite provides real-time spectrum visualization and user control, near-real-time tracking of multiple frequencies, and advanced offline analysis of long-term trends. Through a dedicated SSH/SFTP mechanism, recordings are organized into structured time-indexed directories for seamless retrieval and automated post-processing. The software highlights spectral features including amplitude and phase noise fluctuations that are believed to precede nature-originated events, as supported by recent publications. This system serves as a complete field-deployable research tool for monitoring geophysical anomalies.

Acknowledgements

The authors acknowledge funding provided by the Institute of Physics Belgrade through the grant by the Ministry of Science, Technological Development and Innovation of the Republic of Serbia.

References

Nina, A., Biagi, P. F., Mitrović et al. *Atmosphere*, 12(4), 444.
Nina, A., Pulinets, S., Biagi, P. F., Nico, G., Mitrović, S., Radovanović, M., and Popović, L. Č. (2020). *Sci. Total Environ*., 710, 136406.
Nina, A. (2024). *Remote Sens*., 16(2), 397.
Nina, A. (2024). *Remote Sens*., 16(8), 1330.
Nina, A., Biagi, P. F., Pulinets, et. al (2022). *Front. Environ. Sci*., 10, 1005575.

*Corresponding author

GeosciRA25

Book of Abstracts and Contributed Papers
International Conference on Recent Trends in Geoscience Research and Applications 2025 Belgrade, Serbia and Virtual, 15–19 September 2025
Editors: Aleksandra Nina, Snežana Dragović, Maja Kuzmanoski, Milan Đorđević, and Mrđan Đokić

Original scientific paper
Abstract

VISUALIZATION OF THE SEISMICITY OF GREECE USING THE EARTH TIDE-SEISMICITY COMPLIANCE PARAMETER MAPS

Michael E. CONTADAKIS[1*], Demetrios N. ARABELOS[1], Georgios S. VERGOS[1], Spyros SPATALAS[1]

[1]Aristotle University of Thessaloniki, University GR-54124, Thessaloniki, Greece; e-mails: mcont@topo.auth.gr, darab@topo.auth.gr, vergo@topo.auth.gr, sspatala@topo.auth.gr

Based on the results of our investigations, which indicate a tidal triggering effect on earthquakes when the stress in the focal area is near the critical level, we prepare yearly maps of the earth tide-seismicity compliance index p. It is shown that the earth tide-seismicity compliance p maps point to the broader area of pending strong earthquakes within a year with a confidence level of 99,7%. Thus, we suggest that earth tide-seismicity compliance p maps may be used for earthquake risk mitigation.

References

Cadicheanu, N., van Ruymbeke, M., and Zhu P. (2007). *Nat. Hazards Earth Syst. Sci.* 7, 733.

Contadakis, M. E., Arabelos, D. N., and Spatalas, S. (2009). Evidence for tidal triggering on the shallow earthquakes of the seismic area of Mygdonia basin, North Greece. In D. Arabelos, M. E. Contadakis, C. Kaltsikis, and I. Tziavos (Eds.), Terrestrial and Stellar Environment (p. 223). Ziti Press, Thessaloniki, Greece

Contadakis, M. E., Arabelos, D. N., and Spatalas, S. D. (2012). *Ann. Geophys.*, 55(1), 73.

Forough, S. (2005). Lithospheric structure of the Aegean obtained from P and S receivers, GeoForschungsZentrum, Potsdam, Germany.

Papazachos, C. B., Kyratzi, A. A. (1996). *Tectonophys.*, 253, 129.

Schuster, A. (1897). *Proc. R. Soc. Lond*., 61, 455.

Vergos, G. S., Arabelos, D. N., and Contadakis, M. E. (2015). *Phys. Chem. Earth.*, 85, 210.

**Corresponding author*

Book of Abstracts and Contributed Papers
International Conference on Recent Trends in Geoscience Research and Applications 2025 Belgrade, Serbia and Virtual, 15–19 September 2025
Editors: Aleksandra Nina, Snežana Dragović, Maja Kuzmanoski, Milan Đorđević, and Mrđan Đokić

https://doi.org/10.46793/Geoscira25.095K

Original scientific paper
Contributed paper

COMPARISON OF AEROSOL VERTICAL PROFILES FROM CALIOP AND GROUND-BASED LIDAR IN BELGRADE, SERBIA

Maja KUZMANOSKI[1*], Jovana KOSTIĆ[2], Zoran MIJIĆ[1]

[1]Institute of Physics Belgrade, National Institute of the Republic of Serbia, University of Belgrade, Belgrade, Serbia;
e-mails: maja.kuzmanoski@ipb.ac.rs, zoran.mijic@ipb.ac.rs
[2]Faculty of Physics, University of Belgrade, Belgrade, Serbia;
e-mail: kosticj01@gmail.com

Abstract: Atmospheric aerosols have significant effect on climate and air pollution. However, they are still not well represented in models due to large variability of their sources and limited spatial and temporal measurements of their properties. The Balkan region is marked by significant air pollution, including aerosols originating from regional sources and those transported from distant source regions, such as North Africa. However, it is characterized by scarce ground-based measurements of aerosol properties. Raman lidar in Belgrade provides information on vertical profiles of aerosol optical properties, contributing to understanding the effects of aerosols in this region on climate and environment. This lidar system performs elastic backscatter and Raman measurements at the wavelengths of 355 nm and 387 nm, respectively. Here, the elastic backscatter signal is analyzed to obtain vertical profiles of aerosol backscatter coefficient at 355 nm in 30-min intervals. Satellite-based lidar measurements, such as CALIOP (Cloud-Aerosol Lidar with Orthogonal Polarization) onboard CALIPSO (Cloud Aerosol Infrared Pathfinder Satellite Observation), provide information on vertically-resolved aerosol optical properties on a global scale. We present study cases of comparison of vertical distribution of aerosol layers, based on backscatter coefficients from ground-based lidar in Belgrade and CALIOP, during CALIPSO overpasses. The analyzed cases correspond to clear-sky and different aerosol conditions.

Keywords: Atmospheric aerosols; Aerosol remote sensing; Aerosol lidar; CALIOP

1. Introduction

The atmospheric aerosols play an important role in climate and air pollution processes (Haywood and Boucher, 2000; Li et al., 2017). Diversity of their sources and thus their properties make it challenging to quantify their effects and represent them realistically in weather and climate models. Monitoring temporal and spatial variability of aerosol optical properties is crucial to assess aerosol effect on Earth's radiative balance and in studies of aerosol-cloud interaction. Besides, information on temporal evolution of the vertical extent of aerosol layers is important for analyzing particulate air

*Corresponding author

pollution and differentiation between contributions of long-range transported and locally-emitted aerosols (Bravo-Aranda et al., 2017). Aerosol lidars provide data on vertical profile of aerosol optical properties - backscatter and extinction coefficients. While ground-based lidars trace the temporal changes of these vertical profiles, satellite-based lidars provide a global picture of aerosol vertical distribution.

Aerosol lidar in Belgrade provides data on vertical profiles of aerosol extinction and backscatter coefficients at 355 nm. It is located in region known for elevated air pollution levels, and very limited ground-based aerosol measurements. In this study we present examples of comparison of ground-based lidar in Belgrade and CALIOP measurements onboard CALIPSO satellite. CALIOP provides vertical profiles of aerosol optical properties at 532 nm and 1064 nm. Since the two lidars operated at different wavelengths, in this work we focus on qualitative comparison of aerosol vertical distributions. Furthermore, CALIOP data are used to provide additional information about types of aerosols measured using ground-based lidar.

2. Measurements

2.1. Raman lidar measurements in Belgrade

A combined Raman and elastic-backscatter lidar has been operating at the Institute of Physics Belgrade (44.86 N, 20.39 E, 89 m). The lidar system and quality assurance procedures are described in detail by Mijić et al. (2023), and only a brief description is given here. It is based on a pulsed Nd:YAG laser, with fundamental wavelength of 1064 nm, and additional emissions at 532 nm and 355 nm. The laser pulses of 5 ns duration are transmitted at a repetition rate of 20 Hz. The signals are detected at 355 and 387 nm with high temporal (1 min) and vertical (7.5 m) resolution. In this work only elastically backscattered signals at 355 nm are analyzed. The aerosol backscatter coefficient is derived from lidar signals averaged over 30-min intervals using Klett-Fernald retrieval method (Klett, 1981; Fernald, 1984), assuming lidar ratio value of 50 sr.

2.2. CALIOP aerosol products

The Cloud-Aerosol Lidar with Orthogonal Polarization (CALIOP) operated aboard CALIPSO satellite and performed elastic backscatter measurements at 532 nm and 1064 nm, and linear depolarization measurements at 532 nm (Winker et al., 2009). Each detected aerosol layer is assigned to one of seven aerosol types by the CALIOP retrieval algorithm, based on integrated attenuated backscatter and depolarization ratio, layer altitude and underlying surface. We use aerosol backscatter coefficient data from the CALIPSO 5-km Aerosol Profile product (Level 2, Version 4.51) and information on aerosol types. The products are reported with horizontal resolution of 5 km and vertical resolution of 60 m in the troposphere. In this work we use cloud-free profiles and apply QA criteria described by Tackett et al. (2018).

3. Results

In this study we present a comparison of aerosol backscatter coefficient vertical profiles based on coincident measurements from ground-based lidar and CALIOP during CALIPSO overpasses. As mentioned above, the analysis is limited to a qualitative comparison due to different wavelengths of Belgrade ground-based lidar (355 nm) and CALIOP (532 nm and 1064 nm) measurements. Furthermore, assuming a single lidar ratio value of 50 sr for all cases impacts the backscatter coefficient values obtained from ground-based lidar measurements. Additionally, we use aerosol type classification results from CALIOP to support interpretation of ground-based lidar measurements.

3.1. Case of May 7, 2018

The smallest distance between the CALIPSO ground track during daytime overpass on May 7, 2018, and Belgrade lidar was 47.4 km. Vertical profile of aerosol backscatter coefficient is retrieved from ground-based lidar measurements taken at 11:45-12:15 UT, corresponding to time of CALIPSO overpass. It reveals a two-layer structure (Figure 1), with the boundary layer height of 1 km and an overlying layer extending to the altitude of 3.6 km. Figure 1 also shows the vertical profiles of aerosol backscatter coefficient at 532 nm and 1064 nm from CALIOP, averaged within the maximum distance of 100 km from the location of the Belgrade lidar (28 profiles). It displays a very similar two-layer structure extending to the same altitude, with somewhat larger boundary layer height (1.4 km).

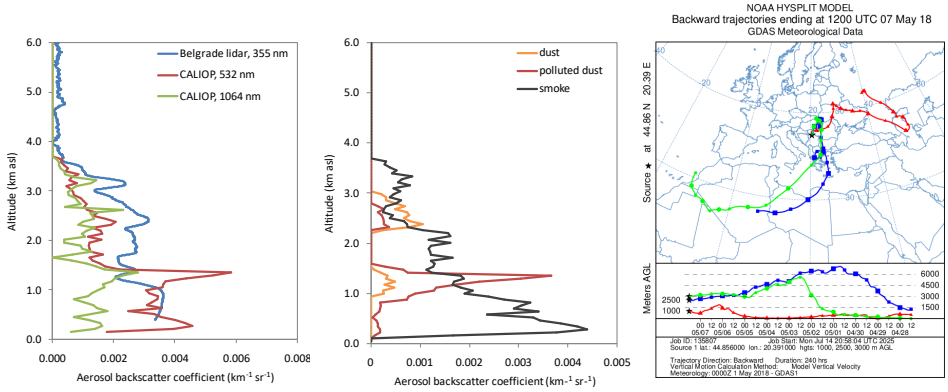

Figure 1. Vertical profiles of aerosol backscatter coefficient derived from ground-based lidar measurements in Belgrade and CALIOP on May 7, 2018 (left panel); corresponding aerosol backscatter coefficient profiles for different aerosol types from CALIOP (middle panel); HYSPLIT airmass backward trajectories at the location of Belgrade lidar station (right panel)

The CALIOP aerosol type classification indicates predominance of smoke, with contributions of dust and polluted dust, mainly in the elevated layer. HYSPLIT backward trajectories (Stein et al., 2015) indicate that the airmasses reaching the boundary layer and the elevated layer originated from the Eastern Europe and North Africa, respectively. The thermal anomalies detected by the Moderate-Resolution Imaging Spectroradiometer (MODIS) sensor (https://worldview.earthdata.nasa.gov)

indicate fire activities in Eastern Europe at the beginning of May, consistent with the aerosol type classification. However, presence of dust in the elevated layer does not align with DREAM model (Nickovic et al., 2001; www.seevccc.rs), which shows the start of the dust episode later, on May 10. The backscatter color ratio, based on vertically integrated aerosol backscatter coefficients at 532 nm and 1064 nm, was 2.5 in the boundary layer and 1.3 in the elevated layer. These are close to the values reported by Groß et al. (2013) for anthropogenic pollution and Saharan dust (2.43 ± 0.27 and 1.30 ± 0.15, respectively).

3.2. Case of March 25, 2019

In this case, the smallest distance between the CALIPSO ground track and Belgrade lidar station was 96.5 km, during daytime overpass. We thus averaged aerosol backscatter coefficients from CALIOP within a 150 km distance from the Belgrade lidar station. Vertical profiles of aerosol backscatter coefficients from both ground-based lidar and CALIOP show a single aerosol layer which extends to an altitude of 3 km, with majority of the later located below 2.5 km (Figure 2). The backscatter coefficient increases with altitude, with maximum found at somewhat different altitudes in the ground-based and CALIOP observations. The CALIOP aerosol classification suggests that smoke is the prevalent aerosol type, with contributions of polluted continental aerosol at altitudes of 1-2 km and some polluted dust at 2.5-3 km. The thermal anomalies detected by MODIS indicate fire activities over the region. Backward trajectories indicate that airmasses arrived from Western and Central Europe. The backscatter color ratio is 2.5, which is close to values observed for anthropogenic pollution (Groß et al., 2013), as noted previously.

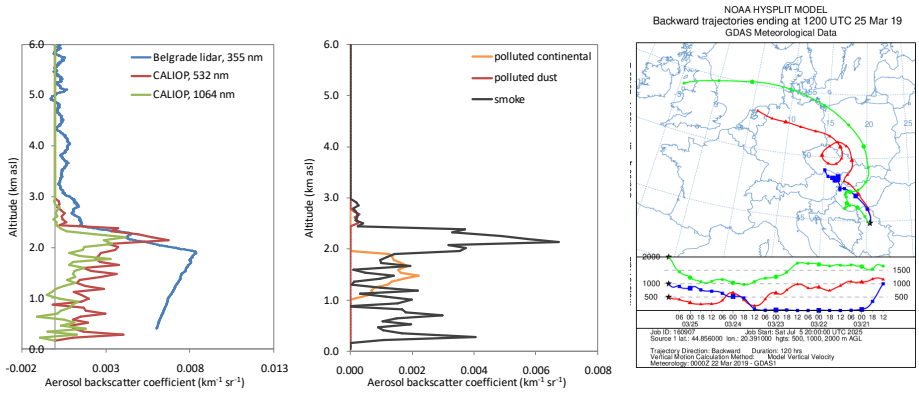

Figure 2. Vertical profiles of aerosol backscatter coefficient derived from ground-based lidar measurements in Belgrade and CALIOP on March 25, 2019 (left panel); corresponding aerosol backscatter coefficient profiles for different aerosol types from CALIOP (middle panel); HYSPLIT airmass backward trajectories at the location of Belgrade lidar station (right panel)

3.3. Case of April 23, 2020

The smallest distance between the CALIPSO ground track during daytime overpass on April 23, 2020 and the lidar station in Belgrade was 27.1 km. The CALIOP aerosol backscatter coefficient profiles within a 100 km distance from the lidar station were averaged (36 profiles). Both CALIOP and ground-based lidar measurements show a single aerosol layer extending to the altitude of 3 km, without significant changes of backscatter coefficient over most of the layer (Figure 3). The CALIOP aerosol type classification suggests that the aerosol is polluted dust. Furthermore, the backscatter color ratio is 1.29, close to the value reported for Saharan dust (Groß et al., 2013). HYSPLIT shows that airmasses were transported from northeastern Europe, passing over Ukraine and Romania. While DREAM model does not show dust event on this day, it shows that the region was affected by a dust episode two days earlier.

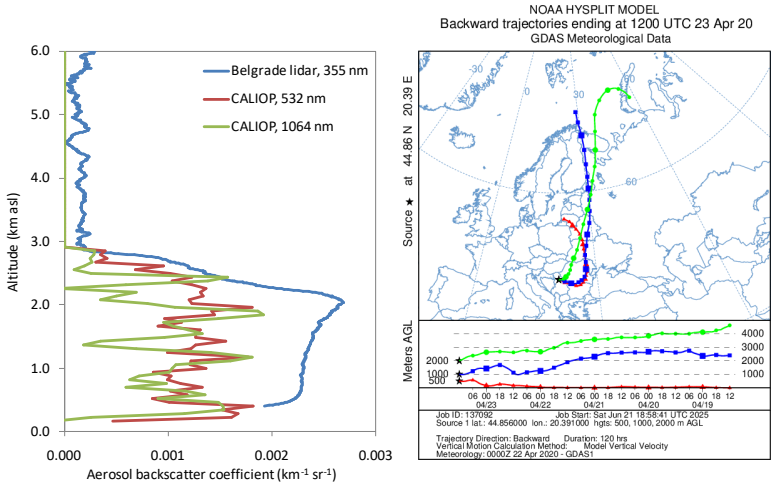

Figure 3. Vertical profiles of aerosol backscatter coefficient derived from ground-based lidar measurements in Belgrade and CALIOP on April 23, 2020 (left panel); HYSPLIT airmass backward trajectories at the location of Belgrade lidar station (right panel)

4. Conclusion

A qualitative comparison of aerosol backscatter coefficients, obtained from ground-based lidar measurements in Belgrade and CALIOP data, is carried out for three cases with different airmass origins. In the analyzed cases, CALIOP data show consistency with data from the ground-based lidar. The vertical profiles of aerosol backscatter coefficient from CALIOP and Belgrade lidar show agreement in extent and vertical structure of aerosol layer. While CALIOP aerosol type classification, along with airmass backward trajectories, provide valuable information, aerosol models are necessary to support interpretation of measured aerosol vertical profiles.

Acknowledgements

MK and ZM acknowledge funding provided by the Institute of Physics Belgrade, through the grant by the Ministry of Science, Technological Development and Innovation of the Republic of Serbia.

References

Bravo-Aranda, J. A., Titos, G., Granados-Muñoz, M. J. et al. (2015). Study of mineral dust entrainment in the planetary boundary layer by lidar depolarisation technique. *Tellus Ser. B-Chem. Phys. Meteorol.* 67, 26180.

Fernald, F. G. (1984). Analysis of atmospheric lidar observations: some comments. *Appl. Opt.*, 23(5), 652.

Groß, S., Esselborn, M., Weinzierl, B. et al. (2013). Aerosol classification by airborne high spectral resolution lidar observations. *Atmos. Chem. Phys*., 12, 25983.

Haywood, J. and Boucher, O. (2000). Estimates of the direct and indirect radiative forcing due to tropospheric aerosols: a review, *Rev. Geophys.*, 38(4), 513.

Klett, J. D. (1981). Stable analytical inversion solution for processing lidar returns. *Appl. Opt.*, 20(2), 211.

Li, M., Wang, T., Xie, M. et al. (2017). Impacts of aerosol-radiation feedback on local air quality during a severe haze episode in Nanjing megacity, eastern China. *Tellus Ser. B-Chem. Phys. Meteorol.* 69, 1339548.

Mijić, Z., Ilić, L. and Kuzmanoski, M. (2023). Data quality assurance for atmospheric probing and modeling: characterization of Belgrade Raman lidar station. *Contrib. Astron. Obs. Skaln. Pleso*, 53(3), 163.

Nickovic, S., Papadopoulos, A., Kakaliagou, O. and Kallos, G. (2001). Model for prediction of desert dust cycle in the atmosphere. *J. Geophys. Res.*, 106, 18113.

Stein, A. F., Draxler, R. R., Rolph, G. D. et al. (2015). NOAA's HYSPLIT atmospheric transport and dispersion modeling system. *Bull. Am. Meteorol. Soc*., 100(5) 2059.

Tackett, J. L., Winker, D. M., Getzewich, B. J. et al. (2018). CALIPSO lidar level 3 aerosol profile product: version 3 algorithm design. *Atmos. Meas. Tech.*, 11, 4129.

Winker, D. M., Vaughan, M. A., Omar, A. et al. (2009). Overview of the CALIPSO Mission and CALIOP Data Processing Algorithms. *J. Atmos. Oceanic Technol.* 26(11), 2310.

Book of Abstracts and Contributed Papers
International Conference on Recent Trends in Geoscience Research and Applications 2025 Belgrade, Serbia and Virtual, 15–19 September 2025
Editors: Aleksandra Nina, Snežana Dragović, Maja Kuzmanoski, Milan Đorđević, and Mrđan Đokić

https://doi.org/10.46793/Geoscira25.101K

Original scientific paper
Contributed paper

CHARACTERIZATION OF VERTICAL PROFILES OF AEROSOL EXTINCTION COEFFICIENT ABOVE GREATER BELGRADE AREA, BASED ON CALIOP DATA

Jovana KOSTIĆ[1*], Maja KUZMANOSKI[2]

[1]Faculty of Physics, University of Belgrade, Belgrade, Serbia; e-mail: kosticj01@gmail.com
[2]Institute of Physics Belgrade, National Institute of the Republic of Serbia, University of Belgrade, Belgrade, Serbia; e-mail: maja.kuzmanoski@ipb.ac.rs

Abstract: Information on the vertical distribution of atmospheric aerosols is essential for understanding their role in climate processes and contribution to air pollution. These profiles can be retrieved from both ground-based and satellite lidar instruments. CALIOP (Cloud-Aerosol Lidar with Orthogonal Polarization), onboard CALIPSO (Cloud-Aerosol Lidar and Infrared Pathfinder Satellite Observations), is a two-wavelength polarization-sensitive lidar that provides vertically-resolved aerosol extinction and backscatter coefficients at 532 and 1064 nm. In this study, we use Level 2, Version 4.51 CALIOP aerosol profile products for the period 2015–2019, in the region of 44–45° N and 20–21° E, covering the greater Belgrade area. This area has seasonal variations in aerosol presence with high surface pollution during colder months and influence of long-range transported aerosols, such as Saharan dust, in warmer periods. Our analysis is based on cloud-free profiles that meet quality control criteria used for CALIOP Level 3 aerosol profile data. Data are grouped by season (spring–summer and fall–winter) and time of day (day and night) to investigate the impact of different aerosol sources and meteorological conditions. We examine the vertical distribution of aerosols, their contribution to total aerosol optical depth (AOD) at different altitudes, and the influence of relative humidity on extinction coefficients.

Keywords: Atmospheric aerosols; Aerosol extinction coefficient; Remote sensing; Aerosol vertical profile; CALIOP

1. Introduction

Atmospheric aerosols play a crucial role in the Earth's climate system and have significant implications for air quality and human health. Fine particulate matter smaller than 2.5 μm (PM2.5) is considered the most hazardous fraction due to its ability to penetrate deep into the human respiratory system (Pope and Dockery, 2006). In terms of climate impact, aerosols influence Earth's radiation balance both directly – by scattering and absorbing solar radiation, and indirectly – through their interactions with clouds – affecting cloud formation, lifetime, and albedo. By scattering light and enhancing cloud

*Corresponding author

brightness, aerosols increase Earth's albedo and contribute to negative radiative forcing, typically counteracting the warming effect of greenhouse gases. The optical properties of aerosols, such as the extinction coefficient, are key parameters in quantifying these effects. The extinction coefficient is primarily determined by particle size distribution, but also depends on complex refractive index, which is linked to chemical composition (Hess et al., 1998). Vertical profiles of aerosol extinction coefficient provide insight into the stratification of aerosols in the atmosphere, allowing us to distinguish between boundary layer pollution – often of anthropogenic origin – and elevated aerosol layers involved in cloud processes and long-range transport. Despite their importance, the overall impact of aerosols on clouds and radiation remains a major source of uncertainty in current climate models, partly due to their diverse sources and the complexity of their interactions with clouds (Stocker et al., 2013).

Studying aerosol vertical distribution over the greater Belgrade area is important due to frequent emissions from anthropogenic sources as well as the influence of long-range transported particles such as Saharan dust and biomass burning aerosols. Serbia has been repeatedly identified by the European Environment Agency (EEA) as one of the most polluted countries in Europe with respect to particulate matter (PM). Annual reports point to exceedances of recommended PM10 and PM2.5 concentrations, especially in urban centers during winter months. However, ground-based measurements are often insufficient to fully capture the vertical extent and dynamics of aerosol layers. Satellite lidar instruments, such as CALIOP onboard the CALIPSO satellite, offer a valuable opportunity to investigate aerosol vertical profiles on a global scale, including regions with limited ground-based observations. This study focuses on the characterization of aerosol extinction coefficient profiles above the greater Belgrade area using CALIOP data, aiming to improve our understanding of aerosol loading and distribution in the lower and middle troposphere over this pollution-prone region.

2. CALIPSO measurements

The CALIPSO mission, launched in 2006 by NASA and the French space agency CNES, operated until 2023 and provided global vertical profiles of aerosols and clouds using the CALIOP lidar. CALIOP is a dual-wavelength elastic backscatter lidar that operated at 532 nm and 1064 nm in near-nadir geometry. It continuously acquired data along the satellite's sun-synchronous orbit, providing both day and night observations with high vertical resolution and global coverage.

In this study, we use the Level 2 Aerosol Profile, Version 4.51 data product, which contains aerosol extinction coefficient profiles with 5 km horizontal and 60 m vertical resolution in the troposphere. The analysis covers the period 2015–2019 and is limited to a spatial grid of 44–45° N and 20–21° E, corresponding to the greater Belgrade area.

To ensure the reliability of the retrieved aerosol extinction profiles, a set of filtering criteria was applied (Tackett et al., 2018). Profiles affected by clouds were excluded. Only aerosol layers with cloud–aerosol discrimination (CAD) score values between −100 and −20 were retained, ensuring a higher confidence in their classification as aerosol rather than cloud. Extinction values associated with high uncertainty or invalid quality flags were removed, along with data below 60 m above ground level. Clear-air regions located below low-altitude aerosol layers (with base height below 250 m) were disregarded. In addition, aerosol layers in contact with ice clouds above 4 km altitude,

where cloud-top temperatures were below 0 °C, were excluded to avoid contamination from cloud–aerosol interaction artifacts.

3. Results

In this analysis, the data were grouped into four categories based on season (spring–summer and fall–winter), as well as time of day (day and night), to reflect the influence of different aerosol sources, types, and meteorological conditions. Data from all vertical profiles were then averaged for each category over the 2015-2019 period. Each category included some clear air profiles at locations distant from local pollution sources. These were assumed to have extinction coefficient of 0 km^{-1}.

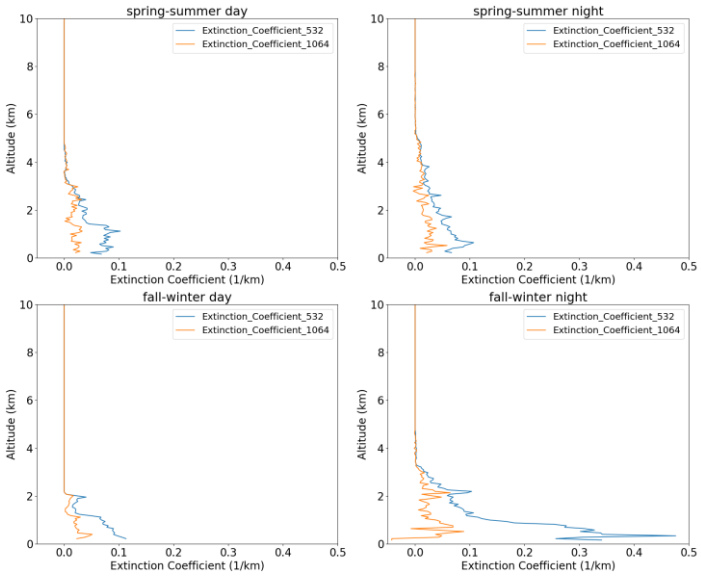

Figure 1. Vertical profiles of filtered extinction coefficients at 532 nm and 1064 nm for four data groups, averaged over the 2015–2019 period

Figure 1 reveals that the main seasonal difference lies in the altitude at which aerosols are detected, especially during daytime. In the spring–summer period, aerosols frequently appear above 2 km, and even at higher altitudes, which is likely associated with long-range transport events such as Saharan dust or biomass burning. In the fall–winter period, aerosol layers tend to be more confined to lower altitudes. A noticeable difference between day and night profiles is also observed: during the day, aerosols are generally found up to 2 km, while at night they can extend up to around 3.5 km. It is also observed that extinction coefficient values at 532 nm during fall–winter nights are notably higher than those in the other data groups.

These patterns can be explained by seasonal and diurnal variations in the atmospheric boundary layer (ABL) height. During winter, the ABL is typically shallower due to lower surface temperatures, and it is also lower at night than during the day. A shallower ABL limits vertical mixing and reduces horizontal air movement, resulting in more

pronounced aerosol accumulation near the surface, especially at night. Additionally, seasonal differences in pollution levels contribute to the observed patterns. In summer, aerosol concentrations are generally lower, which reduces the contrast between day and night profiles.

The consistently lower extinction coefficients at 1064 nm compared to those at 532 nm indicate the predominance of fine-mode aerosol particles, as smaller particles more effectively attenuate shorter wavelengths. This spectral behavior is typical for urban and combustion-related aerosols and is consistent with a high Ångström exponent shown in Table 1.

Table 1. Mean AOD and Ångström exponent values for four data groups

	Spring-summer day	Spring-summer night	Fall-winter day	Fall-winter night
Total AOD	**0.15**	**0.18**	**0.10**	**0.38**
AOD below 1 km	**0.06**	**0.06**	**0.07**	**0.24**
	43.03%	**35.88%**	**72.04%**	**65.86%**
AOD between 1-2 km	**0.05**	**0.05**	**0.03**	**0.08**
	33.65%	**28.51%**	**26.98%**	**20.49%**
AOD above 2 km	**0.03**	**0.06**	**0.00**	**0.05**
	23.32%	**35.61%**	**0.98%**	**13.65%**
Angstrom Exponent	**1.27**	**1.47**	**1.62**	**1.80**

Table 1 presents an overview of the total aerosol optical depth (AOD) values at 532 nm for each data group, along with the contributions to AOD from three altitude ranges, and the mean Ångström exponent derived from AOD at 532 nm and 1064 nm. Several notable patterns can be observed.

Total daytime AOD values are higher during the spring–summer season compared to fall–winter, which is consistent with findings by Ma and Yu (2015) for locations in North America, Europe, and East Asia. In our case, the higher AOD observed during the spring–summer season is primarily attributed to aerosols located above 1 km altitude. In contrast, nighttime AOD values in the lowest altitude range (below 1 km) are significantly higher in fall–winter than in spring–summer, which may reflect enhanced near-surface pollution under stable atmospheric conditions. AOD values above 2 km at night show little difference between the two seasons.

Significant day–night differences in fall–winter AOD are observed across all altitude ranges (Liu et al., 2024), especially below 1 km. During fall–winter daytime conditions, AOD values above 2 km are nearly negligible, whereas in spring–summer, daytime AOD in this altitude range is present but still notably lower than nighttime values. Day and night AOD values below 2 km during the spring–summer season remain comparable.

It is also evident that in the fall–winter season, more than 60% of the total AOD originates from the lowest kilometer of the atmosphere during both day and night. This highlights the dominant contribution of near-surface, anthropogenic aerosols in winter. On the other hand, in the spring–summer period, a substantial portion of the total AOD is located above 2 km, in agreement with the presence of long-range transported aerosols at higher altitudes.

The Table 1 also includes the mean Ångström exponent calculated for each group. It

shows a clear increasing trend from spring–summer day to fall–winter night. This suggests an increased proportion of smaller particles, with fine aerosols likely dominating during fall–winter nights.

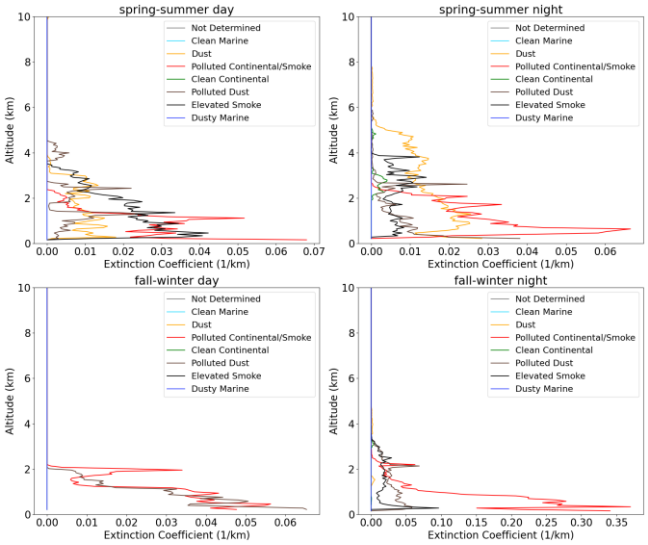

Figure 2. Vertical profiles of extinction coefficients at 532 nm for different aerosol subtypes, averaged over the 2015–2019 period

Focusing on aerosol subtypes, Figure 2 shows that during spring–summer nights, dust and elevated smoke – representing long-range transported aerosols – dominate at altitudes above 2 km, while polluted continental and dust aerosols are prevalent closer to the surface. A similar pattern is observed during spring–summer days, with polluted continental and elevated smoke aerosols being most abundant below 2 km.

In the fall–winter period, the aerosol composition shifts. During daytime, polluted continental and polluted dust aerosols dominate the lower 2 km of the atmosphere. At night, polluted continental aerosols remain the most prominent below 2 km, but there is also a notable presence of polluted dust and elevated smoke both below and above this altitude.

We also investigated the dependence of extinction coefficient at 532 nm on relative humidity (RH). During spring–summer days, RH appears to have little influence on the extinction coefficient. In contrast, fall–winter daytime data show greater variability in extinction values with changing RH, particularly in the 0.8 to 0.9 range. A slight positive correlation between extinction and higher RH is observed during spring–summer nights. Further analysis will focus on assessing the impact of RH on extinction coefficient for each aerosol subtype individually, since the current results reflect the effect across all aerosol types.

4. Conclusion

The aim of this study was to investigate vertical profiles of aerosol extinction coefficients over the greater Belgrade area using CALIOP data for the period 2015–2019, with respect to seasonal and diurnal variability. Results show that higher daytime AOD values during spring–summer are mainly due to elevated aerosol layers above 1 km, likely from long-range transport of Saharan dust and biomass burning. In contrast, fall–winter aerosols are concentrated near the surface, reflecting local anthropogenic pollution, particularly during nighttime. The overall increase in nighttime AOD compared to daytime likely results from a lowered atmospheric boundary layer height, which limits aerosol dispersion. Seasonal and vertical variations in aerosol subtypes were also observed: dust, elevated smoke, and polluted continental aerosols dominate in spring–summer, while polluted continental and polluted dust are prevalent in the lower layers during fall–winter. Analysis of the Ångström exponent indicates a dominance of fine particles in the region, particularly during the colder months. Further research is needed to examine how relative humidity affects the size of specific aerosol subtypes and, consequently, their extinction coefficients.

Acknowledgements

MK acknowledges funding provided by the Institute of Physics Belgrade, through the grant by the Ministry of Science, Technological Development and Innovation of the Republic of Serbia.

References

Hess, M., Koepke, P., and Schult, I. (1998). Optical properties of aerosols and clouds: the software package OPAC. *Bull. Am. Meteorol. Soc*., 79, 831.

Liu, G., Li, J., Li, J. et al. (2024). Estimation of nighttime aerosol optical depths using atmospheric infrared sounder longwave radiances. *Geophys. Res. Lett*., 51, e2023GL108120.

Ma, X. Y., and Yu, F. Q. (2015). Seasonal and spatial variations of global aerosol optical depth: multi-year modelling with GEOS-CHEM-APM and comparisons with multiple-platform observations. *Tellus B*, 67, 25115.

Pope, C. A., and Dockery, D. W. (2006). Health effects of fine particulate air pollution: lines that connect. *J. Air Waste Manag. Assoc.*, 56(6), 709.

Stocker, T. F., Qin, D., Plattner, G.-K. et al. (2013). *Climate change 2013: The physical science basis. Contribution of Working Group I to the Fifth Assessment Report of the Intergovernmental Panel on Climate Change*. Cambridge University Press. UK.

Tackett, J. L., Winker, D. M., Getzewich, B. J. et al. (2018). CALIPSO lidar level 3 aerosol profile product: version 3 algorithm design. *Atmos. Meas. Tech.*, 11, 4129.

Book of Abstracts and Contributed Papers
International Conference on Recent Trends in Geoscience Research and Applications 2025 Belgrade, Serbia and Virtual, 15–19 September 2025
Editors: Aleksandra Nina, Snežana Dragović, Maja Kuzmanoski, Milan Đorđević, and Mrđan Đokić

https://doi.org/10.46793/Geoscira25.107S

Original scientific paper
Contributed paper

DETECTION OF SOLAR FLARES FROM IONOSPHERIC DATA USING DEEP LEARNING

Martin SARNOVSKÝ[1*], Peter BUTKA[1], Peter BEDNÁR[1], Aleksandra NINA[2], Vladimir SREĆKOVIĆ[2], Luka Č. POPOVIĆ[3], Aleksandra KOLARSKI[2], Filip ARNAUT[2]

[1]Department of Cybernetics and Artificial Intelligence, Faculty of Electrical Engineering and Informatics, Technical University of Kosice, Kosice, Slovakia; e-mails: martin.sarnovsky@tuke.sk, peter.butka@tuke.sk, peter.bednar@tuke.sk
[2]Institute of Physics Belgrade, National Institute of the Republic of Serbia, University of Belgrade, Belgrade, Serbia; e-mails: sandrast@ipb.ac.rs, vlada@ipb.ac.rs; aleksandra.kolarski@ipb.ac.rs, arnaut@ipb.ac.rs
[3]Department of Astronomy, Faculty of Mathematics, University of Belgrade, Belgrade, Serbia; e-mail: lpopovic@aob.rs

Abstract: This work addresses the detection of solar flares based on data from low-frequency radio wave signal amplitudes. The work is a cooperation between the Technical University of Košice and the Institute of Physics at the University of Belgrade. The primary goal is to explore the provided data and to look for patterns and connections in the ionosphere's behavior during normal conditions and solar flares. To achieve this goal, an Autoencoder neural network is implemented in Python. Data exploration utilizes various types of data visualizations, including box plots, violin plots, and histograms. The data used included VLF signal amplitudes received in Belgrade and information on solar flares from NASA GOES satellites. Working with an extremely unbalanced dataset, low class distinctiveness, and noisy data presented significant challenges. Despite these difficulties, the final Autoencoder model, trained on non-flare data and using two key features derived from signal statistics, was able to capture 65% of real flare occurrences, although it produced many false positives. The results of this research work demonstrate that subtle differences in the signals related to flares exist and provide a basis for future efforts to improve detection.

Keywords: Solar flares; Machine learning; Deep learning; Neural networks.

1. Introduction

Solar flares are powerful energy impulses originating from the Sun that can induce significant changes in the Earth's ionosphere, consequently affecting the reflection of very low frequency (VLF) radio waves crucial for radiocommunication. Such ionospheric disturbances can lead to signal disruptions, potentially impacting critical navigation, communication, and security systems. With an increasing global reliance on

*Corresponding author

satellite technology, mobile communications, and information systems, the timely and reliable detection of solar flares is paramount for preventing and managing potential damage. In severe scenarios, widespread satellite system outages could lead to the interruption of global telecommunication and energy networks, resulting in catastrophic economic consequences (Šulić, 2016).

The work presented in this paper addresses the detection of solar flares and their influence on ionospheric behavior. The aim of this work is exploratory data research, focusing on identifying patterns in the ionosphere's behavior during both normal periods and during solar flare occurrences. The primary objective is to develop a suitable neural network model capable of reliably and accurately identifying these phenomena. The study places strong emphasis on data analysis, understanding and the identification of key features that might characterize solar flare events. The developed model is intended to at least partially be capable of distinguishing between a normal ionospheric state and one affected by a solar flare. Development of the model was systematically realized using the CRISP-DM (Cross-Industry Standard Process for Data Mining) methodology (Azevedo, 2008).

2. Methodology and data description

The main objective was to develop a machine learning model capable of accurately identifying solar flare occurrences based on frequency changes observed in ionospheric measurements. The standard CRISP-DM methodology was adopted to systematically guide the process, from problem understanding and data preparation to modeling and results evaluation.

2.1. Problem and data understanding

The dataset comprises 375,818 rows, with each entry representing one minute of measurement during the year 2013 (Nina, 2017). Each row included a timestamp, amplitudes for five distinct frequency signals (19.8, 20.27, 22.1, 23.4, and 24 kHz). The VLF signals were transmitted from various global locations and received in Belgrade: 19.8 kHz (NWC, Australia), 20.27 kHz (ICV, Italy), 22.1 kHz (GQD, UK), 23.4 kHz (DHO, Germany), and 24 kHz (NAA, USA). Amplitude measurements were chosen for analysis over phase measurements, as phase signals were found to be more susceptible to noise and less stable. A significant challenge was the extreme data imbalance: out of 375,818 records, only 1,548 indicated a flare occurrence. Additionally, the dataset exhibited long data outages and erroneous values, which were removed during preprocessing. Observations revealed that the sensitivity of individual frequencies varied, with some increasing and others decreasing in amplitude during flares. These factors significantly complicated direct solar flare detection, as the 'flare' and 'non-flare' classes were very similar in terms of amplitude behavior.

2.2. Data Preparation

For data preparation, we integrated the data with daily sunrise and sunset times for Belgrade in 2013, converted to UTC, and trimmed by 30 minutes after sunrise and before sunset to mitigate potential signal disturbances. Subsequent cleaning involved removing records with negative or abnormally low amplitude values (e.g., extreme

sudden drops across all frequencies, indicating measurement errors). The target attribute was then transformed into a binary format (1 for flare, 0 for normal state). The resulting cleaned dataset contained 137,438 records, of which 860 indicated a flare event. Thirty-five distinct flare events were identified, with durations ranging from 4 to 76 minutes and an average duration of 25 minutes.

Then, we aimed to transform the time-series data into aggregated data based on time windows, where we could compute basic characteristics of the signals within a given time window. Based on these characteristics, hourly windows were selected as optimal for aggregation. The aggregated dataset comprised signal statistics for each of the five frequencies within non-overlapping hourly intervals. Signal minimum (*min*) and maximum (*max*) values, delta increase (*delta_inc*), delta decrease (*delta_dec*), and absolute delta (*delta_abs*) were computed for each of five frequencies. The binary target attribute reflected whether at least one flare occurred during that time window. The final dataset used in the modeling phase comprised 2,586 rows, with 2,538 labeled as 'no flare' (0) and only 48 labeled as 'flare' (1).

2.3. Models training

Given the very low number of positive cases and the minimal differences between classes, an anomaly detection approach using an Autoencoder was adopted (Mishra, 2017). Previously, we explored the possibility of using traditional classification approach (Pavlík, 2024), but the performance of the model was very poor (Recall 0.3) due to heavy class imbalance. This model underwent iterative adjustments, testing, and evaluation:

- Model 1: The initial Autoencoder model was trained exclusively on records belonging to class 0. The objective was to train the model to reconstruct typical signal patterns and then detect anomalies (flares) based on the reconstruction error (Mean Squared Error - MSE). The model utilized 25 input attributes (five statistics for each of the five frequencies). Its architecture comprised a Dense layer (32 neurons, ReLU), Dropout (0.2), Dense layer (16 neurons) in the Encoder part. First Dense layer captures non-linear relationship in the input data, Dropout regularizes the model to prevent overfitting (especially useful on smaller datasets) and another Dense layer compresses the input into the lower-dimensional latent representation. Decoder part consists of Dense layer (32 neurons), Dropout (0.2), and a linear output layer. The first Dense layer reconstructs the compressed representation, Dropout again prevents the overfitting and linear output layer is suitable for regression tasks (Berahmand, 2024). The model was trained for 30 epochs with a batch size of 32, using MSE loss, and Adam optimizer. The anomaly threshold was set at the 85th percentile of the error on training data. This model performed well in identifying class 0 (Precision 0.98, Recall 0.95), but was essentially non-functional for class 1 (Precision 0.02, Recall 0.04), indicating a high number of false negatives for flare detection.
    - To enhance model performance, a Kolmogorov-Smirnov test was employed to identify the attributes that most significantly differentiated between classes 0 and 1. Based on the highest differences, six attributes were selected: *20.27kHz_delta_abs*, *22.1kHz_delta_dec*, *24kHz_min*, *22.1kHz_delta_abs*, *22.1kHz_min*, and *24kHz_max*.

- Model 2: A new Autoencoder was built using only these six selected attributes. The architecture remained consistent, trained solely on class 0 data. The anomaly threshold was adjusted to the 80th percentile, as this yielded the highest recall and F1-score for class 1 during testing. This model showed improvement, capturing approximately one-third of all flares (Recall 0.29), though precision for class 1 remained low (0.03).
- Model 3: Further enhancements were made to the Autoencoder, including the addition of another layer, an increase in parameters, L2 kernel regularization to mitigate overfitting, a reduced learning rate for the Adam optimizer, and the incorporation of class weights during loss calculation to specifically emphasize the minority class 1. This version demonstrated greater stability and captured a higher proportion of flares (Recall 0.38), although class 1 precision remained at 0.03.
- Final Model: Based on further visualization and analysis, the two most prominent attributes were identified: 20.27kHz_delta_abs and 24kHz_min. The final Autoencoder model was designed using only these two attributes, with a reduced number of neurons but retaining regularization and class weights. The model was trained for 30 epochs with a batch size of 32, 20% validation, Adam optimizer, and MSE loss. The threshold for anomaly detection was based on the 80th percentile of errors from class 0 data.

2.4. Model evaluation

The final model, which exclusively utilized the two most prominent attributes (*20.27kHz_delta_abs* and *24kHz_min*), yielded the best performance among all tested versions. This model was trained solely on records belonging to class 0 and subsequently evaluated on the entire dataset.

The evaluation of the final model's performance revealed:

- Precision for class 1 (flares) remained very low at 0.06. This indicates a substantial number of false positive predictions, where the model incorrectly identified non-flare events as flares.
- The model successfully captured 65% of all actual flare occurrences (Recall 0.65). This result is considered highly satisfactory, particularly given the extreme imbalance within the dataset.

Tables 1 and 2 depict the confusion matrix and metrics computed for the final model on the testing set.

Table 1. Contingency table for the final model

	Predicted 'no flare'	**Predicted 'flare'**
Real 'no flare'	**2020**	**505**
Real 'flare'	**17**	**31**

Table 2. Classification evaluation for the final model

Class	Precision	Recall	F1	Support
no flare	**0.99**	**0.80**	**0.89**	**2525**
Flare	**0.06**	**0.65**	**0.11**	**48**
Accuracy		**0.80**		**2573**
Macro average	**0.52**	**0.72**	**0.50**	**2573**
Micro average	**0.97**	**0.80**	**0.87**	**2573**

Understanding of the models showed that the real attribute values for samples from both class 0 and class 1 are remarkably small, significantly increasing the classification challenge for the model. Furthermore, observations of amplitude trends throughout the day showed that while a mild fluctuation in the 20.27 kHz signal could be observed around the time of a flare, this difference was relatively indistinct when viewed in the context of normal daily amplitude fluctuations. This inherent subtlety in the data underscores the difficulty of the task, as VLF signal amplitude changes during flares are very similar to those occurring during a typical day.

The most significant challenges encountered during this work included:

- An extremely imbalanced dataset, with only 48 positive (flare) cases out of a total of 2,586 records.
- A low degree of distinctiveness between the two classes (flare vs. no flare).
- The presence of noise and data gaps (including missing and negative values) within the dataset.

Despite these significant obstacles, the developed model successfully captured more than half of the flare occurrences, demonstrating the potential for this approach.

3. Conclusion

The work presented in this paper addressed the detection of solar flares using ionospheric data, continuing the collaborative research with the Institute of Physics at the University of Belgrade. The work was characterized by its research-oriented and exploratory nature, aiming to ascertain the extent to which solar flare occurrences could be identified from changes in VLF signal amplitudes recorded in the D-region of the ionosphere.

The theoretical framework provided fundamental insights into the ionosphere, solar flares, and an introduction to data science and artificial intelligence. The practical implementation adhered strictly to the CRISP-DM methodology. The raw data underwent thorough preprocessing, including the removal of erroneous records, enrichment with necessary statistical features for analysis, and transformation into a suitable format for modeling. For the modeling phase, an Autoencoder neural network model was developed to detect deviations from normal ionospheric behavior. After rigorous testing and parameter optimization, the final model achieved a recall of 65% for the positive class (flares), signifying its ability to correctly identify a significant portion of actual flare events. However, it also produced a considerable number of false positives.

The data suffered from extreme imbalance of the target attribute, the low degree of distinctness between the 'flare' and 'no-flare' classes, and the presence of noise and data

gaps. Although the results of this work are primarily for research purposes, the model's performance confirms the existence of subtle, detectable deviations in the VLF signals related to solar flare occurrences. This study, therefore, provides a foundational basis for future efforts aimed at improving solar flare detection and potentially extending the methodology to other types of geophysical phenomena.

Acknowledgements

This work was supported by the Slovak APVV agency Slovak-Serbian project SK-SRB-23-0029, and the Ministry of Science, Technological Development and Innovation of the Republic of Serbia (Serbian-Slovak project 337-00-3/2024-05/11). The authors acknowledge funding provided by the Institute of Physics Belgrade and the Astronomical Observatory (the contract 451-03-136/2025-03/200002) through the grants by the Ministry of Science, Technological Development and Innovation of the Republic of Serbia.

References

Azevedo, A., and Santos, M. F. (2008). *KDD, SEMMA and CRISP-DM: a parallel overview*. IADIS European Conference Data Mining, Amsterdam, Netherlands, 182.

Berahmand, K., Daneshfar, F., Salehi, E. S. et al. (2024). Autoencoders and their applications in machine learning: a survey. *Artif. Intell. Rev.* 57, 28.

Mishra, C., and Gupta, D. L. (2017). Deep machine learning and neural networks: An overview. *IAES Int. J. Artif. Intell.,* 6(2), 66.

Nina, A., Čadež, V. M., Popović, L. Č. et al. (2017). Diagnostics of plasma in the ionospheric D-region: detection and study of different ionospheric disturbance types. *Eur. Phys. J. D*., 71, 189.

Pavlík, V. (2024). Spracovanie ionosférických dát z rádiových meraní pomocou hlbokého učenia. Technical University of Kosice, Kosice, Slovakia

Šulić, D. M., Srećković, V. A., and Mihajlov, A. A. (2016). A study of VLF signals variations associated with the changes of ionization level in the d-region in consequence of solar conditions. *Adv. Space Res.*, 57(4), 102943.

PROGRAMME

Monday, 15 September

14:00 - 15:30 **Registration**

Chairs: Aleksandra Nina and Snežana Dragović

15:30 – 15:45 **Opening ceremony**

Chair: Snežana Dragović

15:45 – 16:20 **Nejc Bezak, Maximilian Kramer, Sascha Schultes, Jošt Sodnik, Klemen Kozmus Trajkovski, Matjaž Mikoš** Invited lecture
MITIGATION OF TORRENTIAL HAZARDS IN A TYPICAL ALPINE CATCHMENT IN SLOVENIA

16:20 – 16:55 **Ivan Lizaga, Borja Latorre, Montfort Bagalwa, Landry Cizungu, Joseph Okello, Muhumuza Moses, Linus Munishi, Kristof Van Oost, William Blake, Ana Navas, Pascal Boeckx** Invited lecture
DELTASENSE: AFRICA'S REMOTE SENSING GUARDIAN OF LANDSCAPE DEGRADATION

17:00 – 19:00 Welcome cocktail

Tuesday, 16 September

Chair: Sergey Pulinets

9:00 – 9:25 **Milan M. Ćirković**
THE WAITING TIME PARADOX AND GLOBAL RISK ANALYSIS: LESSONS FROM GEOPHYSICAL HAZARDS

9:25 – 9:50 **Monika Andreeska, Svemir Gorin, Katerina Drogreshka, Jasmina Najdovska**
COMPARISON OF METHODS FOR MACROSEISMIC MAPPING: A CASE STUDY OF THE 2016 DEBARCA-PLAKENSKA EARTHQUAKE

9:50 – 10:15 **Zeynep Ceylin Ecer, Vasile Grama**
MINING, ECOSYSTEMS, AND COMMUNITY HEALTH: A ONE HEALTH APPROACH TO THE HOLISTIC IMPACTS OF ACID MINE DRAINAGE IN THE WITWATERSRAND BASIN, SOUTH AFRICA

10:15 – 10:45 Coffee break

Chair: Pier Francesco Biagi

10:45 – 11:20 **Toshiyasu Nagao** Invited lecture
THE ANNOUNCEMENT OF THE LONG-TERM PROBABILITY OF A "MAJOR EARTHQUAKE" OCCURRING IN JAPAN AND THE SOCIAL IMPACT OF "AMBIGUOUS" INFORMATION ANNOUNCED WHEN THE PROBABILITY OF OCCURRENCE BECOMES RELATIVELY HIGH

11:20 – 11:45 **Giovanni Nico, Hans U. Eichelberger, Mohammed Y. Boudjada, Aleksandra Nina, Pier Francesco Biagi, Iren-Adelina Moldovan, Luka Č. Popović**
STUDY OF THE SEISMIC ACTIVITY AT THE DODECANESE ISLANDS (JANUARY AND FEBRUARY 2025) BASED ON THE ANALYSIS OF THE SWARM MISSION DATA

11:45 – 12:10 **Aleksandra Nina, Pier Francesco Biagi, Giovanni Nico, Hans U. Eichelberger, Mohammed Y. Boudjada, Jovan Bajčetić, Danilo Lazović, Peter Butka, Peter Bednár, Martin Sarnovský, Martin Humeník, Luka Č. Popović**
VLF/LF EARTHQUAKE PRECURSORS: REVIEW AND COMPARISONS

12:10 – 14:00 Lunch break

Chair: Toshiyasu Nagao

14:00 – 14:35 **Sergey Pulinets, Konstantin Tsybulya, Nadezhda Kotonaeva** Invited lecture
THE IONOSPHERE AS A SENSITIVE INDICATOR AND MEDIUM OF GEOSPHERES' INTERACTION

14:35 – 15:00 **Aneta Wojnar**
TESTING FUNDAMENTAL PHYSICS WITH SEISMOLOGY

15:00 – 15:25 **Milan Đorđević, Miloš Manić, Mrđan Đokić, Ranko Dragović, Ivana Smičiklas, Snežana Dragović**
EXTRACTION OF GULLY BOUNDARIES IN FORESTED TERRAIN USING HIGH-RESOLUTION UAV LIDAR DATA

15:25 – 15:55 Coffee break

Chair: Ivan Lizaga

15:55 – 16:20 **Sebastian Palacios Vidal, Denys Parra Murrugarra**
COMPARISON OF TWO-DIMENSIONAL AND THREE-DIMENSIONAL DYNAMIC RESPONSE OF AN EARTH AND ROCKFILL DAM

16:20 – 16:45 **Miloslava Stefanova**
MULTISPECTRAL IMAGE ANALYSIS FOR MAPPING EROSION AND DEBRIS FLOW-PRONE AREAS IN THE BUYUKDERE RIVER CATCHMENT (EASTERN RHODOPES, BULGARIA)

16:45 – 17:10 **Nina Nikolova, Simeon Matev, Petko Bozhkov, Martin Gera, Sabina Thaler, Josef Eitzinger, Marian Melo, Jaroslava Slavkova**
A COMPARATIVE DROUGHT ANALYSIS FOR AUSTRIA, SLOVAKIA, AND BULGARIA USING DROUGHT INDICES

Wednesday, 17 September

Chair: Giovanni Nico

11:00 – 11:25 **Lekshmi O Nair, Lijo Jose**
CHARACTERIZATION OF DIURNAL AND SEASONAL VARIABILITY OF IONOSPHERIC TEC OVER THE INDIAN EQUATORIAL REGION USING GPS OBSERVATIONS

11:25 – 11:50 **Danilo Lazović, Olivera Pronić-Rančić, Aleksandra Nina, Jovan Bajčetić**
DETECTION OF VLF TRANSMITTERS USING THE VITRANSFORMER DEEP LEARNING ALGORITHM

11:50 – 12:15 **Valentina Nikolova, Laure Guerit, Asparuh Kamburov, Dobromir Filipov, Ana M. Petrović, Jan Babej, Jiří Jakubínský**
CHARACTERIZATION OF RIVERBED SEDIMENT THROUGH 3D POINT CLOUD PROCESSING AND ANALYSIS

12:15 – 13:30 Lunch break

13:30 **Excursion**

Thursday, 18 September

Chair: Irina Mironova

9:00 – 9:25 **Roman Kislov**
MAGNETIC MOMENT OF THE HELIOSPHERIC CURRENT SHEET

9:25 – 9:50 **Nikola Veselinović, Mihailo Savić, Aleksandar Dragić, Dimitrije Maletić, Dejan Joković, Radomir Banjanac, Vladimir Udovičić**
PRELIMINARY ANALYSIS OF FORBUSH DECREASES IN OCTOBER 2024 USING OBSERVATIONS FROM BELGRADE MUON STATION

9:50 – 10:15 **Rudi Čop**
LOCAL MAGNETIC FIELD CHANGES ON THE ADRIATIC TECTONIC MICROPLATE

10:15 – 10:45 Coffee break

Chair: Xuhui Shen

10:45 – 11:20 **Irina Mironova** Invited lecture
MESOSPHERIC OZONE DEPLETION UNDER SOLAR AND GEOMAGNETIC FORCING IN 2024

11:20 – 11:45 **Mirela Voiculescu, Adrian Roșu, Daniel Constantin, Cătălin Negoiță**
CLIMATOLOGY OF CLOUDS AT AN ACTRIS STATION IN THE SE EUROPE

11:45 – 12:10 **Hans U. Eichelberger, Aleksandra Nina, Mohammed Y. Boudjada, Pier Francesco Biagi, Maria Solovieva, Patrick H. M. Galopeau, Iren-Adelina Moldovan, Giovanni Nico, Aleksandra Kolarski, Nikola Veselinović, Vladimir Srećković, Manfred Stachel, Bruno P. Besser**
IONOSPHERIC VARIATIONS IN THE SOLAR CYCLE 25 INFERRED FROM VLF/LF ELECTRIC FIELD MEASUREMENTS

12:10 – 12:20 **Meeting photo**

12:20 – 14:00 Lunch break

Chair: Mirela Voiculescu

14:00 – 14:35 **Xuhui Shen, Xuemin Zhang, Shufan Zhao, Qinqin Liu, Wenxiu Liu, Yatong Cui** Invited lecture
THE COUPLING PHENOMENA AND MECHANISMS BETWEEN EARTH INTERIOR EVENTS AND SPACE ENVIRONMENT

14:35 – 15:00 **Dragan Lukić**
HOT SPRINGS AND THE ORIGIN OF LIFE: SIMULATING ANCIENT ATMOSPHERES IN MODERN GEOTHERMAL ENVIRONMENTS

Chair: Hans U. Eichelberger

15:00 – 16:30 **Posters**

20:00 **Conference dinner**

Friday, 19 September

Chair: Aleksandra Nina

11:00 – 11:25 **Miloš Marković, Dušan Petković, Miljana Todorović Drakul, Stefan Krstić**
OPTIMIZATION OF OBSERVATION TIME IN PRECISE POINT POSITIONING BY COMBINING ERROR MODELS

11:25 – 11:50 **Marko Stanković, Sanja Grekulović, Danilo Joksimović, Sofija Naod**
GEOID MODELING BASED ON GLOBAL GEOPOTENTIAL MODELS AND DIGITAL TERRAIN MODELS

11:50 – 12:15 **Aleksandra Kolarski** Invited progress report
PERTURBATIONS OF VLF RADIO SIGNALS DUE TO LEP EFFECT MONITORED IN BELGRADE - A CASE STUDY

12:15 – 12:30 **Concluding remarks and closing of the Conference**

LIST OF POSTERS

AUTHORS' INDEX

PARTICIPANTS

Mariana Adam, Romania
Monika Andreeska, North Macedonia
Jovan Bajčetić, Serbia
Peter Bednar, Slovakia
Nejc Bezak, Slovenia
Pier Francesco Biagi , Italy
Peter Butka, Slovakia
Zeynep Ceylin Ecer, Turkey
Michael Contadakis, Greece
Rudi Čop, Slovenia
Aleksandar Čupić, Serbia
Milan Ćirković, Serbia
Ranko Dragović, Serbia
Snežana Dragović, Serbia
Mrđan Đokić, Serbia
Milan Đorđević, Serbia
Hans U. Eichelberger, Austria
Patrick H. M. Galopeau, France
Vasile Grama, Romania
Sanja Grekulović, Serbia
Anđelija Ivkov-Džigurski, Serbia
Roman Kislov, Russia
Aleksandra Kolarski, Serbia
Jovana Kostić, Serbia
Stefan Krstić, Serbia
Maja Kuzmanoski, Serbia
Marko Langović, Serbia
Milica Langović, Serbia
Danilo Lazović, Serbia
Ivan Lizaga, Spain
Dragan Lukić, Serbia
Miloš Marković, Serbia
Simeon Matev, Bulgaria
Spomenko Mihajlović, Serbia
Irina Mironova, Russia
Toshiyasu Nagao, Japan
Giovanni Nico, Italy
Valentina Nikolova, Bulgaria
Aleksandra Nina, Serbia
Lekshmi O Nair, India
Oleg Odalović, Serbia
Sebastian Palacios Vidal, Serbia
Dušan Petković, Serbia
Marko Petrović, Serbia
Luka Popović, Serbia
Sergey Pulinets, Russia
Martin Sarnovsky, Slovakia
Xuhui Shen, China
Ivana Smičiklas, Serbia
Vladimir Srećković, Serbia
Marko Stanković, Serbia
Miloslava Stefanova, Bulgaria
Miljana Todorovic Drakul, Serbia
Đorđe Trajković, Serbia
Nikola Veselinović, Serbia
Mirela Voiculescu, Romania
Aneta Wojnar, Spain, Poland

International Conference on Recent Trends in Geoscience Research and Applications 2025

BOOK OF ABSTRACTS AND CONTRIBUTED PAPERS

Publishers:

Faculty of Civil Engineering, University of Belgrade, Belgrade, Serbia

Institute of Physics Belgrade, National Institute of the Republic of Serbia, University of Belgrade, Belgrade, Serbia

Editors:

Aleksandra Nina, Institute of Physics Belgrade, National Institute of the Republic of Serbia, University of Belgrade, Belgrade, Serbia

Snežana Dragović, "VINČA" Institute of Nuclear Sciences - National Institute of the Republic of Serbia, University of Belgrade, Belgrade, Serbia

Maja Kuzmanoski, Institute of Physics Belgrade, National Institute of the Republic of Serbia, University of Belgrade, Belgrade, Serbia

Milan Đorđević, University of Niš, Faculty of Sciences and Mathematics, Niš, Serbia

Mrđan Đokić, University of Niš, Faculty of Sciences and Mathematics, Niš, Serbia

Editorial support:

Milica Langović, Institute of Physics Belgrade, National Institute of the Republic of Serbia, University of Belgrade, Belgrade, Serbia

Dušan Petković, University of Belgrade, Faculty of Civil Engineering, Department of Geodesy and Geoinformatics, Belgrade, Serbia

Printing:

Snežana Dragović, Belgrade

Circulation:

30 copies

ISBN

978-86-7518-253-5

Belgrade, 2025

CIP - Каталогизација у публикацији
Народна библиотека Србије, Београд

55(048)(0.034.2)

INTERNATIONAL Conference on Recent Trends in Geoscience Research and Applications (2025 ; Beograd)
Book of Abstracts ; and Contributed Papers [Elektronski izvor] / International Conference on Recent Trends in Geoscience Research and Applications 2025, GeosciRA25, 15–19 September 2025, Belgrade, Serbia & virtual ; [organizers University of Belgrade, Faculty of Civil Engineering and University of Belgrade, Institute of Physics Belgrade] ; edited by Aleksandra Nina ... [et al.]. - Belgrade : University, Faculty of Civil Engineering : University, Institute of Physics, 2025 (Beograd : Curent Print). - 1 elektronski optički disk (CD-ROM) ; 12 cm

Sistemski zahtevi: Nisu navedeni. - Nasl. sa naslovne strane dokumenta. - Tiraž 30. - Bibliografija uz pojedine apstrakte.

ISBN 978-86-7518-253-5 (FCE)

а) Геологија -- Апстракти

COBISS.SR-ID 176755209